Degradation of Aspartyl Peptides

Studies on the isomerization and enantiomerization of aspartic acid in model peptides by capillary electrophoresis and high performance liquid chromatography

Dissertation
zur Erlangung des akademischen Grades
Doctor rerum naturalium (Dr. rer. nat.)

vorgelegt dem Rat der Biologisch – Pharmazeutischen Fakultät
der Friedrich – Schiller – Universität Jena

von Diplom – Pharmazeutin Silvia De Boni
geboren am 23. Juli 1975 in Conegliano (Italien)

Gutachter:

1. Prof. Dr. G. Scriba
2. Prof. Dr. J. Lehmann
3. Prof. Dr. G. Blaschke

Tag der mündlichen Prüfung: 14.12.2004

Tag der öffentlichen Verteidigung: 25.01.2005

For Jan

Contents

Abbreviations

AA	amino acid
ACN	acetonitrile
API	atmospheric pressure ionization
3-AP	3-aminopyridine
Asn	asparagine
Asp	aspartic acid
Asu	aminosuccinimidyl
BGE	background electrolyte
Boc	*tert*-butyloxycarbonyl
Bzl	benzyl
CD	cyclodextrin
CE	capillary electrophoresis
CM-β-CD	carboxymethyl-β-cylodextrin
CPA	corrected peak area
CZE	capillary zone electrophoresis
DCM	dichlormethane
DIPEA	diisopropylethylamine
DMF	dimethylformamide
DNA	desoxyribonucleic acid
EOF	electroosmotic flow
ESI	electrospray ionization
FAB	fast atom bombardment
Fmoc	9-fluorenylmethoxycarbonyl
GC	gas chromatography
Gly	glycine
HBTU	*N*-[(1*H*-benzotriazol-1-yl)(dimethylamino)methylene]-*N*-methylmethanaminium hexafluorophosphate *N*-oxide
His	histidine
HP-β-CD	hydroxypropyl-β-cyclodextrin
HPLC	high performance liquid chromatography
ID	internal diameter
LOD	limit of detection
LOQ	limit of quantitation
M-β-CD	methyl-β-cyclodextrin
MS	mass spectrometry
MS/MS	tandem mass spectrometry
OD	outer diameter

pABA	para-aminobenzoic acid
pAMBA	para-aminomethylbenzoic acid
Phe	phenylalanine
PIMT	protein L-isoaspartyl-*O*-methyltransferase
RP	reversed phase
RSD	relative standard deviation
SD	standard deviation
Ser	serine
SPPS	solid phase peptide synthesis
S-β-CD	sulphated β-cyclodextrin
$t_{1/2}$	half-life
tBu	*tert*-butylester
TFA	trifluoroacetic acid
TLC	thin layer chromatography
Trp	tryptophane
UV	ultraviolet

1. Introduction

1.1 Instability of aspartyl peptides

Peptides and proteins are used as pharmaceuticals for many indications and as diagnostics. Advantages of this class of substances are the high activity and high specificity, which correlates with relatively low systemic toxicity. The development of recombinant DNA technology allowed the industrial production of these substances and dramatically increased the number of peptides and proteins on the pharmaceutical market. During the years 2000-2003, a total of 64 biopharmaceuticals was approved for human use in North America and Europe, all of them being protein-based drugs [1]. This represents over a quarter of all new drug approvals of the same period of time. Moreover, in 2003 approximately further 500 candidate biopharmaceutical substances were undergoing clinical evaluation [1]. Of the proteins thus far approved within the European Union, hormones and cytokines represent the largest product categories, additional classes are recombinant blood coagulation factors, subunit vaccines and monoclonal antibodies [2]. In addition, many medical agents are synthetic peptides and peptidomimetics.

Degradation pathways of peptides and proteins comprise chemical and physical instability (figure 1). Chemical instability involves covalent modifications, such as hydrolysis, deamidation, beta-elimination, oxidation, enantiomerization and disulfide exchange [3]. In contrast, physical instability refers to changes in the higher order structure of the proteins, such as denaturation, aggregation, precipitation and adsorption. These processes can lead to loss of structure and physiological activity as well as to the formation of toxic degradation products.

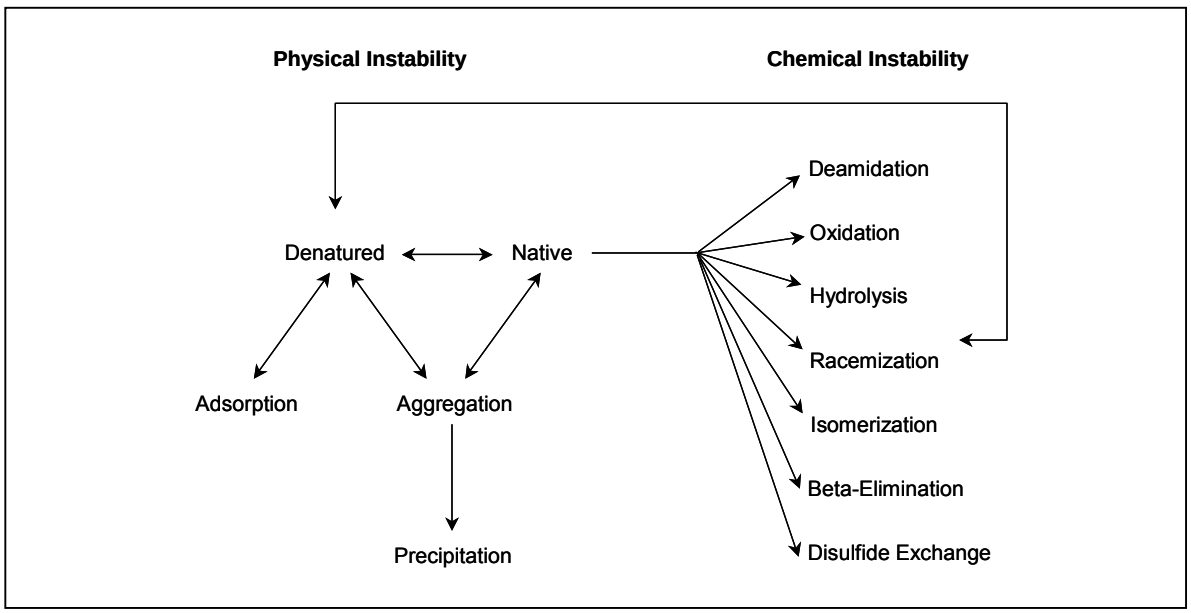

Figure 1: Degradation pathways of peptides and proteins

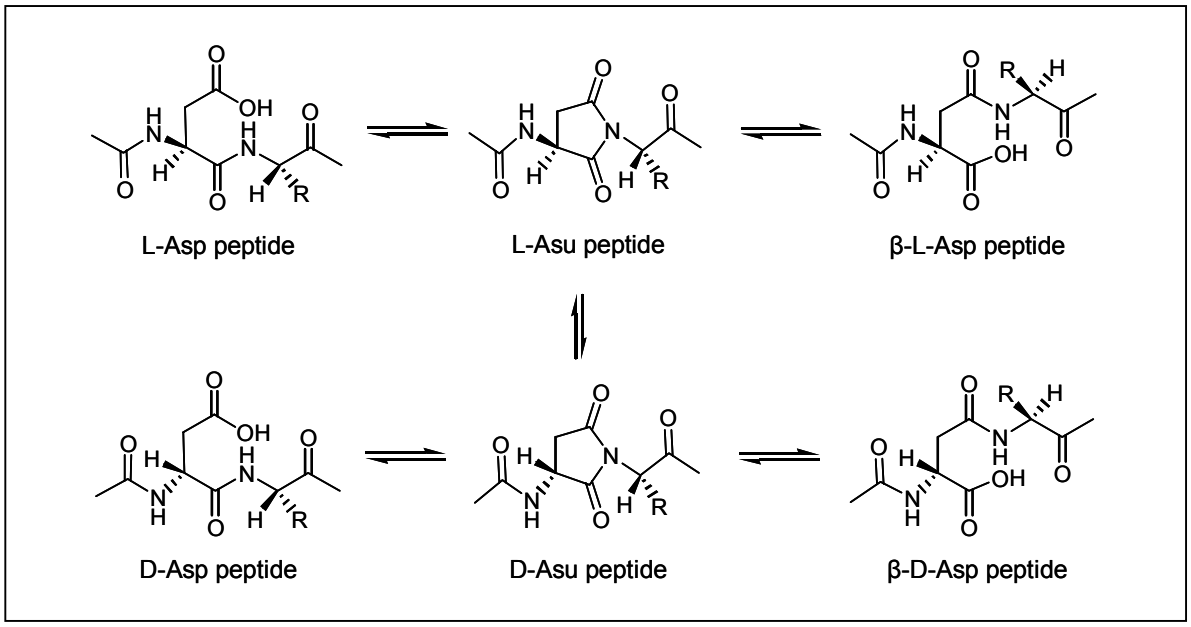

Figure 2: Spontaneous isomerization and enantiomerization of L-Asp in peptides.

Asparagine (Asn) and aspartic acid (Asp) are among the most unstable amino acids in peptides and proteins. Both of them are susceptible to isomerization and enantiomerization and Asn can additionally undergo side chain deamidation [3-5]. The initial event in these nonenzymatic reactions is the formation of an aminosuccinimidyl (Asu) intermediate (figure 2). The mechanism of succinimide formation involves deprotonation of the carboxyl-side backbone amide followed by attack of the anionic nitrogen on the side chain carbonyl group. The rate of the succinimide formation depends on the primary sequence of the peptide as well as temperature, pH, concentration and ionic strength of the solution [3-8]. Neighbouring amino acid residues that allow for chain flexibility and hydrogen-bonding interactions such as Gly or Ser facilitate the formation of the succinimidyl intermediate. The succinimide is subject to spontaneous hydrolysis generating either the native L-aspartyl residue (α-Asp) or L-isoaspartyl residue (iso-Asp or β-Asp), in which the peptide backbone chain is connected *via* the β-carboxyl group of the Asp side chain (figure 2). In addition, enantiomerization of the L-succinimide to D-succinimide may occur, due to the increased acidity of the succinimidyl α-carbon compared to Asp [9]. It has been demonstrated that the rate of Asp enantiomerization in peptides is about 10^5 times faster than that of Asp itself under similar conditions [9, 10]. Successive hydrolysis of the D-succinimide leads to the formation of D-Asp and D-iso-Asp (D-β-Asp) residues (figure 2).

Beside being side reactions in solution and solid phase peptide synthesis [11, 12], deamidation, isomerization and enantiomerization of Asn and Asp are degradation reactions of natural proteins and of peptide and protein drugs [3, 4]. Spontaneous deamidation and isomerization of Asn were found in prion proteins [13]. Nabuchi and coworkers studied the stability of human parathyroid hormone under acidic and alkaline conditions and found deamidation and isomerization of Asn residues after incubation at pH 9 [14]. Fibrillar deposits of β-amyloid proteins containing β-Asp occur in Alzheimer's

disease [15, 16]. Succinimidyl peptides were found in heat stressed solutions of the human amylin synthetic analog pramlintide [17]. Enantiomerization and formation of D-Asp peptides could be detected by RP-HPLC after incubation of the peptidomimetic klerval [18]. Age-dependent accumulation of D-Asp was observed in numerous human tissues, such as tooth dentine, skin, bones and ocular lens [19] and has been used to date paleontological material [20]. To minimize the accumulation of damaged aspartyl residues in cellular proteins, all mammalians tissues possess the protein L-isoaspartyl-*O*-methyl-transferase (PIMT) [4]. This enzyme uses *S*-adenosyl-L-methionine to methylate L-β-Asp residues but not "normal" L-α-Asp residues. Non-enzymatic deesterification of the methylated residues returns them to the succinimide form much more rapidly than in the absence of methylation, resulting in the eventual conversion of most of the damaged residues to the L-Asp form. However, this protection reaction is less efficient in presence of D-β-Asp residues causing accumulation of this form of the amino acid. In addition, proteins containing D-amino acids can normally not be metabolized and β-Asp proteins have been found to be immunogenic [21].

Thus, it is clear that degradation reactions of Asp play a major role in the instability of natural proteins as well as peptide and protein pharmaceuticals. They are relatively rapid reactions and were observed in a number of compounds. Any of these reactions can occur during production, isolation, purification, delivery and storage of peptide and protein drugs. The investigation of the mechanism of these degradation reactions is important for understanding the pathogenesis of some diseases as well as for optimizing processing and formulation conditions of proteins drugs.

1.2 Analytical techniques to investigate aspartic acid degradation

Chemical instability of peptides and proteins has been investigated by different analytical techniques. Changes in mass, size, charge, hydrophobicity as well as in UV absorption and fluorescence are used to monitor the degradation reactions [22].

Replacement of an amide by a carboxylic acid as consequence of deamidation causes changes in hydrophobicity, polarity and charge. Such changes can be studied by chromatographic methods, such as ion-exchange chromatography, reversed phase high performance liquid chromatography (RP-HPLC), hydrophobic and affinity chromatography as well as by electrophoretic techniques, such as isoelectrofocusing, gel electrophoresis and capillary electrophoresis (CE) [4, 22]. Moreover, the mass change ($\Delta m = +1$ *m/z*) can be detected by mass spectrometry.

Isomerization of Asp to β-Asp can be observed through blockage of Edman sequencing, because the extra carbon in the backbone of the β-Asp residue prevents cyclization to form the anilinothiazolone derivative [4]. A direct assay for β-Asp residues involves the use of PIMT for selectively labeling β-Asp sites with a ^{3}H- or ^{14}C-methyl group [23]. Tritiated methanol is released from the methylated intermediate and can be detected by scintillation counting. To obviate the need for radioactive

materials, an alternative method using PIMT analyzes *S*-adenosyl-L-homocystein, which like methanol is produced in stoichiometric amounts by PIMT-dependent methylation of β-Asp residues. UV detection is carried out after separation by RP-HPLC or strong cation-exchange HPLC [24-26]. Recently Cloos and Fledelius [27] developed immunoassays to determine the level of Asp isomerization in collagen.

Enantiomerization of amino acids in peptides was first analyzed after hydrolysis of the peptide in 6 M HCl at 100°C for 6h [28]. Aspartic acid was separated from the other amino acids by anion exchange chromatography and was analyzed by chiral gas chromatography (GC) or by RP-HPLC after derivatisation to give diastereoisomers. This method is time-consuming and, because of the acid-catalyzed enantiomerization occurring during hydrolysis [29-31], does not provide reproducible results. Moreover, the presence of α- and β-Asp linkages in the peptide can not be distinguished by the amino acids analysis and has to be established indirectly through the β-Asp resistance to Edman degradation. Enantiomerization of an amino acid in peptides results in the formation of diastereomers which can be distinguished from one other based on differences in physico-chemical properties. Differences in hydrophobicity and polarity can be exploited relatively easily by RP-HPLC. Because RP-HPLC is a well-established technique, most of the studies on the degradation of Asp were conducted with this method [6, 8, 10, 32].

1.3 Aim of the work

While many studies were published on the factors that influence the formation of the succinimidyl intermediate and the isomerization of Asp [3-8, 33], only few investigated Asp enantiomerization in peptides. Geiger and Clarke demonstrated extensive enantiomerization of Asp in model hexapeptides [10]. Oliyai and Borchardt detected in pH 10 incubations of Asp hexapeptides additional peaks by RP-HPLC that were assigned as the corresponding D-Asp peptides based on the retention time in relation to a standard and by off-line fast atom bombardment mass spectrometry as well as enzymatic cleavage studies [7]. D-Asp peptides could be detected by RP-HPLC after incubation of the peptidomimetics klerval [18] and of human αA-crystallin [32]. To date only the work of Geiger and Clarke reported on the half-life ($t_{1/2}$) of the hydrolysis and enantiomerization of a model hexapeptide [10], but the kinetic of the degradation reaction has not been extensively investigated. Moreover, no report on the kinetic of the succinimidyl intermediate has been published. Most of the studies on Asp degradation were conducted by RP-HPLC with UV detection, while CE was not tested as analytical method.

The present study was conducted in order to investigate the degradation products arising from the degradation of aspartyl peptides in acidic and alkaline media, specifically with respect to the isomerization and enantiomerization of the Asp residue. The tripeptides Phe-Asp-GlyNH_2 and Gly-Asp-PheNH_2 were used as model compounds in order to compare the influence of the steric

hindrance of the Asp-following amino acid on the degradation. For this purpose, the following points were evaluated:

1. Synthesis of α/β-D/L-aspartyl peptides as reference substances
2. Identification of the degradation products arising after incubation of the model tripeptides
3. Development and validation of an analytical method for the separation of the degradation products
4. Quantification of the degradation products and investigation of the kinetics of the degradation reactions
5. Investigation of the degradation of a succinimidyl model peptide.

2. Synthesis of reference substances

In order to investigate the degradation of the model aspartyl peptides Phe-Asp-GlyNH_2 and Gly-Asp-PheNH_2, pure degradation products were required as reference substances. When available, amino acids and dipeptides were purchased from commercial sources. Tripeptides with amidated *C*-terminal end were provided by Dr. Sabbah and were synthesised according to [34]. Tripeptides with a free terminal carboxylic function were synthesised by manual solid phase peptide synthesis (SPPS) according to standard procedures [35].

2.1 Solid phase peptide synthesis of tripeptides with free terminal carboxyl group

In SPPS a polymer matrix serves simultaneously as solid support for the peptide and as permanent *C*-terminal protecting group. Synthesis starts with the attachment of the first N_α-protected amino acid to the linker functionality of the resin. After deprotection of the amino function another activated protected amino acid is added. Chain elongation is accomplished by consecutive deprotection and coupling steps. Finally, the *N*-terminal free peptide is cleaved from the resin with concomitant deprotection of all side chain functionalities. Advantages of SPPS compared to solution synthesis are: (I) the easy and fast washing and filtration steps, (II) the possibility of using reagents in excess thus achieving practically quantitative reactions, (III) the minimization of physical losses as the peptide remains attached to the support throughout the synthesis and (IV) the possibility of automation.

The two most extensively used protecting combinations in SPPS are the Merrifield strategy (Boc/Bzl-chemistry) and the Sheppard strategy (Fmoc/tBu-chemistry). In the Merrifield system *tert*-butyloxycarbonyl (Boc) is used as N_α-protecting group. This can be quantitatively removed using 20-50% trifluoroacetic acid (TFA) in dichloromethane (DCM). Benzyl esther derived (Bzl) side-chain protecting groups as well as the *C*-terminal linker to the solid support are removed simultaneously employing acids like hydrofluoric acid. Other than in the classical Merrifield system, the Sheppard strategy uses 9-fluorenylmethoxycarbonyl (Fmoc) as N_α-protecting group. This group can be rapidly and quantitatively removed in alkaline medium in presence of piperidine. Permanent protection of side-chain groups is provided by *tert*-butyl derivatives (tBu), which can be cleaved in acidic medium under relatively moderate conditions such as 95% TFA in DCM. Because of its milder reaction conditions, the Fmoc strategy is nowadays well established as method of choice in SPPS.

Tripeptides with free terminal carboxylic function were synthesised by Fmoc-based SPPS. A reaction scheme is depicted in figure 3. Polystyrene with a 2-chlorotrityl chloride linker was used as resin. The Fmoc-protecting group was removed treating the peptidyl-resin with piperidine in dimethylformamide (DMF). Amide bond formation involved *in situ* chemical activation of the carboxy group by *N*-[(1*H*-

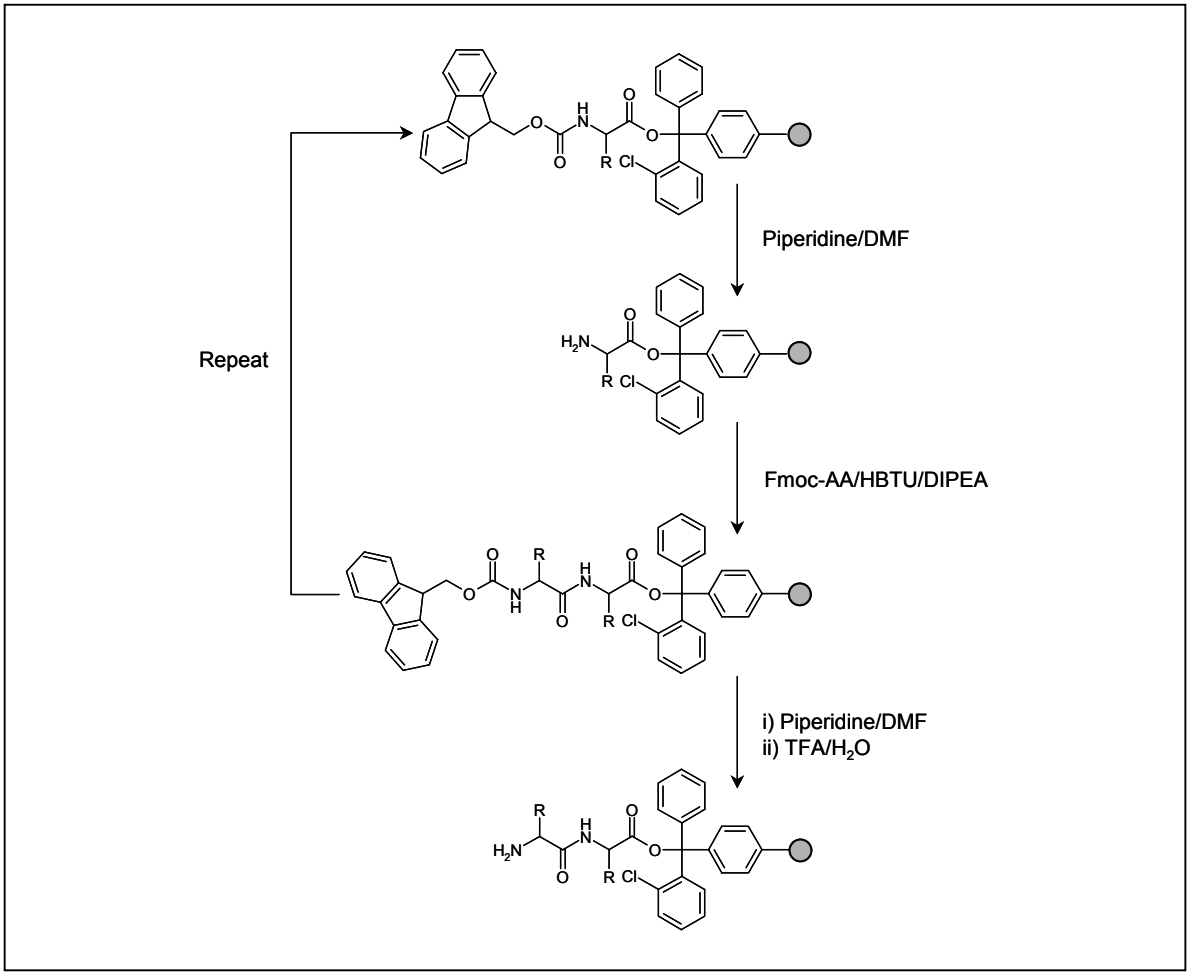

Figure 3: Fmoc-based solid phase peptide synthesis.

benzotriazol-1-yl)(dimethylamino)methylene]-*N*-methylmethanaminium hexafluorophosphate *N*-oxide (HBTU). Cleavage of the products from the resin was achieved with 95% TFA in water. The crude peptides were purified by preparative HPLC and their identity was confirmed by mass spectrometry.

2.2 Synthesis of succinimidyl peptides

Formation of succinimidyl derivatives is a well known side reaction during both in solution and solid phase synthesis of aspartyl peptides [35-37]. Schön and Kisfaludy [38] investigated the formation of Asu peptides during removal of the tBu aspartyl side-chain protecting group under different reaction conditions. While no cyclization occurred in TFA, over 95% transformation of the protected peptide to the Asu peptide was estimated by thin layer chromatography (TLC) after treatment with 3.6 N HCl in acetic acid. A scheme of the reaction is depicted in Figure 4. This reaction was used to synthesise the succinimidyl peptides Phe-Asu-GlyNH_2, Phe-Asu-GlyOH, Gly-Asu-PheNH_2 and Gly-Asu-PheOH by

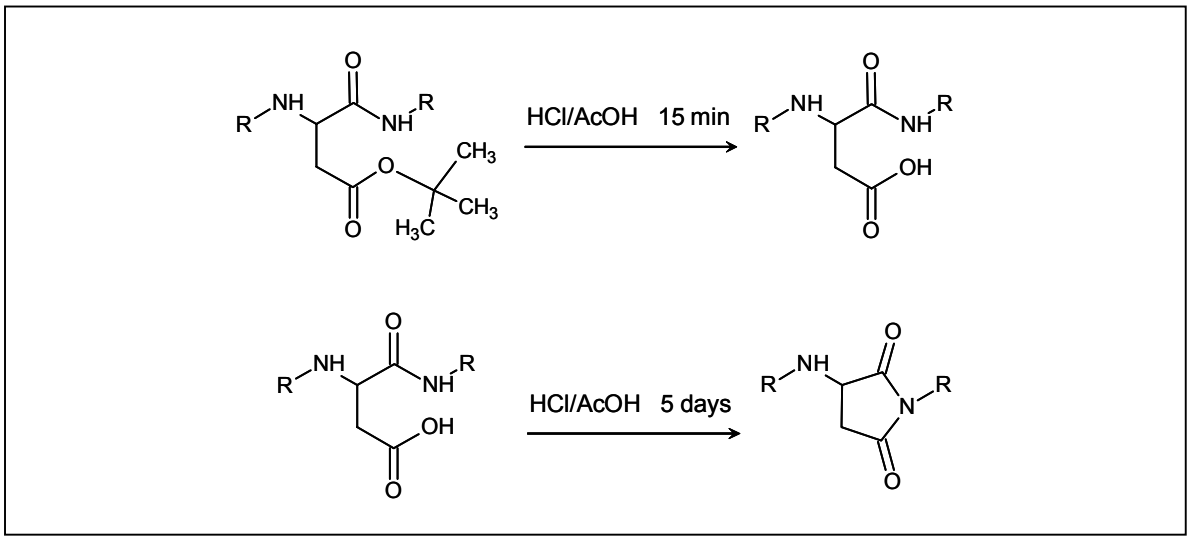

Figure 4: Synthesis of succinimidyl peptides according to [38].

prolonged incubation of the corresponding aspartyl peptides in HCl/acetic acid. The peptides were purified by preparative HPLC and their identity was confirmed by mass spectrometry.

3. Incubation of model peptides

3.1 Incubation of Phe-Asp-GlyNH_2 and Gly-Asp-PheNH_2

The purpose of this work was to study the degradation of aspartic acid in peptides with special regard to the enantiomerization reaction. The model tripeptides Phe-Asp-GlyNH_2 and Gly-Asp-PheNH_2 were selected in order to compare the influence of steric hindrance of the Asp-following amino acid because the initial succinimide formation resulting in the corresponding Asu peptides is known to depend on the amino acid sequence [7, 39, 40]. As it has been demonstrated that different degradation products are formed depending on the pH of the solution [6, 8, 14], the aspartyl peptides were incubated at two different pH values (pH 2 and 10). In addition to isomerization and enantiomerization, further degradation reactions can be expected [3, 5]. Deamidation of the *C*-terminal amide and hydrolysis of the peptide amide backbone can occur. A diketopiperazine derivative can be the result of the nucleophilic attack of the *N*-terminal nitrogen on the amide carbonyl between the second and the third amino acid [41, 42]. Previous studies have shown that hydrolysis of the peptide backbone is predominant at acidic pH while isomerization occurs in alkaline media [6, 14]. Moreover, the succinimide is relatively stable at low pH while it is rapidly hydrolysed under neutral and alkaline conditions [43, 44]. As the enantiomerization of Asp occurs rather slowly, the incubation was performed at 80°C, in order to accelerate the reaction rate.

3.2 Incubation of Phe-Asu-GlyOH

After analysis of the incubations of Phe-Asp-GlyNH_2 and Gly-Asp-PheNH_2 it was clear that various reactions contribute to the degradation of the Asp peptides (see chapter 4). In order to investigate the enantiomerization reaction independently from other degradation pathways, the model compound Phe-Asu-GlyOH was incubated. In this way, the hydrolysis reaction of the Asu ring and the consequent formation of α- and β- D/L-Asp products could be selectively studied. After analysis of the incubation of Phe-Asp-GlyNH_2 it was shown that no ring opening occurs at pH 2 (see paragraph 4.2). For this reason, the Asu peptide was incubated only in alkaline medium (pH 10). A preliminary experiment was conducted incubating Phe-Asu-GlyOH at a temperature of 80°C. Under these conditions the succinimidyl hydrolysis proceeds too fast to allow detection of the degradation of Phe-Asu-GlyOH in reasonable time intervals. An incubation temperature of 30°C proved to be convenient for the analysis.

4. Analysis of degradation products by capillary electrophoresis

4.1 Basic principles of peptide analysis by CE

CE is one of the most important techniques for the separation of charged substances. In capillary zone electrophoresis (CZE) analytes are separated due to their different mobility in a fused-silica capillary filled with an electrolyte solution when an electric field is applied. Equation (1) describes the mobility μ of a compound in terms of the physical parameters q (ion charge), η (solution viscosity) and r (ion radius):

$$\mu = \frac{q}{6 \pi \eta r} \qquad (1)$$

From this equation it is evident that small, highly charged species have high mobilities whereas large, minimally charged species have low mobilities. Electrophoretic mobility depends on: (I) properties of the analyte itself such as charge, size, shape, (II) properties of the background electrolyte (BGE) such as composition, pH, ionic strength, viscosity, temperature and (III) interactions between analytes and components of the BGE such as solvatation, dissociation and complex formation. Another parameter that influences the migration time is the electroosmotic flow (EOF). The EOF is the bulk flow of liquid in the capillary as a consequence of the surface charge on the interior capillary wall. The EOF results from the effect of the applied electric field on the solution double-layer at the wall. Changes in the chemistry of the capillary wall can affect the velocity of the EOF profoundly and subsequently the migration time. Moreover, the EOF causes movement of nearly all species, regardless of charge, in the same direction. Thus, cations, neutral species and anions can be detected in a single run since they all migrate in one direction.

Differences in the primary structure of peptides cause differences in their properties such as electric charge, size, shape and hydrophobicity. Because of its ability to exploit these physico-chemicals properties, CE is a convenient, fast and simple analytical technique for the separation of peptides. In the last years many application of CE for the separation of peptides have been demonstrated [45-47]. In a previous study a CE and a RP-HPLC method for the analysis of Asn peptides were compared. CE showed better resolution in shorter analysis time [48]. Moreover, it has been shown that CE can separate Asp and β-Asp peptides and the corresponding D-Asp and β-D-Asp diastereomers [49-51]. This is due to small differences of the pK_a values of both the α-Asp and β-Asp isomers as well as the respective diastereomers.

4.2 Analysis by CE in achiral buffer

Analysis of the incubation solutions was first performed by CE with UV detection. An aqueous phosphate buffer, pH 3.0, was used as background electrolyte (BGE). Using reference substances it has been previously shown that the diastereomeric pairs L-Phe-α-L-Asp-$GlyNH_2$/L-Phe-α-D-Asp-$GlyNH_2$ and L-Phe-β-L-Asp-$GlyNH_2$/L-Phe-β-D-Asp-$GlyNH_2$ can be separated under these conditions [50]. Identification of the degradation products was carried out by co-injection of reference substances. Potential degradation products that were available as reference substances were injected. Most of the degradation products could be identified in this way. Unequivocal identification was performed by on-line mass spectrometry (MS) detection (see chapter 6). By MS, identification of peaks that were previously not assigned by co-injection was achieved. Subsequently, missing reference substances were synthesised and co-injected.

As it can be seen in Figure 5, a phosphate buffer, pH 3.0 (CE-System 1, see Materials and Methods, paragraph 10.4), was suitable for the analysis of most degradation products in the presence of p-aminomethylbenzoic acid (pAMBA) as internal standard. Most of the expected degradation products could be identified in the solutions after incubation at pH 2 (see Figures 5A and 5C). Deamidation of the C-terminal amide resulted in the free acid form of the tripeptides. The dipeptides Phe-Asp and Gly-Asp and the amino acid amides $PheNH_2$ and $GlyNH_2$ were the result of hydrolysis of the peptide amide backbone. The Asu peptides could be detected due to their relative stability in acidic solution. Peptides containing D-Asp were not observed as the acidity of the succinimidyl α-carbon is not sufficiently high to be deprotonated at pH 2, so that no significant epimerization occurred.

As expected, incubations at pH 10 resulted in different degradation patterns compared to pH 2 (see Figure 5B and 5D). Cleavage of the backbone amide was not significant while isomerization and enantiomerization *via* the cyclic imide dominated. Deamidation of the C-terminal amide to yield the corresponding free acids was observed for all isomers of the tripeptides. The intermediate Asu-peptides were not detected, due to their low stability under these incubation conditions.

As predicted from the pK_a values for the α- and β-Asp free carboxyl groups, the β-Asp peptides showed longer migration times than the corresponding α-Asp peptides. In fact, studies on glycin-Asp peptides showed that the α-Asp side chain carboxyl group is less acidic than the α-carboxyl group of β-Asp, having pK_a values of 4.0 and 3.4, respectively [43, 44]. Interestingly, the succinimidyl peptides Phe-Asu-GlyOH and Gly-Asu-PheOH migrated slower than the corresponding aspartyl peptides Phe-Asp-GlyOH and Gly-Asp-PheOH, despite the fact that the Asp peptides possess two carboxyl groups and a higher molecular mass compared to the Asu peptides. This may be explained by an increased acidity of the *C*-terminal carboxyl group due to succinimide formation, so that the succinimidyl peptides carry a lower overall positive charge than the Asp peptides. Alternatively, this behaviour may be attributed to different hydrodynamic volumes of the compounds.

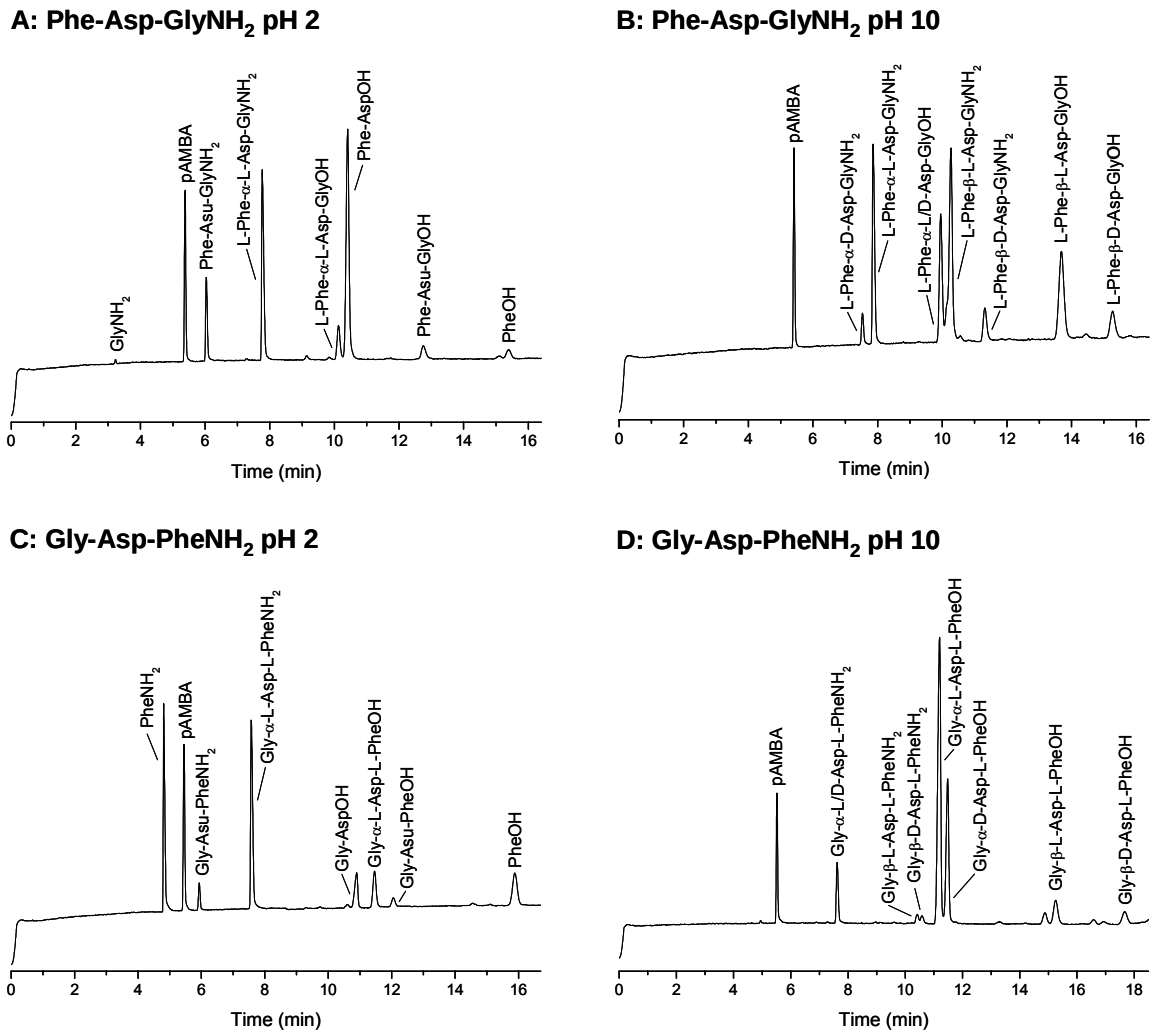

Figure 5: Electropherograms of Phe-Asp-$GlyNH_2$ incubated at pH 2 for 12 h (A) and at pH 10 for 24 h (B) and Gly-Asp-$PheNH_2$ incubated at pH 2 for 36 h (C) and at pH 10 for 96 h (D). Analysis conditions: 50 mM phosphate buffer, pH 3.0. For details see Materials and Method, CE-System 1, paragraph 10.4.

4.3 Analysis by CE using cyclodextrins

Under the conditions used in CE-system 1 (phosphate buffer, pH 3.0), resolution of all analytes could not be achieved. As it can be seen in Figures 5D and 5B, the diastereomeric pair Gly-α-L-Asp-L-$PheNH_2$ and Gly-α-D-Asp-L-$PheNH_2$ was not resolved and only partial separation of L-Phe-β-L-Asp-$GlyNH_2$, L-Phe-α-L-Asp-GlyOH and L-Phe-α-D-Asp-GlyOH was possible. An additional selectivity can be reached by addition of a chiral compound into the BGE. Cyclodextrins (CDs) are the most popular chiral selectors for peptide enantioseparations in CE [52, 53]. CDs are dissolved in the BGE and form with analytes host-guest inclusion complexes. These transient diastereomeric complexes differ in their physico-chemical properties and can thus be separated. Similarly to enantiomers, diastereomers can

form complexes with CDs which have different properties and thus electrophoretic mobilities. Consequently, separations that can not be achieved in an achiral medium can be often observed in the presence of CDs.

Resolution of Gly-α-L/D-Asp-L-PheNH$_2$ and of L-Phe-β-L-Asp-GlyNH$_2$ and L-Phe-α-L/D-Asp-GlyOH was attempted by addition of cyclodextrins to the BGE. Various uncharged and negatively charged CDs such as β-CD, methyl-β-CD (M-β-CD), carboxymethyl-β-CD (CM-β-CD), hydroxypropyl-β-CD (HP-β-CD) and sulfated-β-CD (S-β-CD) were tested. Concentrations of the selector, pH of the BGE and applied voltage were optimized for every sample by injection of reference substances.

4.3.1 Analysis of Gly-α-L-Asp-L-PheNH$_2$ and Gly-α-D-Asp-L-PheNH$_2$

Figure 6 A shows the separation of the diastereomeric pair Gly-α-L-Asp-L-PheNH$_2$ and Gly-α-D-Asp-L-PheNH$_2$. Base-line resolution was obtained by the addition of 3 mg/ml S-β-CD to 50 mM phosphate buffer, pH 3.0 (CE-System 2, Materials and Methods, paragraph 10.4). The DL diastereomer migrates faster than the LL diastereomer which can be of advantage because of the low concentration of the DL diastereomer in the incubation solutions. In fact, it is always desirable that the minor substance migrates ahead of the principal component, in order to avoid the minor peak to be obscured by eventual tailing of the major peak.

A negative consequence of the use of CDs is that the internal standard pAMBA can not be detected. This is probably due to the strong interaction between CDs and pAMBA. Negatively charged CDs, such as S-β-CD, migrate towards the anode. Substances which interact strongly with the chiral selector form negatively charged complexes which migrate towards the anode as well. Because analyte detection is carried out at the cathodic end of the capillary, these negatively charged complexes can not reach the detection window and can consequently not be detected. Assuming that the UV-absorption properties of the diastereomers are identical, the total concentration of Gly-α-L-Asp-L-PheNH$_2$ and Gly-α-D-Asp-L-PheNH$_2$ were calculated from the area of the peak corresponding to both peptides in the analysis in the achiral BGE (CE-system 1). After separation with CDs (CE-system 2) the peak-area ratio of the two analytes and consequently the amount of Gly-α-L-Asp-L-PheNH$_2$ and Gly-α-D-Asp-L-PheNH$_2$ were determined.

4.3.2 Analysis of L-Phe-β-L-Asp-GlyNH$_2$, L-Phe-α-L-Asp-GlyOH and L-Phe-α-D-Asp-GlyOH

The best separation of L-Phe-β-L-Asp-GlyNH$_2$, L-Phe-α-L-Asp-GlyOH and L-Phe-α-D-Asp-GlyOH was achieved by the addition of CM-β-CD to the phosphate buffer. As already discussed for the use of S-β-CD, the internal standard was not detected under these conditions. While L-Phe-α-L-Asp-GlyOH

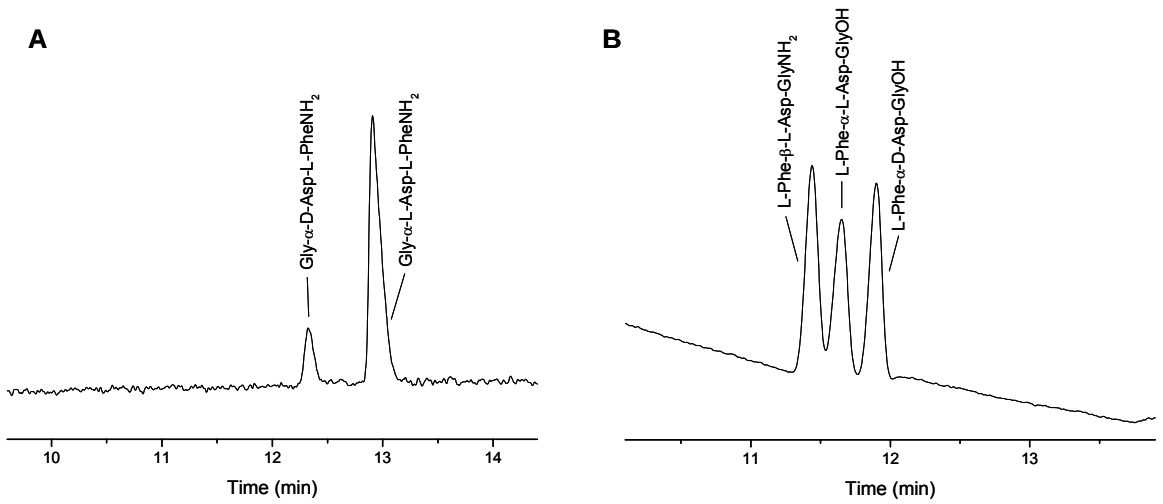

Figure 6: Separation of the reference substances Gly-α-L-Asp-L-PheNH$_2$ and Gly-α-D-Asp-L-PheNH$_2$ in CE-System 2 (A) and L-Phe-β-L-Asp-GlyNH$_2$, L-Phe-α-L-Asp-GlyOH and L-Phe-α-D-Asp-GlyOH in CE-System 3 (B). Analysis conditions in (A): 50 mM phosphate buffer, pH 3.0, 3 mg/ml S-β-CD. Analysis conditions in (B): 50 mM phosphate buffer, pH 3.0, 16 mg/ml CM-β-CD, containing 5% acetonitrile. For details see Materials and Method, paragraph 10.4.

and L-Phe-α-D-Asp-GlyOH are diastereomers, L-Phe-β-L-Asp-GlyNH$_2$ is a different peptide. It possesses an additional amide group which absorbs at 215 nm. For this reason, the UV-absorption properties of the three substances can not be considered identical and the amount of the analytes could not be calculated from the peak-area ratio as discussed for the analysis of Gly-α-L-Asp-L-PheNH$_2$ and Gly-α-D-Asp-L-PheNH$_2$ (see paragraph 4.3.1).

The addition of an organic solvent such as acetonitrile (ACN) causes a decrease of the viscosity of the BGE and a stronger EOF. As a consequence, negatively charged complexes such as those between pAMBA and CDs can be transported to the cathode and can be detected after the EOF. Different amounts of ACN in the phosphate/CM-β-CD buffer were tested. The addition of 5% acetonitrile (see CE-System 3, Materials and Methods) allowed the detection of pAMBA after the EOF with a still acceptable resolution of the three peptides (see Figure 6B).

4.4 Analysis of the diketopiperazine derivatives cyclo(Phe-Asp) and cyclo(Gly-Asp)

In incubations at pH 2 significant formation of the diketopiperazine derivates cyclo(Phe-Asp) and cyclo(Gly-Asp) was observed. These compounds were not detected at first by analysis with CE-System 1. In fact, at a pH value of 3.0 they are partially negatively charged and migrate after the EOF. During CE-MS analysis (see paragraph 6.1), the phosphate buffer had to be replaced by an

ammonium formate/acetonitrile buffer. As already discussed in paragraph 4.3.2, the presence of a low viscous organic solvent like acetonitrile increases the EOF and allows the detection of negatively charged substances, which reach the detection window after the EOF. Separations in the organic buffer were faster at the expense of resolution compared to phosphate buffer. A 50 mM formate buffer, pH 3.0, containing 10% acetonitrile (CE-System 4, see Materials and Methods, paragraph 10.4) was used for the analysis of cyclo(Phe-Asp) and cyclo(Gly-Asp). Figure 7A shows the separation of the reference substances cyclo(Phe-Asp) and cyclo(Gly-Asp) which migrate after the EOF at 11.9 and 12.5 min respectively.

4.5 Analysis of the degradation products after incubation of Phe-Asu-GlyOH

In order to investigate the Asp enantiomerization separately from the other degradation reactions, the model compound Phe-Asu-GlyOH was incubated at pH 10 at 30°C. A suitable system for the separation of the degradation products had to be developed, because Phe-Asu-GlyOH and L-Phe-β-L-Asp-GlyOH could not be resolved in CE-System 1. Changes in the pH value of the phosphate buffer were first tested. Resolution of the critical pair Phe-Asu-GlyOH/L-Phe-β-L-Asp-GlyOH was achieved at a pH value of 2.7 or lower. However, under these conditions separation of Phe-Asu-GlyOH and L-Phe-β-D-Asp-GlyOH was not possible. Partial separation of the three substances was obtained at pH 2.9. Because it has been shown that lower capillary temperatures can result in an enhancement of peptide resolutions [54], different temperatures were tested. Separation of all substances was achieved in phosphate buffer, pH 2.9, at a temperature of 15°C (CE-System 5, Materials and Methods, paragraph 10.4). Separation of the reference substances is shown in Figure 7B.

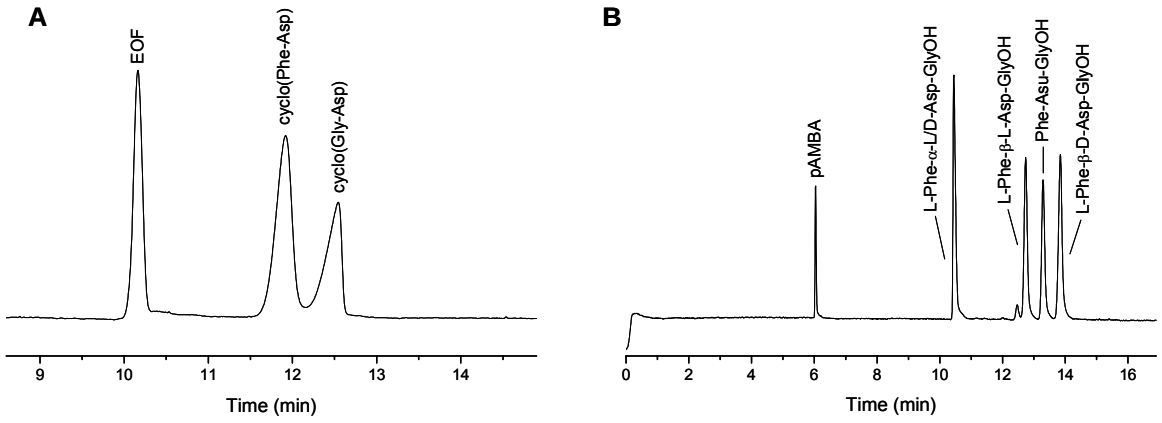

Figure 7: Separation of the reference substances cyclo(Phe-Asp) and cyclo(Gly-Asp) in CE-System 4 (A) and of the standards corresponding to the degradation products arising after incubation of Phe-Asu-GlyOH at pH 10 in CE-System 5 (B). Analysis conditions in (A): 50 mM formic acid, pH 3.0 (ammonia), containing 10% acetonitrile. Analysis conditions in (B): 50 mM phosphate buffer, pH 2.9. For details see Materials and Method, paragraph 10.4.

5. Analysis of degradation products by RP-HPLC

RP-HPLC is the most commonly used technique for peptide and protein analysis. The partitioning separation mechanism of RP-HPLC mainly based on the hydrophobic character of the analytes can be considered orthogonal to the separation mechanism of CE based on the charge-to-mass ratio. Consequently, differences in the elution and migration order as well as in the resolution of the compounds can be expected [51]. Because HPLC is a well-established technique, most of the studies on the isomerization and enantiomerization of Asp were conducted with this method [6, 8, 10, 14, 17, 18, 32]. In this work a gradient RP-HPLC for the analysis of the model aspartyl peptides Phe-Asp-$GlyNH_2$ and Gly-Asp-$PheNH_2$ and their degradation products was developed as an alternative to CE. A direct comparison of the two methods can be interesting to understand advantages and disadvantages of both techniques.

5.1 Analysis by RP-HPLC in water/acetonitrile

The RP-HPLC method that was developed consisted of a gradient of two eluents. The gradient utilising eluent A (0.1% TFA in water) and eluent B (0.1% TFA in water/acetonitrile 5:95 v/v) was optimized for each sample. Figure 8A shows the separation of the degradation products of Phe-Asp-$GlyNH_2$ after incubation at pH 2. This was achieved with a gradient of 7-20% eluent B within 15 min (HPLC-System 1a, see Material and Methods, paragraph 10.5). All substances that were detected by CE could also be analyzed by RP-HPLC, except for $GlyNH_2$ whose peak was obscured by the tailing of the neighbouring peak corresponding to PheOH. Generally, the amidated peptides had shorter retention times compared to the corresponding peptides with free carboxyl groups. The succinimidyl intermediates Phe-Asu-$GlyNH_2$ and Phe-Asu-GlyOH eluted after the corresponding aspartyl peptides because of the higher hydrophobicity of the succinimide moiety compared to Asp. The diketopiperazine cyclo(Phe-Asp) had the longest retention time.

The best separation of the degradation products in incubations of Gly-Asp-$PheNH_2$ at pH 2 was achieved with a gradient of 1-39% eluent B within 20 min (HPLC-System 1c, see Material and Methods, paragraph 10.5). A chromatogram of an incubated sample is depicted in Figure 8C. As already observed for Phe-Asp-$GlyNH_2$, the amide eluted before the deamidated peptide and the succinimide had the longest retention time. Due to their high polarity, Gly-Asp and cyclo(Gly-Asp) did not interact with the stationary phase and eluted in the solvent front.

A representative chromatogram of the degradation products of Phe-Asp-$GlyNH_2$ after incubation at pH 10 is shown in Figure 8B. The best separation was achieved with a gradient of 2-13% eluent B within 30 min (HPLC-System 1b, see Material and Methods, paragraph 10.5). Except for the

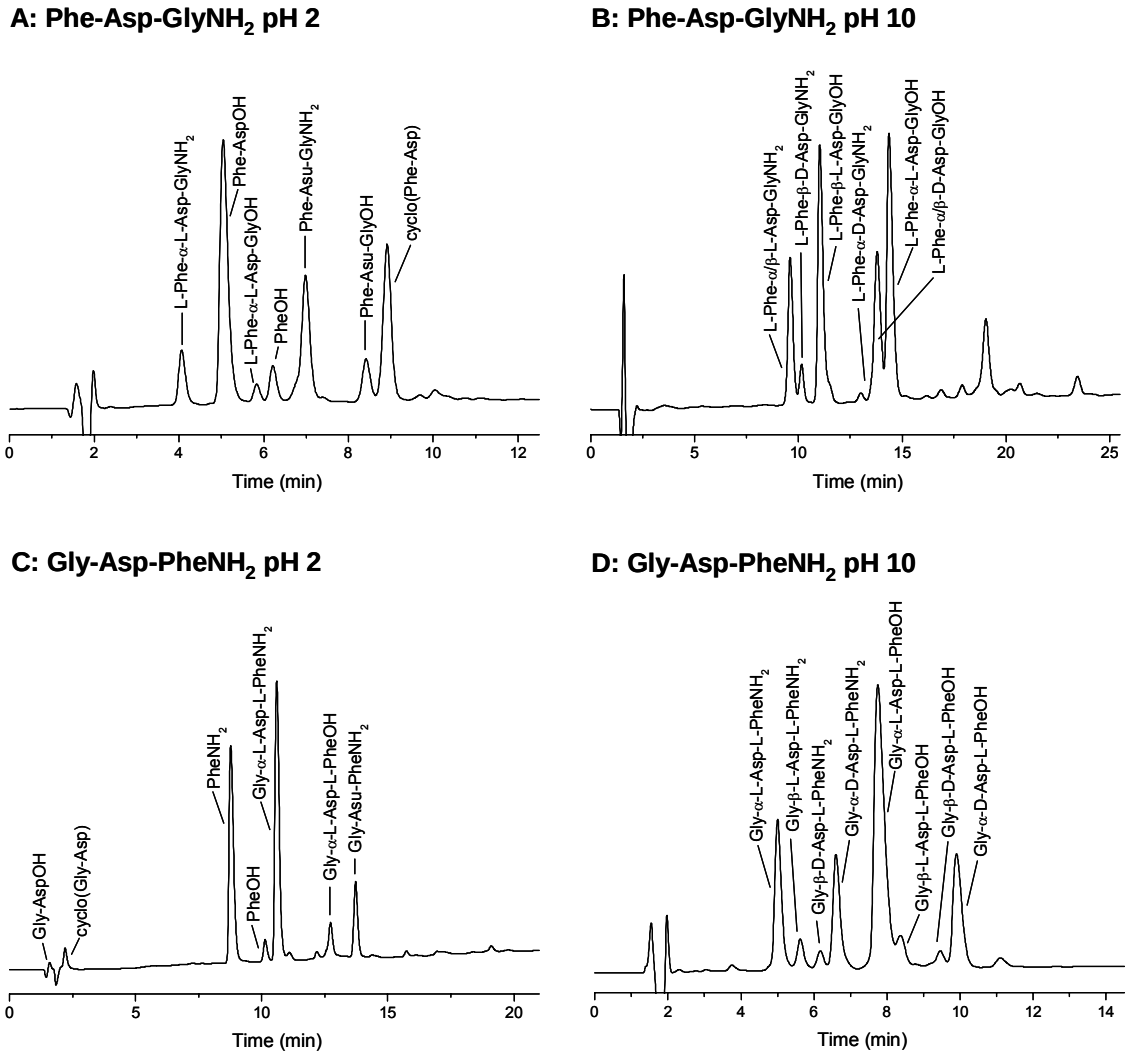

Figure 8: Chromatograms of Phe-Asp-GlyNH$_2$ incubated at pH 2 for 24 h (A) and at pH 10 for 48 h (B) and of Gly-Asp-PheNH$_2$ incubated at pH 2 for 24 h (C) and at pH 10 for 48 h (D). Analysis conditions: mobile phase gradient 7-20% B within 15 min (A), 2-13% B within 30 min (B), 1-39% B within 20 min (C) and 10-20% B within 15 min (D). Eluent A was 0.1% TFA in water and eluent B was 0.1% TFA in water-acetonitrile (5:95 v/v). Flow: 0.2 ml/min. Detection at 215 nm. For details see HPLC-System 1a,b,c, and d in Materials and Methods, paragraph 10.5.

diastereomeric pair L-Phe-α-L-Asp-GlyOH/L-Phe-α-D-Asp-GlyOH the L-Asp-containing peptides eluted faster than the corresponding D-Asp peptides. The isomeric pairs L-Phe-α-L-Asp-GlyNH$_2$/ L-Phe-β-L-Asp-GlyNH$_2$ and L-Phe-α-D-Asp-GlyOH/L-Phe-β-D-Asp-GlyOH could not be resolved in water-acetonitrile mixtures containing TFA.

Separation of the degradation products of Gly-Asp-PheNH$_2$ after incubation at pH 10 was achieved with a gradient of 10-20% of eluent B within 15 min (see Figure 8D). In contrast to Phe-Asp-GlyNH$_2$, all isomers of Gly-Asp-PheNH$_2$ could be separated. The amide peptides eluted before the deamidated compounds and L-Asp containing peptides eluted faster than the corresponding D-Asp peptides.

5.2 Analysis by RP-HPLC in phosphate buffer

The isomeric pairs L-Phe-α-L-Asp-GlyNH_2/L-Phe-β-L-Asp-GlyNH_2 and L-Phe-α-D-Asp-GlyOH/L-Phe-β-D-Asp-GlyOH could not be resolved in water-acetonitrile mixtures containing TFA. Kaneda et al. [55] reported on the separation of isomeric peptides of αA-crystallin using 15 mM phosphate buffer instead of aqueous TFA. Subsequently, various isocratic acetonitrile-phosphate buffer mixtures were investigated as mobile phases. Partial resolution of L-Phe-α-L-Asp-GlyNH_2 and L-Phe-β-L-Asp-GlyNH_2 could be achieved at pH 5.0 with an 85:15 (v/v) mixture phosphate buffer/acetonitrile. Baseline resolution of L-Phe-α-D-Asp-GlyOH and L-Phe-β-D-Asp-GlyOH was achieved at pH 4.0 under otherwise identical conditions. Figure 9 shows the chromatogram of a Phe-Asp-GlyNH_2 sample incubated at pH 10 for 48 h and analyzed with an acetonitrile/phosphate buffer, pH 5.0, gradient (2% - 13% eluent B within 30 min, HPLC-System 2, see Materials and Methods, paragraph 10.5). The compounds that were not separated in the water-TFA/acetonitrile gradient could be resolved in the phosphate system. However, only partial resolution of the pair L-Phe-α-L-Asp-GlyOH and L-Phe-β-D-Asp-GlyOH was achieved. At pH 5.0 all peptides with free carboxyl groups eluted faster than the amidated peptides, because of the higher polarity of the deprotonated terminal carboxyl group.

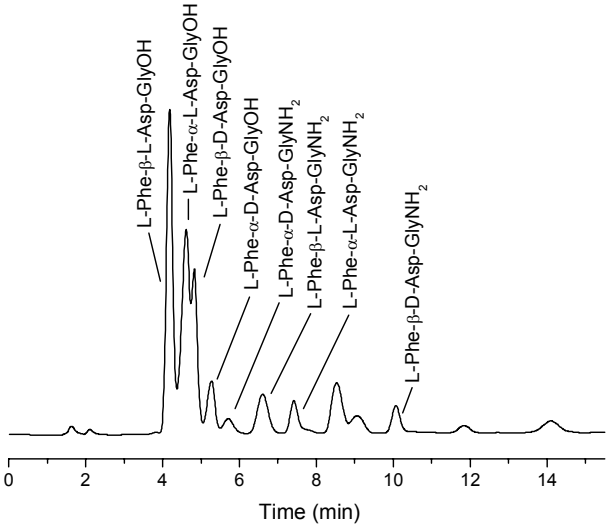

Figure 9: Chromatogram of Phe-Asp-GlyNH_2 incubated at pH 10 for 48 h and analyzed with HPLC-System 2. Analysis conditions: mobile phase gradient 2-13% eluent B within 30 min. Eluent A was 15 mM aqueous phosphate, pH 5.0, and eluent B was water-acetonitrile (5:95 v/v). Flow: 0.2 ml/min. Detection at 215 nm. For details see Materials and Methods, paragraph 10.5.

5.3 Comparison between CE and RP-HPLC

RP-HPLC is a well-established and the most frequently used technique for peptide analysis. In contrast, CE is not yet established in all laboratories, although in the last years it has been recognized as a fast and simple technique for the separation of peptides including stereoisomer analysis [45-47, 53]. A disadvantage of CE in comparison to HPLC is the strong dependence of the migration time on the electroosmotic flow (EOF). Changes in the chemistry of the capillary wall can affect the velocity of the EOF profoundly and subsequently the migration time. On the other hand, the EOF is responsible for the flat profile of the flow in CE, since the driving force is uniformly distributed along the capillary. The flat flow profile is advantageous because it does not directly contribute to the dispersion of the solute zones. This is in contrast to that generated by an external pump in HPLC which yields a laminar or parabolic flow profile.

Compared to HPLC, method development in CE is more rapid. This involves the use of various BGEs (composition of the buffer, pH, additives, temperature), whereas in HPLC the approach normally is to use various columns with different stationary phases. As a consequence, the optimization of the separation parameters is much faster and cheaper in CE. Furthermore, high separation can be achieved in CE. Another advantage of CE is that it requires much smaller sample and reagent volumes. Sample consumption is normally in the order of nanoliters in CE and microliters in HPLC. If UV detection is applied, CE is generally less sensitive than HPLC. This is due to the short optical path-length afforded by the small internal diameter of the capillary. A significant advantage of HPLC is the ability to collect fractions of even minor peaks for further characterization.

In incubations at pH 2, all compounds analyzed by RP-HPLC could also be detected by CE except for the diketopiperazines cyclo(Phe-Asp) and cyclo(Gly-Asp) which migrated as a anionic compounds behind the EOF at pH 3.0. However, these compounds were analysed by switching to a formate buffer, pH 3.0, containing 10% acetonitrile (see Figure 7A). On the other hand, Gly-Asp and cyclo(Gly-Asp) eluted in the solvent front in RP-HPLC and can, therefore, not be reliably analyzed in this system (Figure 8C). Moreover, $GlyNH_2$ could not be detected in RP-HPLC because its small peak was obscured from the tailing of the neighbouring peak corresponding to PheOH. As pointed out above, the analytes had different migration orders compared to the elution orders in RP-HPLC due to the different separation mechanisms of both techniques. Interestingly, the deamidated peptides displayed longer migration times in CE compared to the *C*-terminal amidated analogs similarly to RP-HPLC using aqueous TFA in the mobile phase where the amides eluted faster than the corresponding peptides with a free terminal carboxyl group.

CE analysis of the pH 10 incubations revealed that the diastereomeric pairs Phe-α-L/D-Asp-GlyOH and Gly-α-L/D-Asp-$PheNH_2$ could not be resolved using a pH 3.0 run buffer. These pairs could be easily resolved by RP-HPLC. However, while all isomers of the Gly-Asp-Phe series could be at least

partially separated by RP-HPLC, the α-Asp and β-Asp pairs Phe-α/β-L-Asp-GlyNH_2 and Phe-α/β-D-Asp-GlyOH could not be resolved by RP-HPLC using TFA in water-acetonitrile. As discussed in paragraph 5.2, resolution of these compounds was achieved using a phosphate buffer, pH 5.0, instead of aqueous TFA in the mobile phase. The use of CDs allowed the separation of those substances which could not be resolved by CE in phosphate buffer, pH 3.0.

Concluding, both methods allowed the analysis of most compounds. While two pairs of diastereomers could not be separated by CE, RP-HPLC was less efficient resolving peptides containing α-Asp and β-Asp linkages. Overall, separations that were difficult with one technique proved to be easily achieved by the other method illustrating the complementary of HPLC and CE in peptide analysis.

6. Identification of degradation products by on-line mass spectrometry

In both, CE and RP-HPLC, on-line MS studies were performed in order to confirm the identification of the compounds derived from co-injection of reference substances and primarily to identify unknown products. Peptide fragments were labelled according to standard rules [56, 57]. A scheme of the fragments arising from MS analysis of peptides is shown in Figure 10.

6.1 CE-MS/MS

Coupling of CE with mass spectrometry is a useful tool to characterize peptides. This detection allows high selectivity and sensitivity in addition to providing information about the mass and the structure of the analytes. For electrospray ionization mass spectrometry (ESI) sheathless interface, liquid junction and sheath-liquid interface have been applied [58-61]. A scheme of the coaxial sheat-flow interface is shown in Figure 11. The sheath liquid is infused into the ESI source at a constant rate trough the coaxial sheath capillary which surrounds the end of the separation capillary. The sheath liquid mixes with the separation buffer as it elutes from the tip of the CE capillary, thus providing the necessary

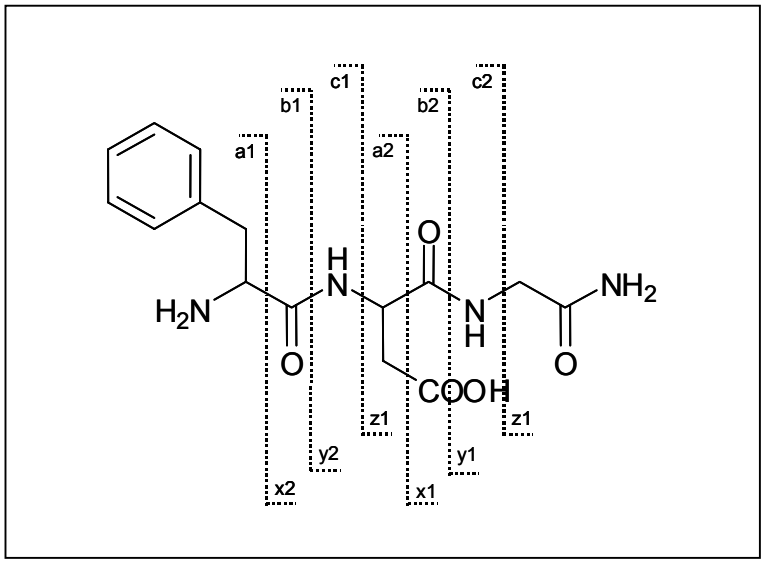

Figure 10: Schematic representation of the fragments arising from MS analysis of Phe-Asp-GlyNH_2 according to [56, 57]. The three possible cleavage points of the peptide backbone are called a, b and c when the charge is retained at the *N*-terminal fragment of the peptide and x, y and z when the charge is retained by the *C*-terminal fragment.

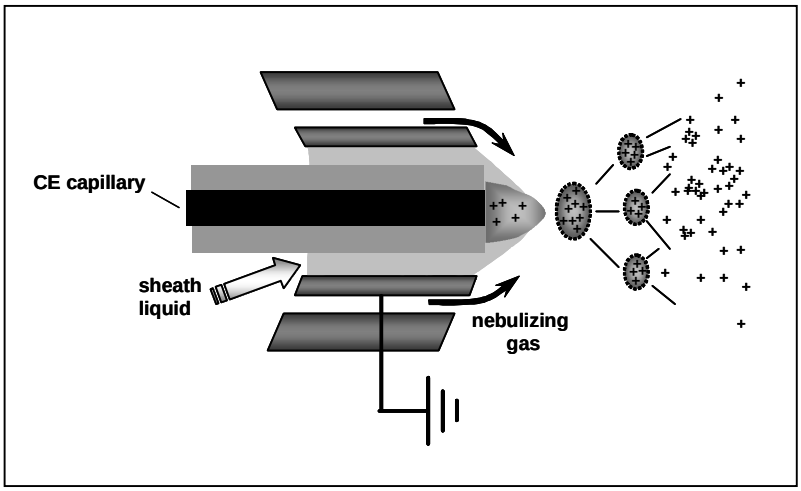

Figure 11: Schematic representation of the CE-MS sprayer coaxial sheat-flow interface.

electrical contact between the ESI needle and the CE buffer. Recent studies show the robustness and competitive sensitivity of the sheath-liquid coupling [62]. The number of applications of CE-MS is still limited although a broad range of applications have been demonstrated, including studies of protein identification [63, 64], peptide glycosylation [65, 66] and peptide phosphorylation [67]. CE-MS has also been employed to study the degradation of peptides [68].

MS detection in CE was carried out with electrospray ionization. Tandem mass spectrometry was performed. Analysis of daughter fragments arising from fragmentation of the $[M+H]^+$-ion gave additional information about the structure of the compounds. Because of its low volatility, the aqueous phosphate buffer used for the CE-UV analysis is not compatible with MS detection. For this reason, an ammonium formate buffer, pH 2.9, containing 10% v/v acetonitrile was used as BGE for CE-MS analysis. Due to the increased EOF, separations in this buffer were faster at the expense of resolution compared to phosphate buffer. However, the specificity of the MS detection compensated for the loss of resolution.

All compounds were detected as $[M+H]^+$-ions, as summarized in Table 1. Representative MS/MS spectra of the aspartyl succinimide Phe-Asu-GlyNH_2 and Phe-Asu-GlyOH derivatives are shown in Figure 12. These were identified from the $[M+H]^+$-ions at *m/z* 319 (amide) and *m/z* 320 (acid) respectively. Tandem mass spectrometry of these ions yielded predominantly a fragment at *m/z* 120 which can be assigned to the a_1 fragment $[C_8H_{10}N]^+$ resulting from fragmentation of the Phe CH-CO bond with retention of the charge in the amino terminal fragment. The fragments at *m/z* 302 and *m/z* 245 can be assigned to the $[M\text{-}NH_2]^+$-ion and the $[b_2\text{-}H_2O]^+$-ion, respectively. The peaks at *m/z* 341 and *m/z* 356 in the spectrum of the amide represent the sodium and the potassium adducts of the molecular ion.

Table 1: $[M+H]^+$-ions of the substances detected after incubations of Phe-Asp-GlyNH_2 and Gly-Asp-PheNH_2. The compounds were observed either from incubations at pH 2 or form incubations at pH 10.

Sequence	Peptide/amino acid	$[M+H]^+$	Sequence	Peptide/amino acid	$[M+H]^+$
Phe-Asp-Gly	Phe-Asp-GlyNH_2	337	**Gly-Asp-Phe**	Gly-Asp-PheNH_2	337
	Phe-β-Asp-GlyNH_2	337		Gly-β-Asp-PheNH_2	337
	Phe-Asp-GlyOH	338		Gly-Asp-PheOH	338
	Phe-β-Asp-GlyOH	338		Gly-β-Asp-PheOH	338
	Phe-Asu-GlyNH_2	319		Gly-Asu-PheNH_2	319
	Phe-Asu-GlyOH	320		Gly-Asu-PheOH	320
	Phe-AspOH	281		Gly-AspOH	191
	cyclo(Phe-Asp)	263		cyclo(Gly-Asp)	173
	PheOH	166		PheOH	166
	PheNH_2	165		PheNH_2	165

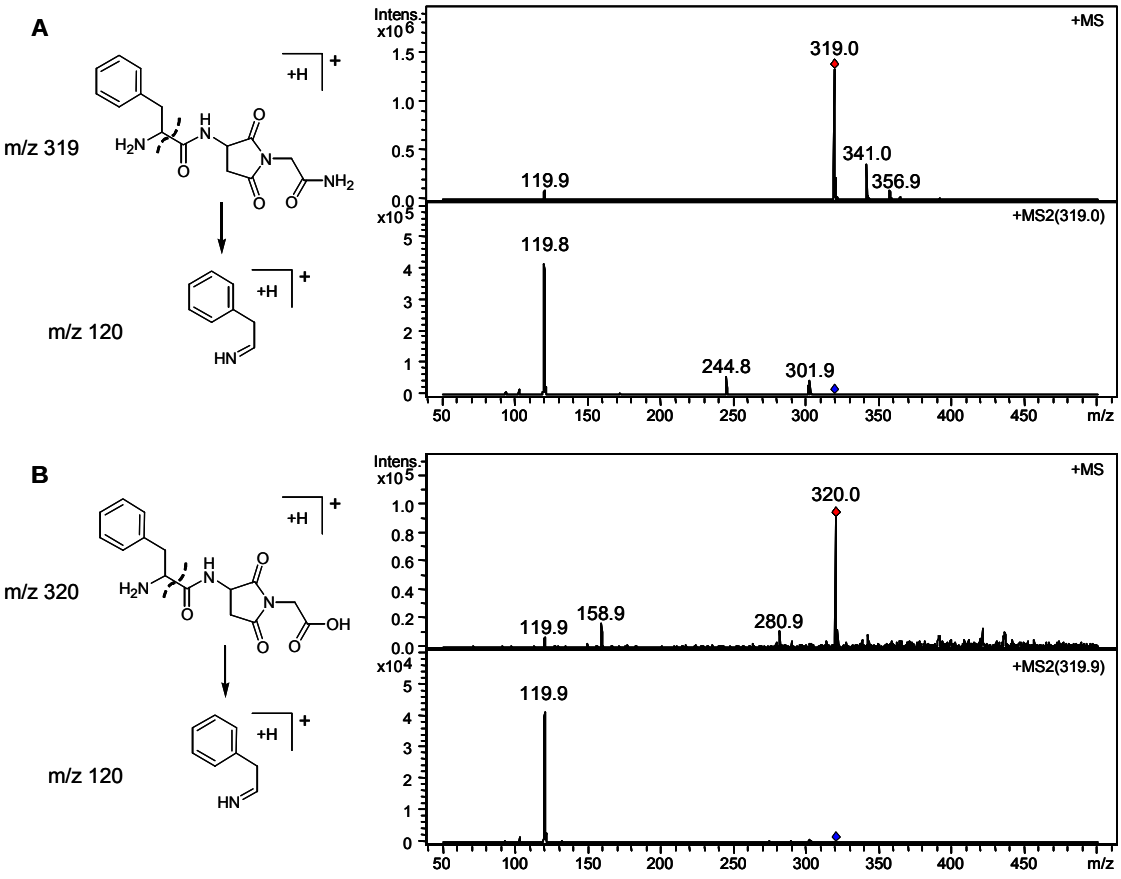

Figure 12: Electrospray tandem mass spectra of the Phe-Asu-GlyNH_2 ion at *m/z* 319 (A) and of the Phe-Asu-GlyOH ion at *m/z* 320 (B).

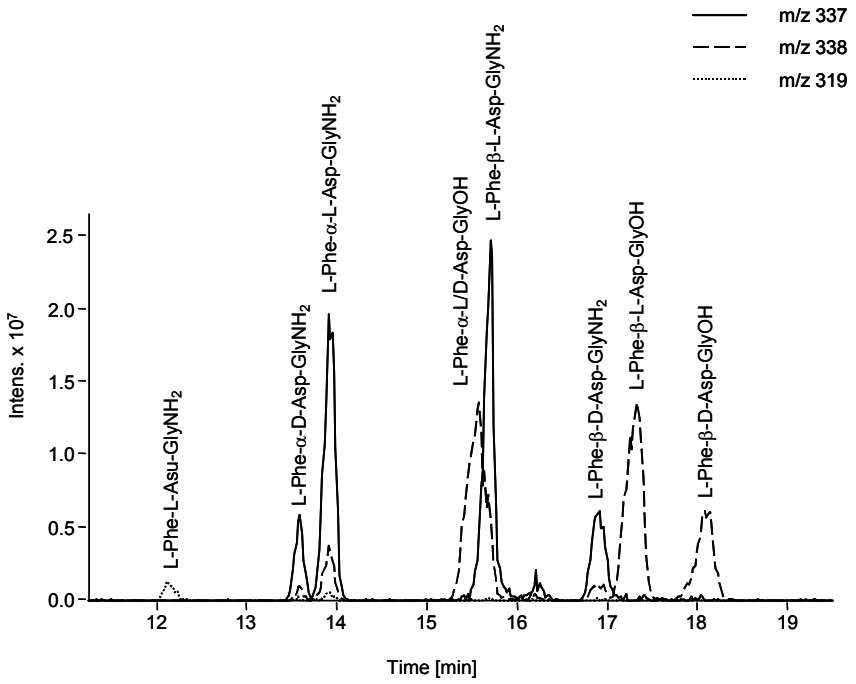

Figure 13: CE-MS traces of incubations of Phe-Asp-$GlyNH_2$ at pH 10 after 24 h.

The mass traces of the CE-MS analysis of an incubation of Phe-Asp-$GlyNH_2$ at pH 10 are shown in Figure 13. The trace of the ion at *m/z* 337 (solid line) displayed four peaks corresponding to the α-L-Asp peptide, the β-L-Asp peptide and their D-Asp containing diastereomers, which are separated under the experimental conditions. The small peak of the trace of the ion at *m/z* 319 at 12.1 min corresponds to the cyclic imide Phe-Asu-$GlyNH_2$ (dotted line). Moreover, four peaks with *m/z* 338 could be observed (hatched line). These peaks correspond to the $[M+H]^+$-ions of the free acid forms of the tripeptides resulting from deamidation of the terminal $GlyNH_2$ residue.

Tandem mass spectrometry was used to assign the peaks at *m/z* 337 and *m/z* 338 to the α-Asp and β-Asp series. Mass spectrometric differentiation of α-Asp and β-Asp peptides has been reported by Lloyd and coworkers [69], who noticed differences in the loss of CO from aspartyl fragment ions. Different relative intensities of b and y fragments of a tryptic heptapeptide of recombinant human stem cell factor depending on the presence of α-Asp or β-Asp linkages have been observed [70]. Lehmann and coworkers [71] distinguished α-Asp and β-Asp peptides based on the decrease of the b/y ratio of b- and y-ions generated by electrospray tandem mass spectrometry.

Figure 14 summarizes the MS/MS spectra of the peaks of the traces at *m/z* 337 and *m/z* 338 in the analysis of the incubation of Phe-Asp-$GlyNH_2$ at pH 10 represented in Figure 13. Differences in the daughter ions depending on the presence of α-Asp and β-Asp linkage can be noticed. Beside the ubiquitous b_3 fragments at *m/z* 319 or *m/z* 320, MS/MS of L-Phe-α-D-Asp-$GlyNH_2$ and L-Phe-α-L-Asp-

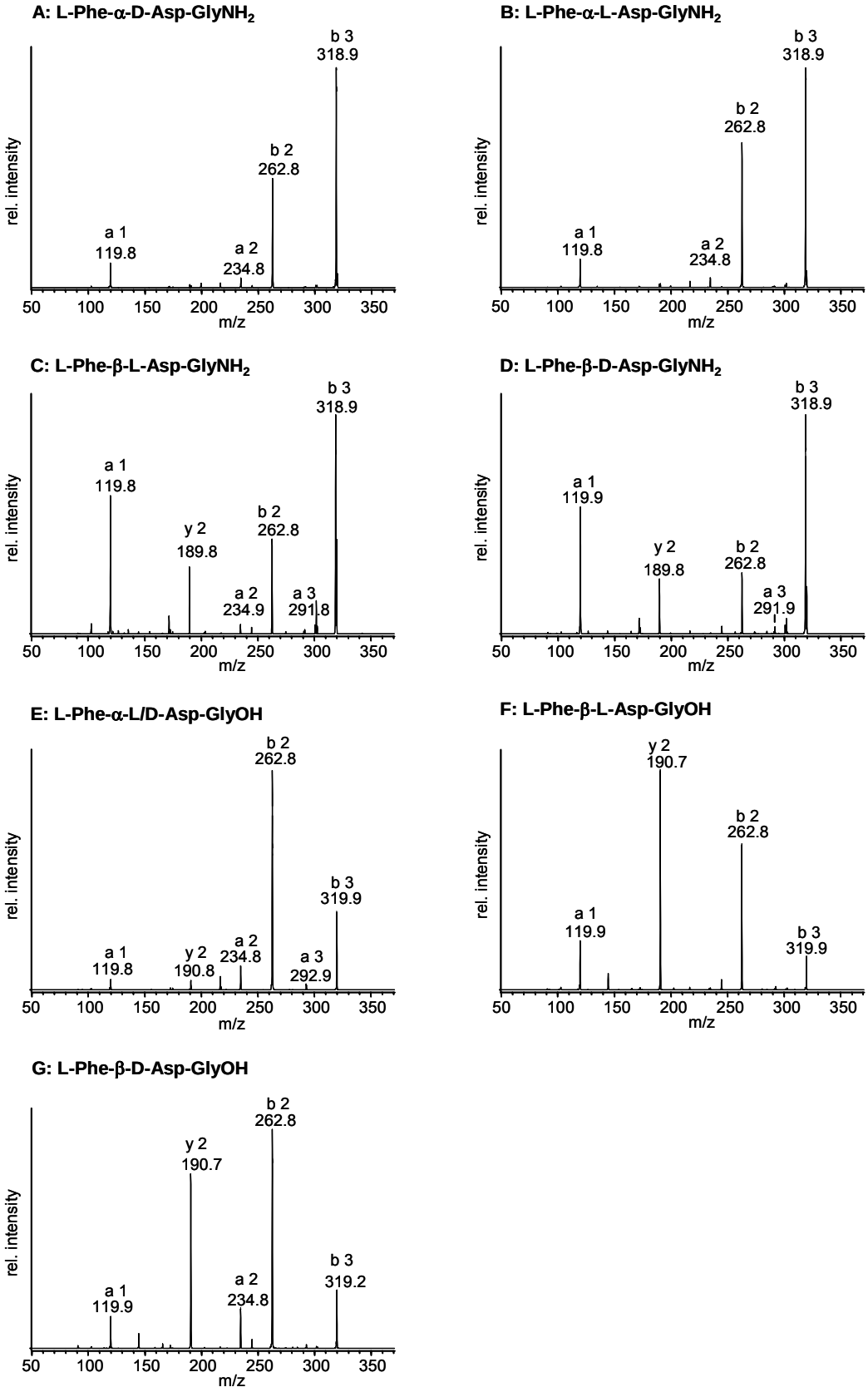

Figure 14: MS/MS spectra of a CE-MS/MS analysis of an incubation of Phe-Asp-GlyNH$_2$ at pH 10 after 24h, under identical conditions as shown in Figure 13.

$GlyNH_2$ showed a dominant b_2 fragment ion at *m/z* 263 while the y_2 fragment ion at *m/z* 190 was hardly detectable. Low-abundant a_1 and a_2 fragments at *m/z* 120 and *m/z* 235, respectively, could be observed. In contrast, the intensity of the y_2 fragment ion in the daughter spectra of Phe-β-L-Asp-$GlyNH_2$ and L-Phe-β-D-Asp-$GlyNH_2$ was similar to that of the b_2 fragment ion. In addition, the a_1 fragment $[C_8H_{10}N]^+$ at *m/z* 120 exhibited a higher abundance compared to the peptides containing α-Asp. Similar results were obtained for the analysis of the corresponding reference substances. According to the literature [71], a decrease of the b/y ratio of complimentary b- and y-ions allowed to discriminate between α-Asp and β-Asp peptides.

In the same way the α-Asp and β-Asp form of the deamidated peptides could be assigned to the peaks observed for the trace of the ion at *m/z* 338 (Figures 14E, 14F and 14G). All spectra showed a b_3 fragments at *m/z* 320 due to the loss of water from the $[M+H]^+$-ion and a a_1 fragment at *m/z* 120 corresponding to $[C_8H_{10}N]^+$. Peptides containing α-Asp displayed a highly abundant b_2 fragment ion at *m/z* 263 while the y_2 fragment at *m/z* 191 had very low intensity. In contrast, the spectra of the daughter ions of β-Asp containing peptides showed higher abundant y_2 fragment ions at m/z 191. In addition, the a_1 fragments at *m/z* 120 exhibited a higher relative intensity if compared to the same fragment of α-Asp containing peptides.

Similar results were obtained for the incubations of the peptide with inverse amino acid sequence Gly-Asp-Phe. Figure 15 depicts the MS/MS spectra of the traces at *m/z* 337 and *m/z* 338 in the analysis of an incubation of Gly-Asp-$PheNH_2$ at pH 10. Because of the increased EOF in the formate/acetonitrile buffer, resolution of the diastereomeric pairs Gly-β-L-Asp-L-$PheNH_2$/Gly-β-D-Asp-L-$PheNH_2$ and Gly-α-L-Asp-L-PheOH/Gly-α-D-Asp-L-PheOH, which could be separated in phosphate buffer, was not achieved. All spectra show intensive y_1 fragments at *m/z* 166 and *m/z* 165 for the acid and the amide, respectively, and the ion at *m/z* 120 which can be assigned to the fragment $[C_8H_{10}N]^+$ confirming the presence of Phe in the peptide structure. All spectra show the b_3 fragment at *m/z* 320 and *m/z* 319, corresponding to the loss of water. Moreover loss of NH_3 was observed for the amide structure (fragment at *m/z* 320). Differences in the fragmentation patterns of Gly-α-Asp-Phe and Gly-β-Asp-Phe are small if compared to those of the peptides with inverse amino acid sequence. Apparently, the tendency to form ions with charge retention at the *N*-terminus is lower, possibly due to the fact that Gly is the *N*-terminal amino acid. A small relative increase of the b_2 fragment ion at *m/z* 173 and of the ion at *m/z* 274 can be observed in case of the presence of a β-Asp linkage. In the spectra of β-Asp containing peptides fragments at *m/z* 292 and *m/z* 281 are also detected. The fragment at *m/z* 292 can be attributed to the loss of CO and H_2O and CO and NH_3 from Gly-α-Asp-PheOH and Gly-β-Asp-$PheNH_2$, respectively. CE-MS/MS analysis of the corresponding reference substances gave similar results. Although not as distinct as for the peptides with *N*-terminal Phe the observed differences in the MS/MS spectra allowed the assignment of the peptides to the α-Asp and β-Asp series.

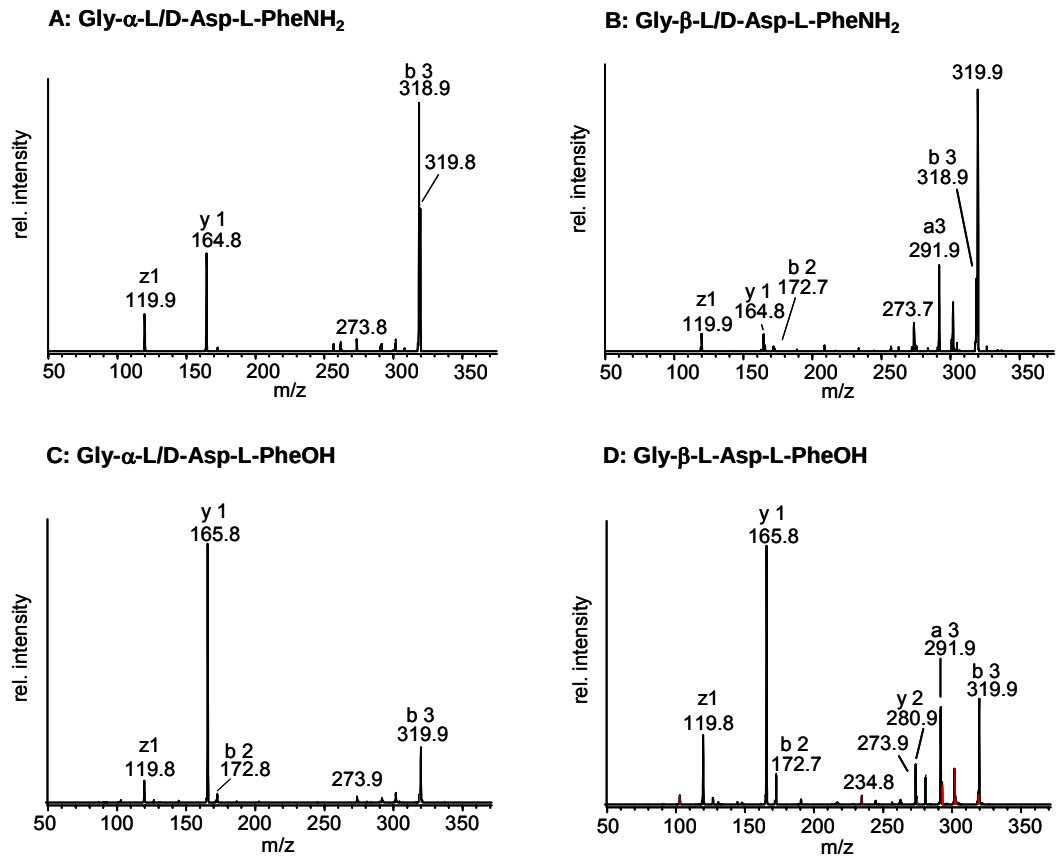

Figure 15: MS/MS spectra of a CE-MS/MS analysis of an incubation of Gly-Asp-PheNH$_2$ at pH 10 after 24h.

Reliable differences in the MS and MS/MS spectra of D-Asp and L-Asp containing peptides could not be observed. Thus identification of diastereomers was performed by comparison with synthetic peptides containing Asp with known configuration.

6.2 HPLC-MS

Chromatographic separations combined with MS detection are nowadays a standard analytical tool. HPLC-MS combines the good efficiency of HPLC with the high sensitivity and selectivity of MS. This technique is widely applied in many areas of environmental, pharmaceutical and biochemical analysis [72]. Many ionization methods such as electron impact ionization, chemical ionization, ion evaporation and fast atom bombardment were used in HPLC-MS [72]. From the wide variety of interfaces developed over the years basically only atmospheric pressure ionization techniques (API) are nowadays commonly applied [73]. For peptide analysis the most used method of ionization is atmospheric pressure electrospray ionization, in which biomolecules are detected after soft ionization without significant fragmentation.

HPLC-MS experiments were performed with an API single quadrupole MS system with turbo ion spray interface. Tandem mass spectrometry was not possible with the present instrument. Nevertheless, information about the structure of the analysed compounds could be achieved from the fragmentation pattern of the substances. The water/acetonitrile gradient used in RP-HPLC is compatible with MS detection and could be used for HPLC-MS analysis. Because of the high flow rate during HPLC separation, the flow was split 1:4 before MS detection.

The results obtained by HPLC-MS were similar to those obtained by CE-MS. Figure 16 shows the mass spectra of representative substances after RP-HPLC-MS detection. All peptides were detected as $[M+H]^+$-ions (see Table 1). As it can be seen in Figures 16A and 16C, the native peptides could be easily discriminated from their deamidated forms by the molecular ions at *m/z* 337 (amides) and *m/z* 338 (carboxylic acid).

In addition, α-Asp and β-Asp peptides could be distinguished by careful analysis of the fragmentation pattern as shown for L-Phe-α-L-Asp-$GlyNH_2$ (Figure 16A) and L-Phe-β-L-Asp-$GlyNH_2$ (Figure 16B). Besides the $[M+H]^+$- and $[M+Na]^+$-ions the spectra displayed the a_1 ion at *m/z* 120, the y_2 ion at *m/z* 190 and the b_2 ion at *m/z* 263. The α-Asp peptide exhibited a more intense b_2 fragment ion and a low abundant y_2 fragment ion, while in the case of the β-Asp peptide the b_2 ion had lower intensity if compared to the y_2 fragment ion (Figures 16A and 16B). L-Phe-α-L-Asp-GlyOH and L-Phe-β-L-Asp-GlyOH (Figures 16C and 16D) displayed a similar fragmentation pattern, with the a_1 ion at *m/z* 120, the y_2 ion at *m/z* 191 and the b_2 ion at *m/z* 263. Both the amidated and the deamidated form of the α-Asp peptides showed the x_2 ion at *m/z* 217 and the a_2 ion at *m/z* 235, which were not present in the spectra of the corresponding β-Asp peptides. In order to confirm these results, reference substances were injected. The MS spectra obtained for α-Asp and β-Asp reference peptides were similar to those obtained for incubated samples. As already discussed in paragraph 6.1, α-Asp and β-Asp linkages could be discriminated from the b/y ratio of complimentary b- and y-ions.

As in CE-MS already observed, differences in the mass spectra of α- and β-Asp peptides derived from Gly-Asp-$PheNH_2$ were less pronounced. All spectra showed an intense a_1 fragment at m/z 120, an intense y_1 fragment at m/z 166, and a b_3 fragment at m/z 319 or m/z 320 for the native peptide and its deamidated form, respectively (Figures 16E and 16F). Less intense ions at *m/z* 173 and *m/z* 281 corresponding to the fragments b_2 and y_2 respectively could be detected in both α- and β-Asp peptides, the b_2 fragment having a higher intensity in case of the α linkage. As already discussed for CE-MS analysis, the tendency to form ions with charge retention at the *N*-terminus is lower for the Gly-Asp-$PheNH_2$ series.

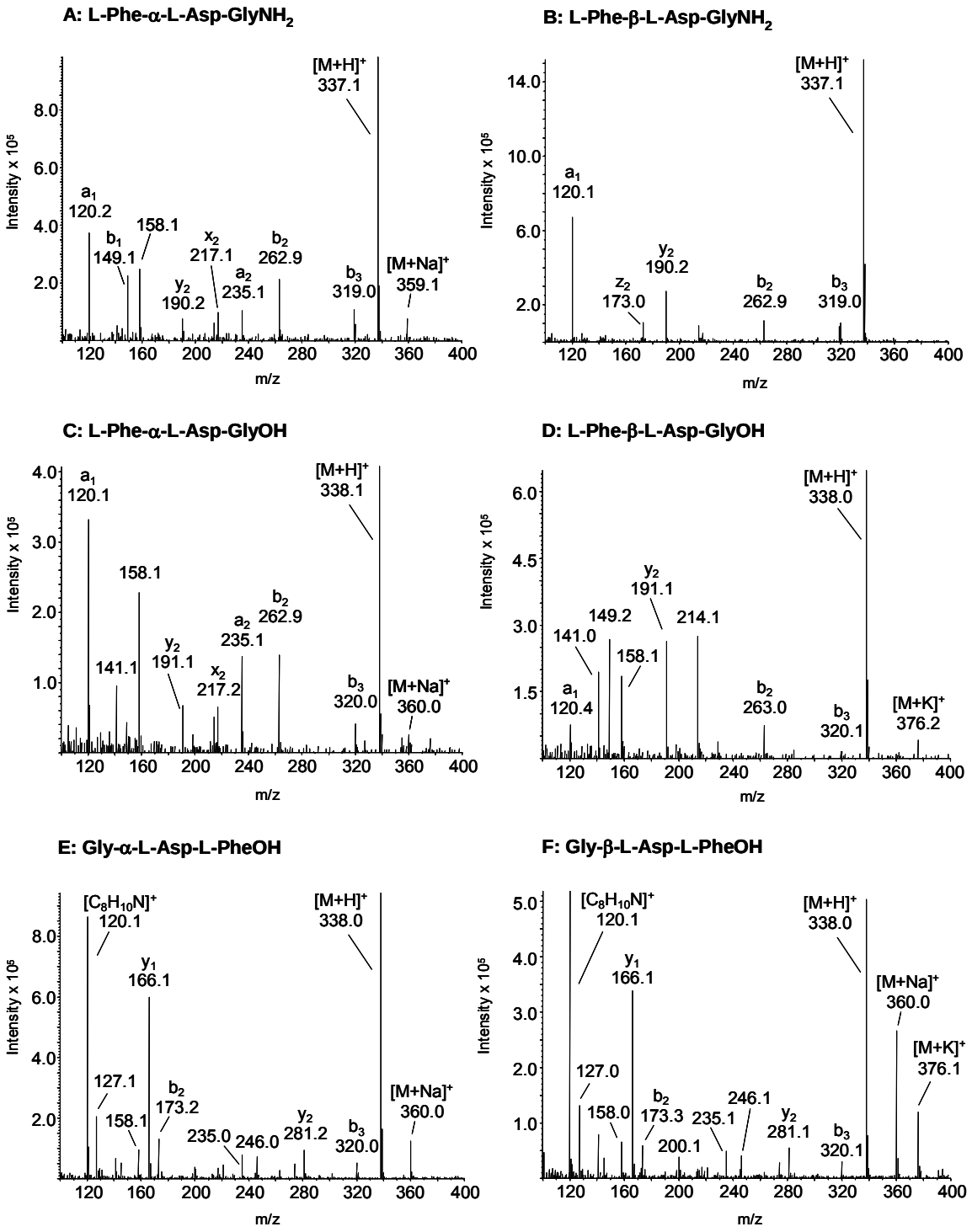

Figure 16: Mass spectra of L-Phe-α-L-Asp-GlyNH_2 (A), L-Phe-β-L-Asp-GlyNH_2 (B), L-Phe-α-L-Asp-GlyOH (C), L-Phe-β-L-Asp-GlyOH (D), Gly-α-L-Asp-L-PheOH (E) and Gly-β-L-Asp-L-PheOH (F). (A) and (B) were analyzed by injection of reference substances, (C)-(F) were recorded from samples of Phe-Asp-GlyNH_2 and Gly-Asp-PheNH_2 after incubation at pH 10.

7. Quantification of degradation products

In this work a CE and a RP-HPLC method for the analysis of the model tripeptides Phe-Asp-GlyNH_2 and Gly-Asp-PheNH_2 and their degradation products were developed. Both methods allowed analysis of most degradation products. On the other hand, separation of all degradation products could not be achieved in a single running system for both CE and RP-HPLC. In both techniques several experimental conditions had to be developed in order to analyse all compounds.

The CE method was chosen for the quantitative analysis of the degradation products. Because of the low dispersion of the solute zones, better resolution and efficiency were achieved in CE. Moreover, CE allowed analysis in much shorter times, which is of great advantage when many repetitive runs have to be performed. In fact, although sample analysis can be performed in approximately 15 min in both CE and RP-HPLC (see Figures 5 and 8), HPLC-column equilibration time is much longer than CE-capillary rinse time, especially when a gradient is run. Furthermore, analysis of Gly-Asp and cyclo(Gly-Asp) was not possible by RP-HPLC, because of the high polarity of these compounds, resulting in their elution in the solvent front.

7.1 Selection of an internal standard

The use of an internal standard proved to be crucial for reproducibility in CE in order to compensate for injection errors and minor fluctuations of the migration times [74-76]. Moreover, an internal standard is necessary to avoid errors during sample preparation. A suitable substance is stable during incubation at pH 2 and 10 at 80°C, has a chromophore which absorbs at the measuring wavelength (215 nm) and does not comigrate with any of the analytes. Tryptophane (Trp), histidine (His), 3-aminopyridine (3-AP), p-aminobenzoic acid (pABA) and p-aminomethylbenzoic acid (pAMBA) were tested as internal standard. While Trp was not stable under alkaline conditions, His, 3-AP and pABA comigrated with one of the degradation products. Under the analysis conditions, pAMBA proved to be the most convenient compound.

7.2 Calibration of reference substances

The assay was validated with respect of linearity. Calibration curves of reference substances were recorded from seven different concentrations in a range between 3 and 0.015 µmol/ml (see Materials and Methods, paragraph 10.4). The peak area ratio method was used. Each concentration was injected three times. For every compound calibration and analysis in the incubation samples were carried out under the same conditions (CE-Systems 1-4, see Materials and Methods, paragraph 10.4). Good linearity was observed for all substances. Slope of regression and linearity for the reference

compounds are listed in Tables 2 and 3. As it can be seen in Table 2, linear relationships with regression coefficient, r^2, of at least 0.9996 were found for all substances that were calibrated in phosphate buffer (CE-System 1). In presence of CM-β-CD (CE-System 3) calibration curves had a regression coefficient of at least 0.9949 (Table 3). For calibration of the diketopiperazine derivatives cyclo(Phe-Asp) and cylo(Gly-Asp) (CE-System 4) the regression coefficient was at least 0.9986. The limit of detection (LOD) was in the range between 0.1 µmol/ml and 0.005 µmol/ml for $GlyNH_2$ and the amidated tripeptides, respectively. The limit of quantification (LOQ) of the compound ranged between 0.3 µmol/ml ($GlyNH_2$)and 0.015 µmol/ml (amidated tripeptides).

Table 2: Slope and linearity of the regression curves obtained for CE analysis of reference substances in CE-System 1 (for details see Materials and Methods, paragraph 10.8).

CE-System 1 (phosphate)					
Compound	**Slope**	**r^2**	**Compound**	**Slope**	**r^2**
L-Phe-α-L-Asp-$GlyNH_2$	1.8080	1.0000	Gly-β-L-Asp-L-PheOH	2.5016	0.9999
L-Phe-α-D-Asp-$GlyNH_2$	1.6991	0.9999	Gly-β-D-Asp-L-PheOH	2.6071	0.9999
L-Phe-β-D-Asp-$GlyNH_2$	1.4748	0.9996	Phe-Asu-$GlyNH_2$	2.3288	0.9999
L-Phe-β-L-Asp-GlyOH	2.1308	0.9999	Phe-Asu-GlyOH	2.5904	0.9999
L-Phe-β-D-Asp-GlyOH	2.1292	0.9998	Gly-Asu-$PheNH_2$	2.2639	0.9999
Gly-α-L-Asp-L-$PheNH_2$	2.2737	0.9999	Gly-Asu-PheOH	2.0965	0.9999
Gly-α-D-Asp-L-$PheNH_2$	2.3092	1.0000	Phe-AspOH	2.6416	0.9999
Gly-β-L-Asp-L-$PheNH_2$	2.2993	0.9999	Gly-AspOH	0.4067	0.9999
Gly-β-D-Asp-L-$PheNH_2$	2.2985	0.9999	$PheNH_2$	1.7532	0.9999
Gly-α-L-Asp-L-PheOH	1.8852	0.9999	PheOH	1.8570	0.9999
Gly-α-D-Asp-L-PheOH	2.2660	0.9998	$GlyNH_2$	0.0420	0.9997

Table 3: Slope and linearity of the regression curves obtained for CE analysis of reference substances in CE-Systems 3 and 4 (for details see Materials and Methods, paragraph 10.8).

CE-System 3 (CM-β-CD)			CE-System 4 (formate)		
Compound	**Slope**	**r^2**	**Compound**	**Slope**	**r^2**
L-Phe-β-L-Asp-$GlyNH_2$	2.0804	0.9949	cyclo(Phe-Asp)	2.7411	0.9986
L-Phe-α-L-Asp-GlyOH	1.5479	0.9981	cyclo(Gly-Asp)	0.5532	0.9992
L-Phe-α-D-Asp-GlyOH	1.5586	0.9999			

7.3 Precision

The assay was validated with respect of intraday and interday precision. Two concentrations of each compound were analyzed by triplicate injections on the same day (intraday precision) and on three consecutive days (interday precision). Acceptable repeatability of the area ratios within one day and within three days was observed. The minimal and maximal values of the relative standard deviation (RSD) for the lowest and the highest concentration for both intraday and interday precision for all compounds are listed in Table 4. The complete data of the ratio corrected area of the individual reference substances versus corrected area of the internal standard are summarised in Appendix (paragraph 13.1).

The RSD values of the area ratios was 9.34% or lower for calibration in phosphate buffer (CE-Systems 1 and 5). The RSD values for calibration of the diketopiperazine derivative cyclo(Phe-Asp) and cyclo(Gly-Asp) in CE-System 4 (formate buffer containing 10% ACN) were considerably higher. This is due to the fact that these negatively charged substances migrate after the EOF and show relatively broad peaks, which causes a larger integration error. Moreover, while the RSD values for cyclo(Phe-Asp) are good (0.31%-6.07% for intraday precision and 3.69%-12.11% for interday precision), the values of cyclo(Gly-Asp) are considerably higher. This is due to the lack of a good chromophore and the consequent low absorption of the substance.

Table 4: Intraday and interday precision of the peak-area ratios (CPA of the analyte related to CPA of internal standard) in CE-System 1, 3 and 4. For details see Materials and Methods, paragraph 10.8.

CE-System	Intraday precision			Interday precision		
	Conc. (µmol/ml)	Min RSD (%)	Max RSD (%)	Conc. (µmol/ml)	Min RSD (%)	Max RSD (%)
1 (phosphate)	0.015	0.46	9.34	0.06	0.28	5.19
	3.00	0.03	3.70	0.75	0.18	4.79
3 (CM-β-CD)	0.015	4.94	8.34	0.06	5.73	6.32
	3.00	4.35	5.67	0.75	1.96	6.76
4 (formate)	0.015	2.83	8.14	0.06	12.11	29.45
	3.00	6.20	7.74	0.75	3.69	14.00

8. Kinetics of degradation reactions

8.1 Kinetics of the degradation of Phe-Asp-GlyNH_2 and Gly-Asp-PheNH_2

The model peptides Phe-Asp-GlyNH_2 and Gly-Asp-PheNH_2 were incubated at pH 2 and 10. Samples were withdrawn after 6, 12, 24, 36, 48, 72, 96, 120, 192 and 240 h (for details see Materials and Methods, paragraph 10.3). The concentration of the compounds in each sample was calculated using equations obtained from calibration curves of reference substances.

8.1.1 Incubations at pH 2

Hydrolysis was the main degradation pathway after incubation of Phe-Asp-GlyNH_2 at pH 2. A scheme of the formation of the degradation products is depicted in Figure 17. Phe-Asp-GlyNH_2 can undergo hydrolysis of the peptide bond between Asp and GlyNH_2 with consequent formation of the dipeptide Phe-Asp and GlyNH_2. Further deamidation of GlyNH_2 yielded GlyOH, which could not be detected by UV because of its poor absorption at 215 nm. The dipeptide Phe-AspOH could be further hydrolysed to the amino acids PheOH and AspOH. Due to the lack of a chromophore Asp could also not be detected. Moreover, nucleophilic attack of the *N*-terminal nitrogen on the α-carbonyl of Asp in the dipeptide Phe-AspOH leaded to the formation of the diketopiperazine derivative cyclo(Phe-Asp).

In addition, Phe-Asp-GlyNH_2 can undergo deamidation of the *C*-terminal amide to yield Phe-Asp-GlyOH (Figure 17). As already observed for Phe-Asp-GlyNH_2, the deamidated peptide was hydrolysed to GlyOH and Phe-AspOH, which could be further hydrolysed to PheOH and AspOH. Both the amidated and the deamidated form of the tripeptide yielded the corresponding succinimidyl peptides. Because the succinimide ring is relatively stable at pH 2, both Phe-Asu-GlyNH_2 and Phe-Asu-GlyOH could be detected. Deamidation of the terminal end of Phe-Asu-GlyNH_2 could also yield Phe-Asu-GlyOH.

Figure 18 shows the kinetic profiles of Phe-Asp-GlyNH_2 and its degradation products after incubation at pH 2. The concentration of the compounds in the incubated samples is depicted as a function of time. The points represent experimental data and the lines were calculated by non-linear curve fitting according to the Bateman equation. The degradation of Phe-Asp-GlyNH_2 followed apparent first order kinetics with half-life of 7.5 h (Figure 18A). Table 5 summarises the apparent half-lives for the formation and the degradation of all substances observed in incubations of Phe-Asp-GlyNH_2 at pH 2. Phe-AspOH and GlyNH_2 were the most abundant degradation products after 24 h of incubation. As expected, the formation rate for these two substances were comparable. Formation of Phe-AspOH was slightly faster than that of GlyNH_2, probably due to the fact that Phe-AspOH can be formed from

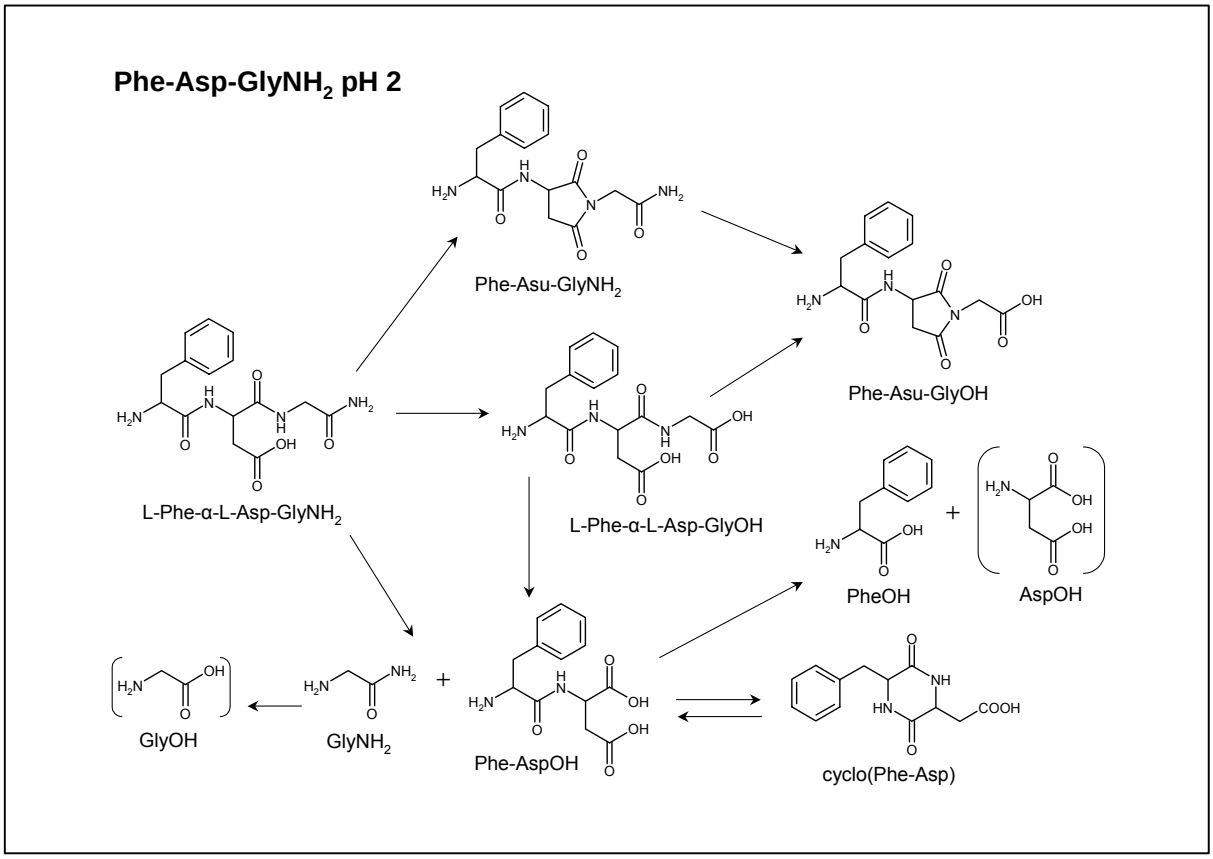

Figure 17: Schematic degradation pathway of Phe-Asp-$GlyNH_2$ at pH 2. Brackets show substances that could not be detected.

hydrolysis of both Phe-Asp-$GlyNH_2$ and Phe-Asp-GlyOH (see Figure 17). After 6 h of incubation significant deamidation of the terminal carboxyl group was observed (Figure 18B). However, this compound was further degradated very fast to the dipeptide and amino acids. As it can be seen from the kinetic profiles for the formation of Phe-Asp-GlyOH, Phe-AspOH and $GlyNH_2$ (Figures 18B, 18E and 18G), hydrolysis of the peptide backbone occurred faster than deamidation of the amide of the carboxy terminus. Hydrolysis as main degradation pathway was confirmed by the fact that after 240 h the main degradation product was PheOH. Due to the fact that PheOH is formed by hydrolysis of Phe-AspOH, the kinetic profile of PheOH showed an initial lag phase (Figure 18F).

Similarly to PheOH, cyclo(Phe-Asp) was formed relatively slowly and showed an initial lag phase (Figure 18H). Although formation of cyclo(Phe-Asp) can occur in alkaline medium [41, 77], it was not noticed in our experiments in incubations at pH 10 where backbone hydrolysis was not observed (see paragraph 8.1.2). It can be concluded that this cyclic compound does not directly result from the tripeptide but is formed from the dipeptide. Moreover, cyclo(Phe-Asp) was further degradated and its concentration decreased after 72 h of incubation. The diketopiperazine ring could be hydrolysed to the

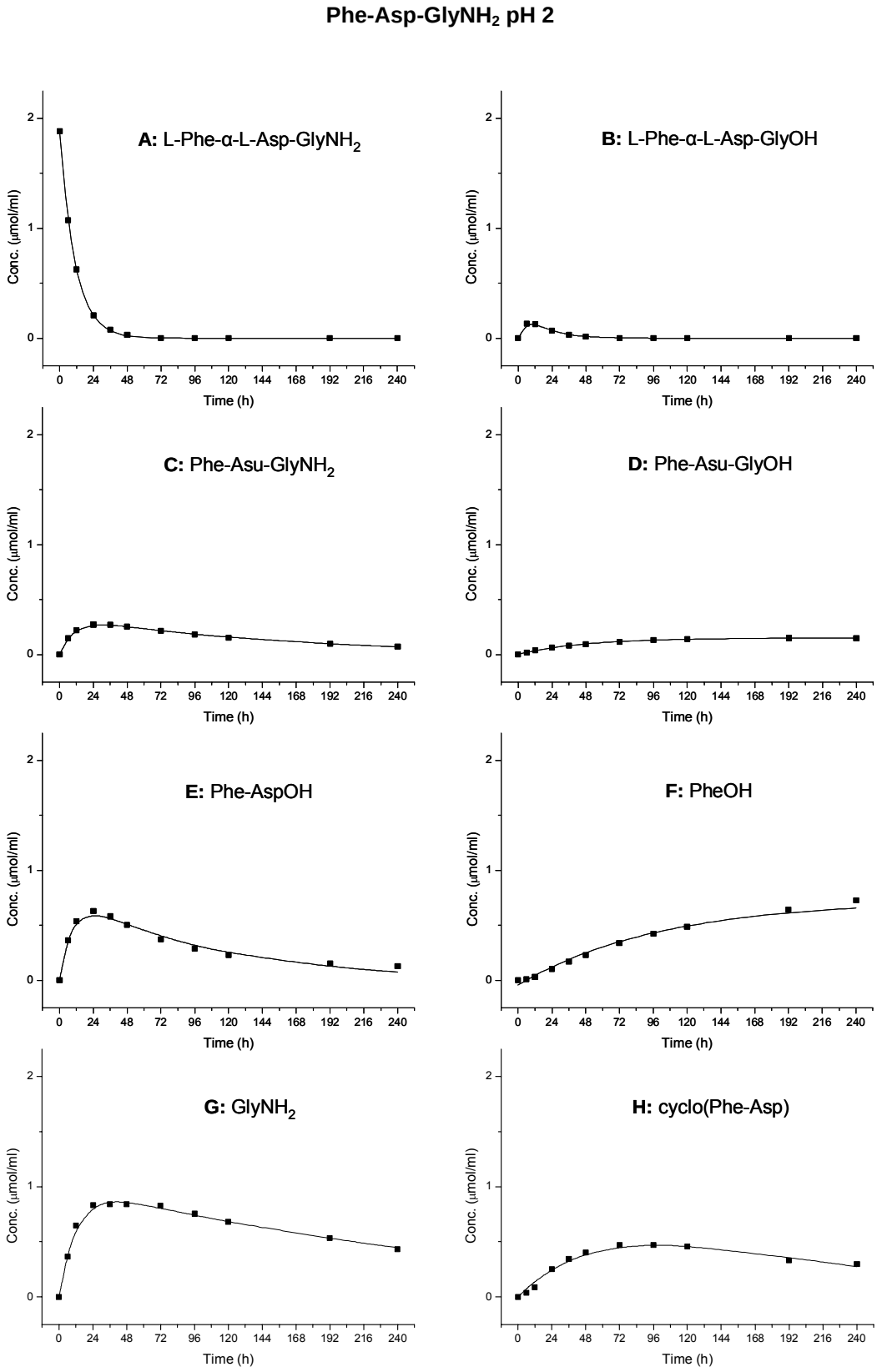

Figure 18: Kinetic profiles of Phe-Asp-$GlyNH_2$ and its degradation products after incubation at pH 2. The squares represent the experimental data obtained as the means of two incubations, each injected in triplicate. The lines were calculated by non-linear curve fitting.

Table 5: Apparent half-lives for the formation and degradation of the compounds observed in incubations of Phe-Asp-GlyNH_2 at pH 2.

Phe-Asp-GlyNH_2 pH 2		
Compound	**$t_{1/2}$ formation (h)**	**$t_{1/2}$ degradation (h)**
L-Phe-α-L-Asp-GlyNH_2	-	7.5
L-Phe-α-L-Asp-GlyOH	9.8	3.7
Phe-Asu-GlyNH_2	6.7	102.1
Phe-Asu-GlyOH	32.5	-
Phe-AspOH	5.7	69.4
PheOH	69.8	-
GlyNH_2	8.2	196.3
Cyclo(Phe-Asp)	57.4	81.2

dipeptide Phe-AspOH which was further degradated to PheOH and AspOH, as mentioned above. Decrease of the concentration of cyclo(Phe-Asp) proved that the hydrolysis reaction of the dipeptide to give amino acids was faster than its cyclization reaction. Sequence inversion and formation of the dipeptide Asp-PheOH was not observed. This is in accordance with literature data on diketopiperazines [41].

The kinetic profiles of the formation of the succinimidyl derivatives Phe-Asu-GlyNH_2 and Phe-Asu-GlyOH are depicted in Figures 18C and 18D. Phe-Asu-GlyOH is relatively stable in acidic medium and even after 240 h of incubation significant degradation of this compound was not observed. On the other side, the amidated compound Phe-Asu-GlyNH_2 reached its highest concentration after 24 h and after this time was further degradated. This is probably due to the deamidation of the terminal amide with consequent formation of Phe-Asu-GlyOH.

Similar results were obtained for incubations at pH 2 of the peptide with inverse amino acid sequence Gly-Asp-PheNH_2. Figure 19 depicts a scheme of the formation of the degradation products. As already discussed for Phe-Asp-GlyNH_2, hydrolysis of the peptide backbone gave the dipeptide Gly-AspOH and PheNH_2. The latter underwent deamidation to PheOH. Gly-AspOH may be further hydrolysed to the amino acids GlyOH and AspOH. Cyclization of the dipeptide Gly-AspOH yielded the diketopiperazine cyclo(Gly-Asp). Similar to Phe-Asp-GlyNH_2, Gly-Asp-PheNH_2 underwent deamidation of the *C*-terminal amide. The deamidated peptide was then further hydrolysed to a dipeptide and amino acids. Both Asu peptides Gly-Asu-PheNH_2 and Gly-Asu-PheOH were formed and were stable under the incubation conditions.

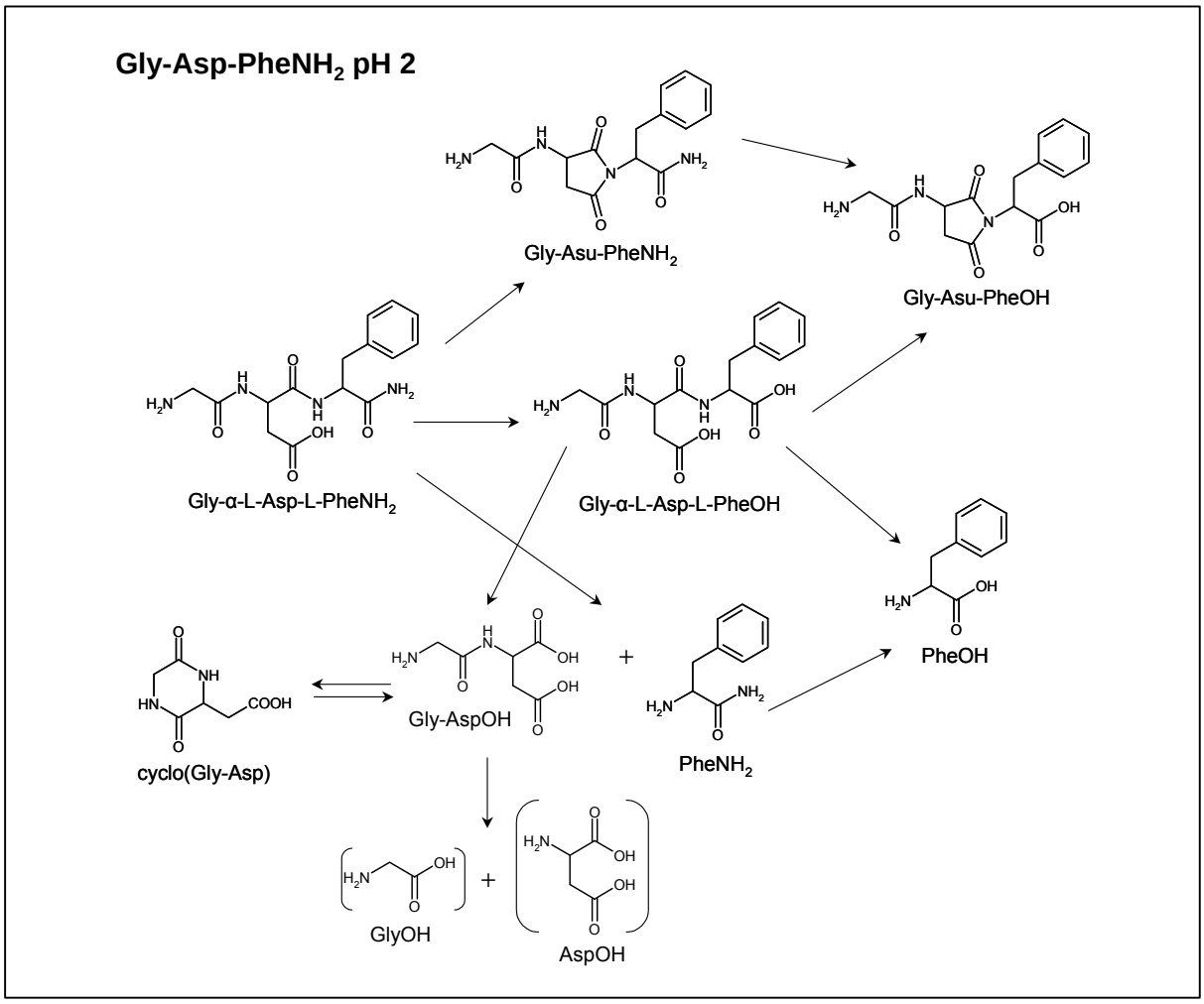

Figure 19: Schematic degradation pathway of Gly-Asp-PheNH$_2$ at pH 2. Brackets show substances that could not be detected.

The kinetic profiles of the degradation of Gly-Asp-PheNH$_2$ and its subsequent products at pH 2 are depicted in Figure 20. The degradation reaction of the tripeptide followed apparent first order kinetics with a half-life of 18.3 h. The curves corresponding to the degradation products were obtained by non-linear fitting according to the Bateman equation. Table 6 summarises the apparent half-lives for the formation and the degradation of all substances observed in incubations of Gly-Asp-PheNH$_2$ at pH 2. Hydrolysis of the peptide backbone was the major degradation pathway. Gly-AspOH reached its maximal concentration after 48 h and was further hydrolysed to GlyOH and AspOH, which could not be detected by UV. Because the deamidation reaction occurred slower than the hydrolysis reaction, the maximal concentration of PheNH$_2$ was reached after 96 h and further degradation of this compound proceeded slowly (Figure 20G). The fact that deamidation occured slower than backbone hydrolysis was confirmed from the kinetic profile of Gly-Asp-PheOH (Figure 20B), the concentration of which increased more slowly than that of the dipeptide Gly-AspOH. Furthermore, the concentration of Gly-Asp-PheOH reached a maximum after 24 h and the compound was rapidly further degradated.

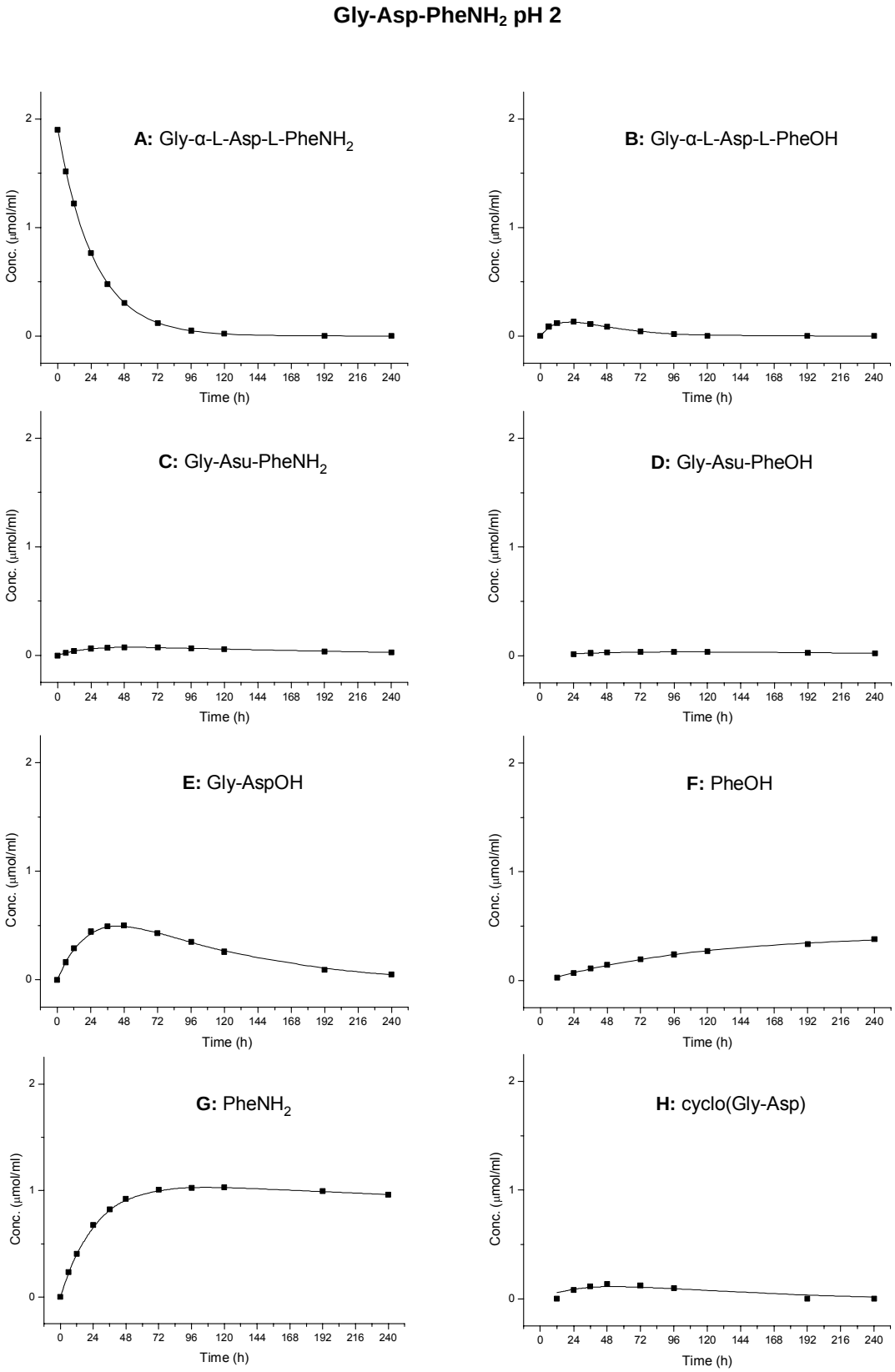

Figure 20: Kinetic profiles of Gly-Asp-PheNH$_2$ and its degradation products after incubation at pH 2. The squares represent the experimental data obtained as the means of two incubations, each injected in triplicate. The lines were calculated by non-linear curve fitting.

Table 6: Apparent half-lives for the formation and degradation of the compounds observed in incubations of Gly-Asp-$PheNH_2$ at pH 2.

Gly-Asp-$PheNH_2$ pH 2		
Compound	**$t_{1/2}$ formation (h)**	**$t_{1/2}$ degradation (h)**
Gly-α-L-Asp-L-$PheNH_2$	-	18.3
Gly-α-L-Asp-L-PheOH	10.2	19.4
Gly-Asu-$PheNH_2$	15.6	117.5
Gly-Asu-PheOH	44.7	-
Gly-AspOH	20.4	46.9
PheOH	76.6	-
$PheNH_2$	17.7	1050
Cyclo(Gly-Asp)	31.7	55.6

Both Asu peptides, Gly-Asu-$PheNH_2$ and Gly-Asu-PheOH, were detected but only small amounts of these products were observed. This is probably due to the steric hindrance of Phe as Asp following amino acid. The diketopiperazine cyclo(Gly-Asp) could be detected, although its amount was smaller that that of cyclo(Phe-Asp) in incubations of Phe-Asp-$GlyNH_2$ at pH 2. As already described for cylo(Phe-Asp), a decrease in the concentration of cyclo(Gly-Asp) after 48 h of incubation was observed. This is due to the diketopiperazine ring opening with consequent formation of the dipeptide Gly-AspOH. Sequence inversion was not noticed.

As expected, degradation proceeded faster for Phe-Asp-$GlyNH_2$ than for Gly-Asp-$PheNH_2$. As it can be seen in Tables 5 und 6, the formation of all degradation products observed in incubations of Gly-Asp-$PheNH_2$ showed higher half-life values compared to those of Phe-Asp-$GlyNH_2$. This may be explained by the steric hindrance of Phe as Asp following amino acid. On the other hand, the deamidation rate of the *C*-terminus was similar for both tripeptides, suggesting that this reaction is not influenced by the presence of the Phe side-chain.

8.1.2 Incubations at pH 10

In incubations at pH 10 isomerization and enantiomerization *via* formation of the succinimidyl intermediate were observed. The degradation pathways were very similar for both model compounds. Figure 21 shows a scheme of the formation of the degradation products after incubation of Phe-Asp-$GlyNH_2$ at pH 10. The tripeptide underwent isomerization with formation of the corresponding β-Asp peptide. Enantiomerization of Asp was observed for both the α-Asp and the β-Asp peptides.

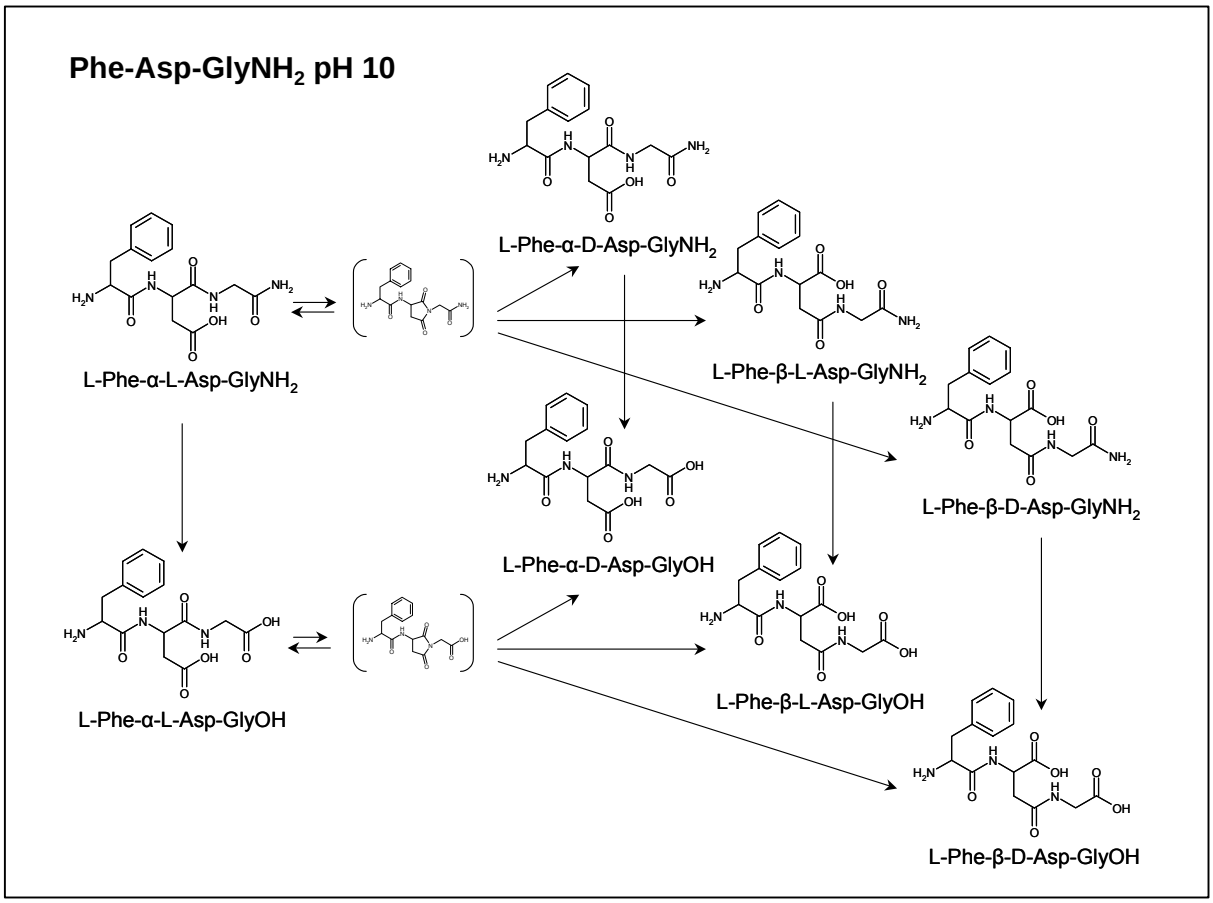

Figure 21: Schematic degradation pathway of Phe-Asp-GlyNH_2 at pH 10. Brackets show substances that could not be detected.

Deamidation of the terminal amide of Phe-Asp-GlyNH_2 yielded Phe-Asp-GlyOH which can also undergo isomerization and enantiomerization *via* formation of the succinimidyl intermediate. Moreover, the α-D-Asp, β-L-Asp and β-D-Asp forms of the amidated peptide may be hydrolysed to the corresponding peptides with free terminal carboxyl groups. Due to their low stability in alkaline medium, the Asu intermediates could not be detected in the incubations.

Figure 22 shows the kinetic profiles for Phe-Asp-GlyNH_2 and its degradation products after incubation at pH 10. The concentration of the compounds in the samples is depicted as a function of time. The points represent experimental data and the lines were calculated from non-linear fitting according to the Bateman equation. The degradation of Phe-Asp-GlyNH_2 followed apparent first order kinetics with a half-life of 18.3 h. Table 7 summarises the apparent half-lives for the formation and the degradation of all substances observed in incubations of Phe-Asp-GlyNH_2 at pH 10. After 24 h of incubation the main degradation product was L-Phe-α-L-Asp-GlyOH (Figure 22E), which resulted from hydrolysis of the terminal amide. This compound reached its highest concentration after 36 h of incubation and it was relatively slowly further degradated presumably via the corresponding Asu intermediate to form

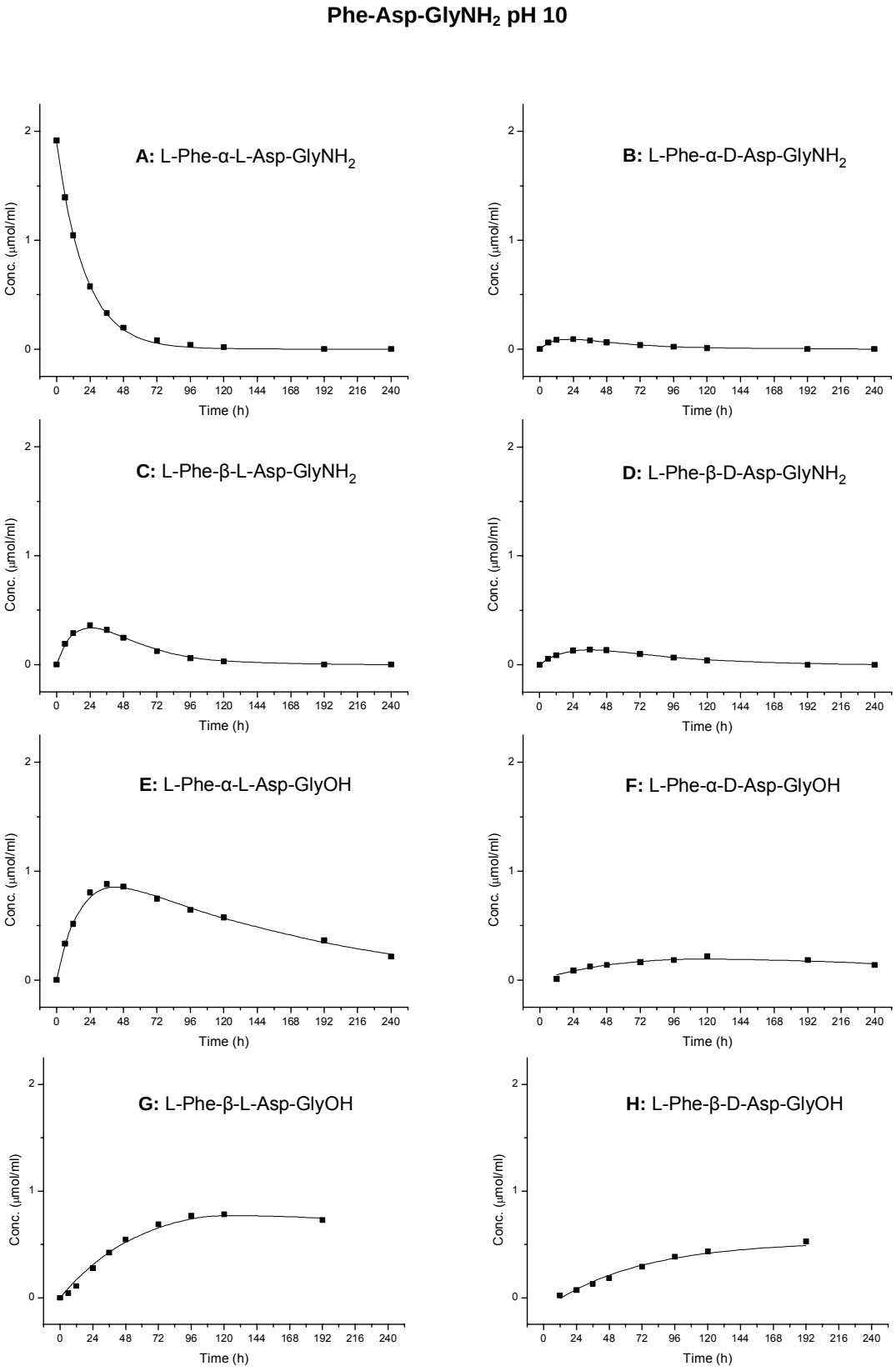

Figure 22: Kinetic profiles of Phe-Asp-GlyNH$_2$ and its degradation products after incubation at pH 10. The squares represent the experimental data obtained as the means of two incubations, each injected in triplicate. The lines were calculated by non-linear curve fitting.

Table 7: Apparent half-lives for the formation and degradation of the compounds observed in incubations of Phe-Asp-GlyNH_2 at pH 10.

Phe-Asp-GlyNH_2 pH 10		
Compound	**$t_{1/2}$ formation (h)**	**$t_{1/2}$ degradation (h)**
L-Phe-α-L-Asp-GlyNH_2	-	14.1
L-Phe-α-D-Asp-GlyNH_2	7.4	29.5
L-Phe-β-L-Asp-GlyNH_2	14.1	18.0
L-Phe-β-D-Asp-GlyNH_2	23.6	24.5
L-Phe-α-L-Asp-GlyOH	12.1	96.5
L-Phe-α-D-Asp-GlyOH	16.3	-
L-Phe-β-L-Asp-GlyOH	95.2	-
L-Phe-β-D-Asp-GlyOH	47.8	-

the isomerization and enantiomerization products. After 192 h the main degradation product was L-Phe-β-L-Asp-GlyOH (Figure 22G). In accordance to literature data [10, 55], the amount of β-Asp containing peptides was higher than that of the corresponding α-Asp peptides. This is evident from Figures 22F and 22H for L-Phe-α-D-Asp-GlyOH and L-Phe-β-D-Asp-GlyOH, respectively.

Significant formation of D-Asp containing peptides was also observed. As it can be seen in Figures 22B and 22D, the peptides Phe-α-D-Asp-GlyNH_2 and Phe-β-D-Asp-GlyNH_2 were formed relatively fast and reached their maximal concentrations after 24 h. These compounds were further degradated by hydrolysis of the terminal amide to yield the corresponding peptides with free terminal carboxyl groups. As it can be seen in Figures 22F, 22G and 22H, the kinetic profiles of L-Phe-α-D-Asp-GlyOH, L-Phe-β-L-Asp-GlyOH and L-Phe-β-D-Asp-GlyOH show an initial lag phase. This is in accordance to the fact that this compounds were not directly formed from degradation of the starting peptide but only after its deamidation to L-Phe-α-L-Asp-GlyOH or its isomerization and enantiomerization to L-Phe-α-D-Asp-GlyNH_2, L-Phe-β-L-Asp-GlyNH_2 and L-Phe-β-D-Asp-GlyNH_2 (Figure 21). On the other hand, the deamidated peptides were relatively stable under the applied conditions and further significant degradation of these substances was not observed up to 240 h of incubation.

The degradation of Gly-Asp-PheNH_2 was very similar to that of Phe-Asp-GlyNH_2 and is shown in Figure 23. The kinetic profiles of the degradation products are depicted in Figure 24. Non-linear fitting according to the Bateman equation was performed. The degradation of the model compound Gly-Asp-PheNH_2 followed apparent first order kinetics with a half-life of 26.5 h. Table 8 summarises the apparent half-lives for the formation and the degradation of all substances observed in incubations of

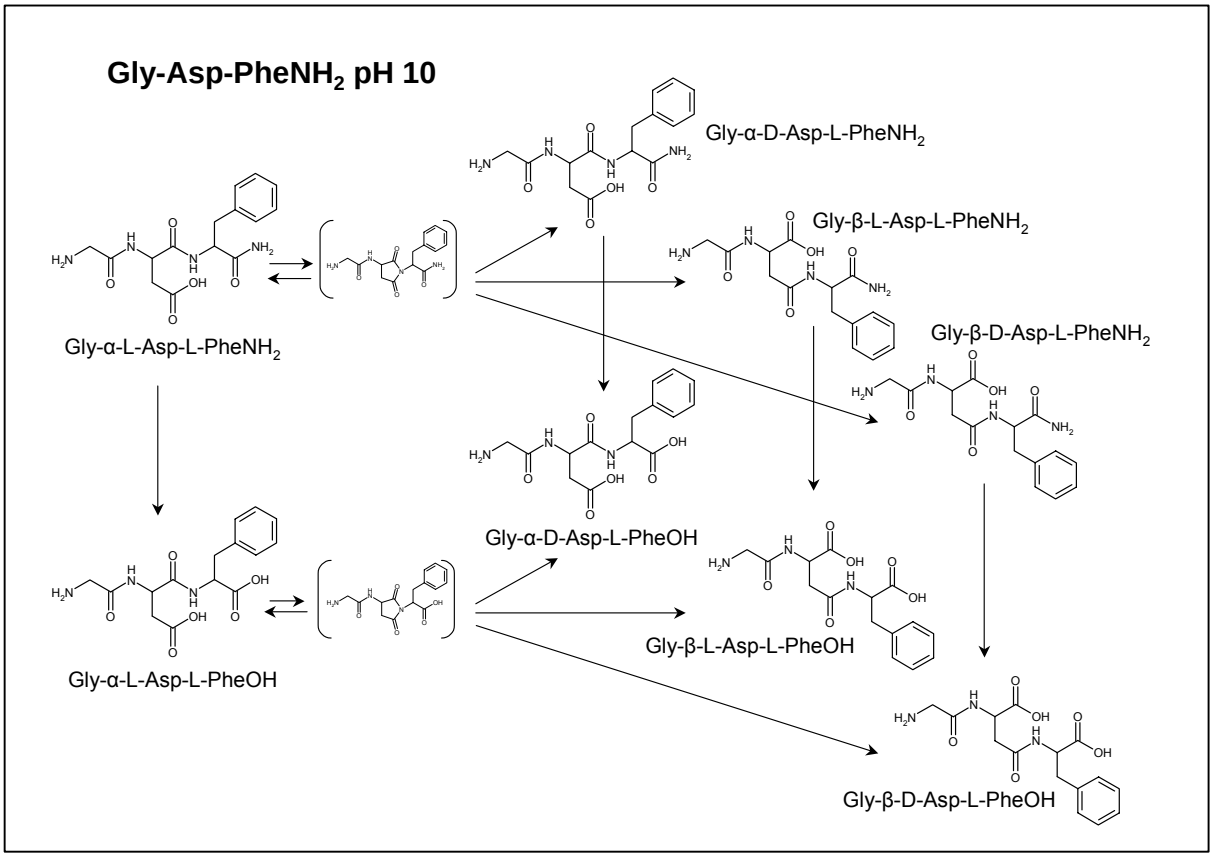

Figure 23: Schematic degradation pathway of Gly-Asp-PheNH$_2$ at pH 10. Brackets show substances that could not be detected.

Gly-Asp-PheNH$_2$ at pH 10. Isomerization and enantiomerization of Asp proceeded relatively slowly and the most abundant degradation product was the deamidated peptide Gly-α-L-Asp-L-PheOH (Figure 24E). A significant difference from the degradation of Phe-Asp-GlyNH$_2$ was found in the ratio between α-Asp and β-Asp peptides. In incubations of Gly-Asp-Phe-NH$_2$, the amount of α-Asp peptides was higher than that of the corresponding β-Asp peptides. This can be seen in Figures 24E and 24G for Gly-α-L-Asp-L-PheOH and Gly-β-L-Asp-L-PheOH and in Figures 24F and 24H for Gly-α-D-Asp-L-PheOH and Gly-β-D-Asp-L-PheOH, respectively. This can be explained by the steric hindrance of the Phe side chain, which probably allows the hydrolysis of the Asu intermediates only from one side of the ring. The most abundant peptide of the D-Asp series was Gly-α-D-Asp-L-PheOH (Figure 24F). The deamidated forms of the peptide were relatively stable up to 240 h incubation, while the amidated forms were further degradated to their corresponding peptides with free carboxyl group.

As already discussed for incubations at pH 2, degradation of Gly-Asp-PheNH$_2$ at pH 10 proceeded more slowly than that of Phe-Asp-GlyNH$_2$. This can be seen in Tables 7 and 8 from the apparent half-lives for the formation and the degradation of the compounds observed in incubations of Phe-Asp-

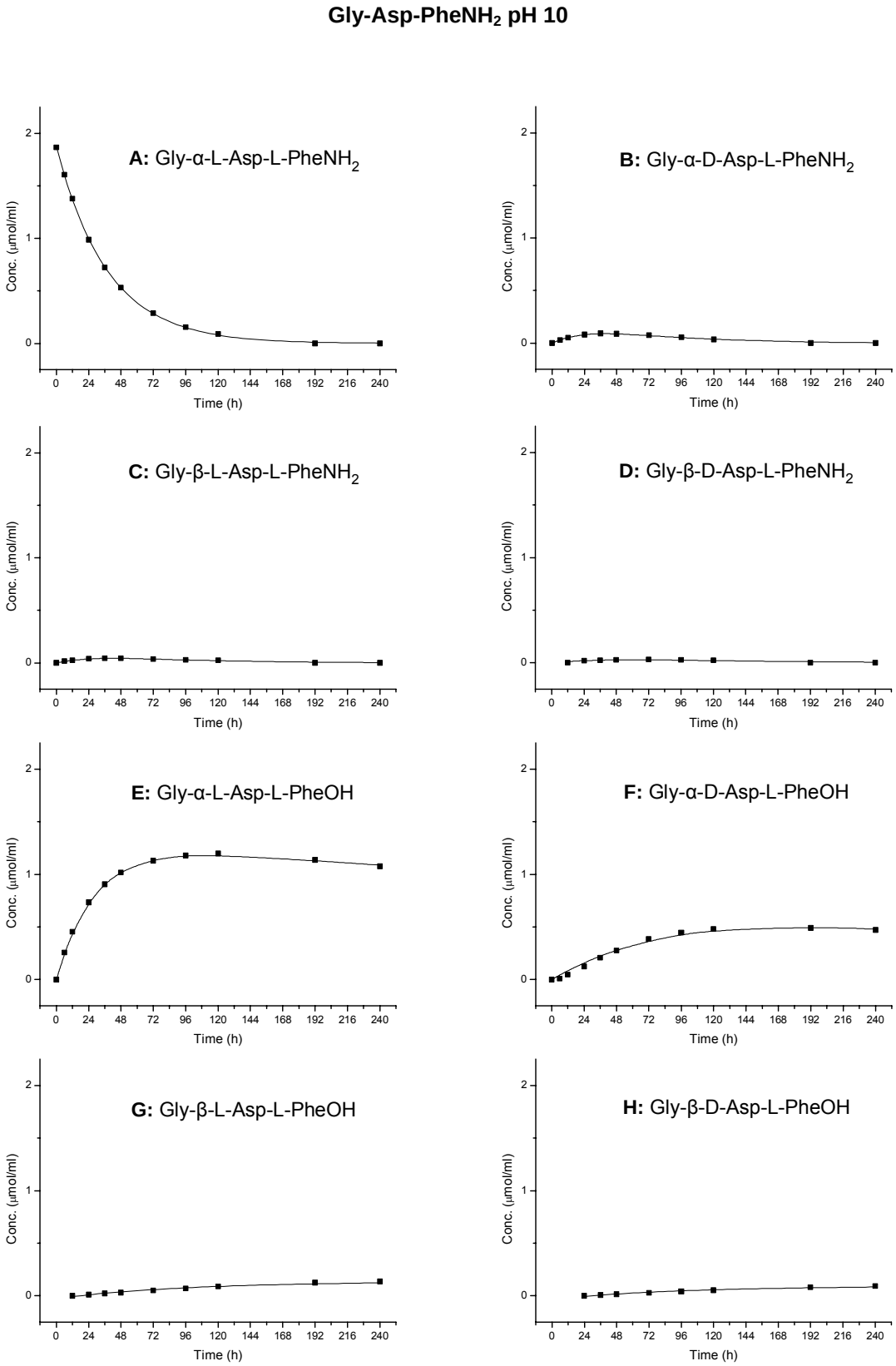

Figure 24: Kinetic profiles of Gly-Asp-PheNH$_2$ and its degradation products after incubation at pH 10. The squares represent the experimental data obtained as the means of two incubations, each injected in triplicate. The lines were calculated by non-linear curve fitting.

Table 8: Apparent half-lives for the formation and degradation of the compounds observed in incubations of Gly-Asp-$PheNH_2$ at pH 10.

Gly-Asp-$PheNH_2$ pH 10		
Compound	**$t_{1/2}$ formation (h)**	**$t_{1/2}$ degradation (h)**
Gly-α-L-Asp-L-$PheNH_2$	-	26.5
Gly-α-D-Asp-L-$PheNH_2$	25.2	30.3
Gly-β-L-Asp-L-$PheNH_2$	22.2	41.2
Gly-β-D-Asp-L-$PheNH_2$	18.2	83.9
Gly-α-L-Asp-L-PheOH	19.7	845.1
Gly-α-D-Asp-L-PheOH	51.7	-
Gly-β-L-Asp-L-PheOH	66.2	-
Gly-β-D-Asp-L-PheOH	67.6	-

$GlyNH_2$ and Gly-Asp-$PheNH_2$ at pH 10. Isomerization and enantiomerization of Asp proceeded more slowly in Gly-Asp-$PheNH_2$ because of the steric hindrance of Phe as Asp-following amino acid. This is in accordance with previous studies on the influence of the amino acid sequence on the degradation of peptides [7, 39, 40]. Compared to incubations at pH 2, the rate of the degradation at pH 10 was slower for both tripeptides. The apparent half-life of the degradation of the Phe-Asp-$GlyNH_2$ was 7.5 h at pH 2 and 18.3 at pH 10. For Gly-Asp-$PheNH_2$, the apparent half-life was 14.1 h and 26.5 h at pH 2 and 10, respectively.

8.2 Kinetics of the degradation of Phe-Asu-GlyOH

In order to investigate the enantiomerization reaction independently from other degradation pathways, the succinimidyl peptide Phe-Asu-GlyOH was incubated at pH 10. In this way, the enantiomerization reaction of the succinimidyl ring and its hydrolysis to give α- and β- D/L-Asp products could be selectively studied. A reaction scheme is shown in Figure 25. As already discussed in paragraph 3.2, the peptide was incubated at 30°C because at 80°C the succinimidyl hydrolysis proceeds too fast to allow detection of the degradation products in reasonable time intervals. Samples were withdrawn after 5, 10, 15, 30, 60, 90 and 120 minutes (see Materials and Methods, paragraph 10.3). A preliminary experiment showed that after this time an equilibrium was reached and significant further degradation did not occur.

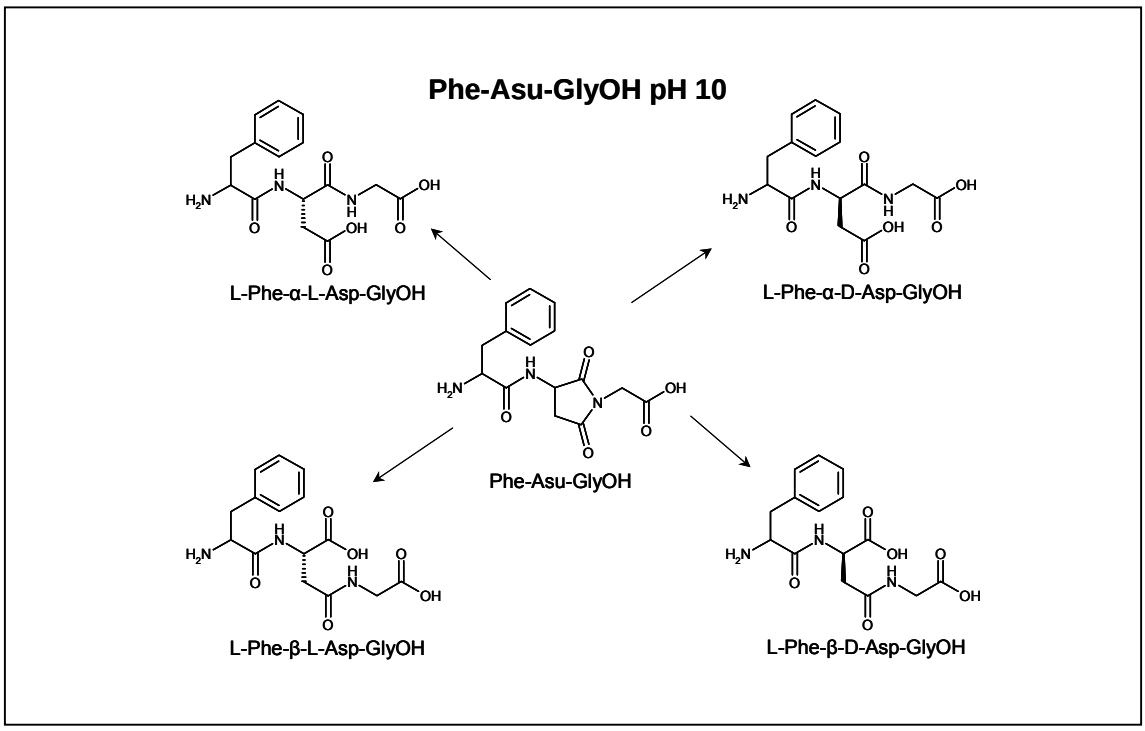

Figure 25: Schematic degradation pathway of Phe-Asu-GlyOH at pH 10.

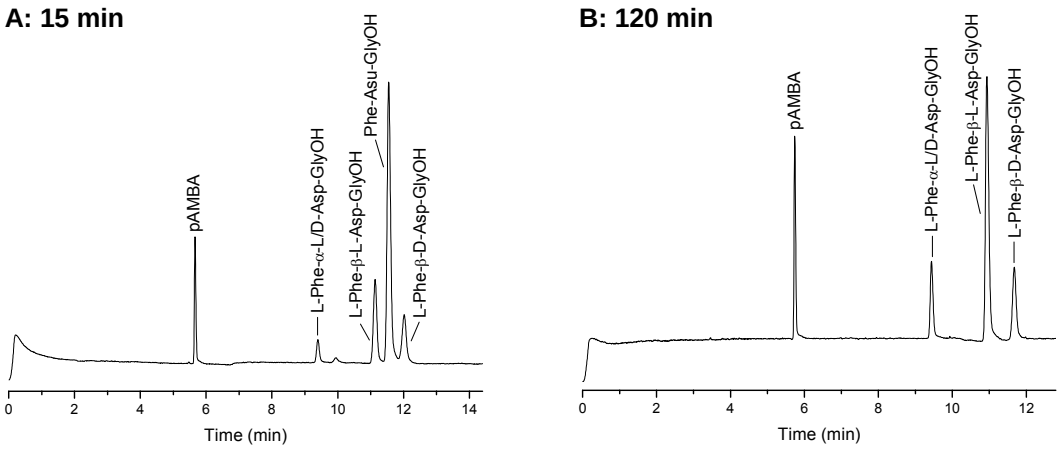

Figure 26: Electropherograms of the analysis of the incubation of Phe-Asu-GlyOH at pH 10 after 15 min (A) and 120 min (B). Analysis conditions: 50 mM phosphate buffer, pH 2.9, 15°C (CE-System 5). For details see Materials and Methods, paragraph 10.4.

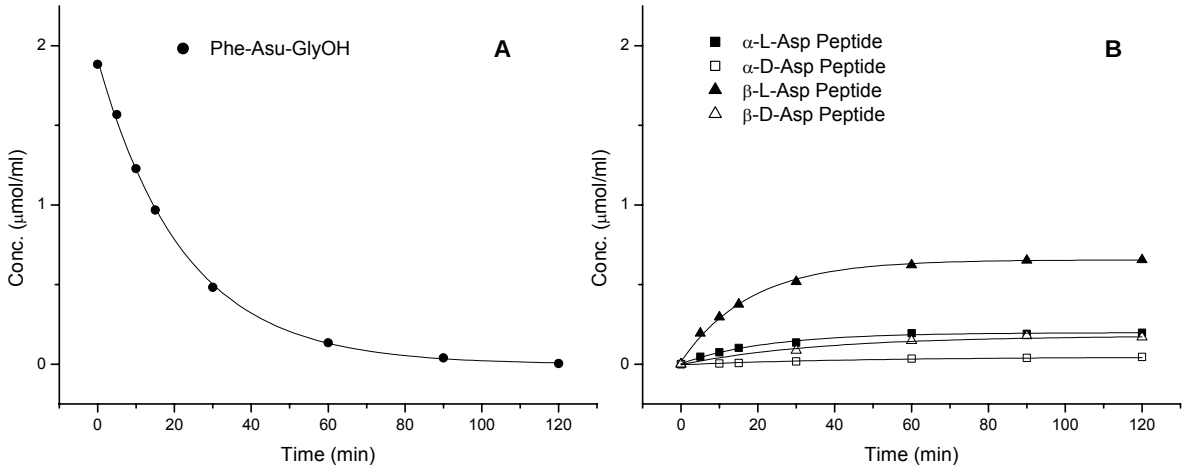

Figure 27: Kinetic profiles for the degradation of Phe-Asu-GlyOH at pH 10 (A) and for the formation of its degradation products (B). The squares represent the experimental data obtained as the means of two incubations, each injected in triplicate. The lines were calculated by non-linear curve fitting.

Figure 26 shows the CE-analysis of an incubation of Phe-Asu-GlyOH at pH 10 after 15 min and 120 min. Separation of the diastereomeric pair L-Phe-α-L-Asp-GlyOH / L-Phe-α-D-Asp-GlyOH was achieved in 50 mM phosphate, pH 3.0, containing 16 mg/ml CM-β-CD and 5% acetonitrile (CE-System 3, see paragraph 4.3.2). At the zero time a single peak corresponding to the Asu peptide was found. After a few minutes, four degradation products corresponding to the α-L, β-L, α-D and β-D forms of the Asp peptide appeared. After 120 min of incubation the peak of the starting compound had completely disappeared and an equilibrium was reached. The kinetic profiles of the compounds are depicted in Figure 27. The most abundant degradation product was the β-L-Asp peptide. Moreover, significant formation of the α-L-Asp and β-D-Asp peptides was noticed while only small amounts of the α-D-Asp peptide were detected. The degradation of the Asu peptide followed apparent first order kinetics with a half-life of 15.7 min. The kinetic profiles for the formation of the four degradation products could be fitted with an exponential equation of the apparent first order as well. The apparent half-lives of these reactions are summarised in Table 9.

The concentration ratio between β-Asp and α-Asp peptides was 3.4:1, which is in accordance with literature data [10, 55, 78, 79]. It is interesting to note that the D/L ratio was similar for both the α-Asp and the β-Asp containing peptides. The α-D-Asp/α-L-Asp ratio was 0.23:1 and the β-D-Asp/β-L-Asp was 0.26:1. Moreover, the apparent half-lives for the formation of both L-Asp peptides were similar (13.7 h and 12.6 h for L-Phe-α-L-Asp-GlyOH and L-Phe-β-L-Asp-GlyOH, respectively). For L-Phe-α-D-Asp-GlyOH and L-Phe-β-D-Asp-GlyOH the the halflives were 28.4 h and 25.4 h. This demonstrates that the succinimidyl ring opening is independent of the stereochemistry of the ring. Moreover, it is

Table 9: Apparent half-lives for the formation of the compounds observed in incubations of Phe-Asu-GlyOH at pH 10.

Phe-Asu-GlyOH pH 10		
Compound	**$t_{1/2}$ formation (min)**	**$t_{1/2}$ degradation (min)**
Phe-Asu-GlyOH	-	15.7
L-Phe-α-L-Asp-GlyOH	13.7	-
L-Phe-α-D-Asp-GlyOH	28.4	-
L-Phe-β-L-Asp-GlyOH	12.6	-
L-Phe-β-D-Asp-GlyOH	25.4	-

evident that the enantiomerization is much slower than ring opening. This is in accordance with the data found by Aylin and coworkers [79] who investigated the hydrolysis reaction of the succinimidyl ring by molecular modelling.

9. Conclusions

The present study was conducted in order to investigate the degradation products of aspartyl peptides in acidic and alkaline media, specifically with respect to the isomerization and enantiomerization of the Asp residue. The tripeptides Phe-Asp-GlyNH_2 and Gly-Asp-PheNH_2 were used as model compounds and were incubated at pH 2 and pH 10 at 80°C.

Analysis of the incubated samples was first performed by capillary electrophoresis (CE) with UV detection. CE was able to separate most α-Asp and β-Asp peptides and the corresponding α-D-Asp and β-D-Asp diastereomers due to small differences of the pK_a values of the free carboxyl group of both the α-Asp and β-Asp isomers as well as the respective diastereomers. A 50 mM phosphate buffer, pH 3.0, was suitable to resolve most of the degradation products. Separations that were not possible in this system were achieved by the addition of cyclodextrins to the buffer.

In addition, a RP-HPLC method for the analysis of the degradation products was developed as an alternative to the CE method. Most of the compounds could be separated with a gradient of acetonitrile in water containing 0.1% trifluoroacetic acid. Resolution of the isomeric pairs L-Phe-α/β-L-Asp-GlyNH_2 and L-Phe-α/β-D-Asp-GlyOH was achieved with a gradient of acetonitrile in phosphate buffer, pH 5.0.

Due to the different separation mechanisms, differences in the elution and migration order as well as in the resolution of the compounds were observed. Both methods allowed the analysis of most compounds. Interestingly, while the two pairs of diastereomers Phe-α-L/D-Asp-GlyOH and Gly-α-L/D-Asp-PheNH_2 could not be separated by CE, HPLC was less efficient resolving peptides containing α-Asp and β-Asp linkages. Overall, separations that were difficult to achieve with one technique proved to be easily accomplished by the other method.

The degradation products were first identified by coinjection of reference substances. Additional on-line MS detection was performed for both techniques in order to unequivocally identify the compounds. All substances were detected as $[M+H]^+$-ions. Analysis of the MS spectra of the peptides allowed the assignment of degradation products to the α-Asp or β-Asp series. Differences between peptides with an α- and β-linkage were observed in the ratio of the b- and y-ions generated by cleavage of the α/β-Asp-X bond and Y-α/β-Asp, respectively. The α-Asp peptide exhibited a more intense b_2 fragment ion and a low abundant y_2 fragment ion, while in the case of the β-Asp peptide the b_2 ion had lower intensity if compared to the y_2 fragment ion. Reliable differences in the spectra of D-Asp and L-Asp containing peptides could not be observed. Thus, the stereochemistry of the degradation products had to be performed by comparison to synthetic peptides with known configuration.

A CE assay for the analysis of the degradation products arising by incubation of the model peptides by pH 2 and 10 was developed and validated with respect of linearity, intraday and interday precision. Good linearity and repeatability of the area ratios within one day and within three days were observed for all substances. For the tripeptides the limit of detection (LOD) and the limit of quantitation were 0.005 µmol/ml and 0.015 µmol/ml, respectively.

At pH 2, the major degradation pathway was cleavage of the peptide backbone amide bonds yielding dipeptides and amino acids, C-terminal deamidation as well as formation of succinimidyl peptides. Hydrolysis of the peptide backbone occurred faster than deamidation, so that only small amounts of deamidated tripeptides could be found. The succinimide ring was stable at pH 2 and significant degradation of the Asu peptides with free carboxyl groups was not observed. Relatively slow formation of diketopiperazine derivatives was found. The diketopiperazines were hydrolysed, but sequence inversion was not observed. Amino acids were the most abundant degradation products after 10 days of incubation.

In alkaline madium (pH 10) both deamidation of the *C*-terminal amide as well as isomerization and concomitant enantiomerization of Asp were observed for the native amide as well as for the resulting deamidated tripeptides. According to a study on hexapeptides by Geiger and Clarke [10], the amount of β-Asp containing peptides was higher than that of the corresponding α-Asp peptides for the sequence Phe-Asp-Gly. The peptide with the inverse amino acid sequence Gly-Asp-Phe yielded α-Asp peptides in higher amounts than β-Asp peptides. This was probably due to the steric hindrance of Phe, which allowed hydrolysis of the Asu ring only from one side. Significant formation of D-Asp containing peptides was found but proceeded relatively slowly.

The degradation of Phe-Asp-GlyNH_2 and Gly-Asp-PheNH_2 both at pH 2 and 10 followed apparent first order kinetics. The formation and degradation of the resulting products could be fitted with a non-linear model according to the Bateman equation.

Incubation of Phe-Asu-GlyOH at pH 10 gave additional information on the enantiomerization and on the opening reaction of the succinimidyl ring. The degradation of Phe-Asu-GlyOH and the formation of the four products L-Phe-α-L-Asp-GlyOH, L-Phe-α-D-Asp-GlyOH, L-Phe-β-L-Asp-GlyOH and L-Phe-β-D-Asp-GlyOH followed apparent first order kinetics. The ratio between β-Asp and α-Asp peptide concentration was 3.4. The α-D-Asp/α-L-Asp ratio was 0.23 and the β-D-Asp/β-L-Asp ratio was 0.26.

Summarising, CE proved to be a powerful technique for the analysis of Asp peptides including the isomerization and enantiomerization of the Asp residue. Additional studies will be necessary to explain the prevalent formation of α-Asp peptides in model substances with Phe as Asp-following amino acid. Moreover, investigations on Asu peptides with different amino acid sequence will be useful to understand the influence of the Asp neighbouring amino acid on the enantiomerization.

10. Materials and Methods

10.1 Fmoc-Solid phase peptide synthesis

200 mg of 2-chlorotrityl chloride resin with a substitution grade of 1.05 mmol/g (corresponding to 0.21 mmol of the resulting peptide) were allowed to swell in dry DMF. The attachment of the first residue to the resin linker was achieved by adding 1.2 equivalents of the Fmoc-protected amino acid dissolved in 1 ml dry DCM in the presence of 4 equivalents of DIPEA. The mixture was shaken for 3 h at room temperature. After this time the resin was washed with DCM/MeOH/DIPEA (17:2:1 v/v/v), DCM and DMF. Removal of the *N*-Fmoc group was achieved by treatment with 5% piperidine in DCM/DMF (50:50 v/v) for 10 min followed by 20% piperidine in DMF for 15 min. The resin was then washed several times with dry DMF. The coupling of the second amino acid was achieved in the presence of HBTU as coupling reagent. 4 equivalents of HBTU were dissolved in 1 ml dry DMF and added to 1.2 equivalent of the Fmoc-protected amino acid in the presence of 8 equivalents of DIPEA. The resin was shaken for 1 h at room temperature. After this time the resin was washed with dry DMF and the coupling reaction was repeated as mentioned before. After washing with DMF the resin was treated with 20% piperidine in DMF in order to remove the Fmoc-protecting group. The next amino acid was coupled following the same procedure described for the second one. After removing the Fmoc-protecting group from the third amino acid the resin was washed with DMF and DCM. Simultaneous cleavage of the peptide from the resin and of the aspartyl side chain protecting group (tBu) was achieved treating the resin with 95% TFA in water for 1 h. The resin was filtered and the peptide was precipitated in ice-cold diethylether. The peptide was then dissolved in *tert*-butanol/water (80:20 v/v), frozen and lyophilized.

The crude peptides were purified by preparative RP-HPLC and their identity was confirmed by fast atom bombardement (FAB) mass spectrometry.

Table 10: $[M+H]^+$ of the peptides synthesised by SPPS. Spectra were obtained by FAB mass spectrometry in glycerol.

Sequence	Peptide	$[M+H]^+$	Sequence	Peptide	$[M+H]^+$
Phe-Asp-Gly	L-Phe-L-α-Asp-GlyOH	338	**Gly-Asp-Phe**	Gly-L-α-Asp-L-PheOH	338
	L-Phe-D-α-Asp-GlyOH	338		Gly-D-α-Asp-L-PheOH	338
	L-Phe-L-β-Asp-GlyOH	338		Gly-L-β-Asp-L-PheOH	338
	L-Phe-D-β-Asp-GlyOH	338		Gly-D-β-Asp-L-PheOH	338

10.2 Synthesis of succinimidyl peptides

20 mg of aspartyl peptide were dissolved in 0.5 ml of 1.85 M HCl in glacial acetic acid and incubated at room temperature for 5 days. After this time over 95% transformation of the Asp peptide to the corresponding Asu peptide could be estimated by RP-HPLC. The reaction mixture was purified by preparative HPLC and the product was lyophilized. The identity was confirmed by mass spectrometry.

Table 11: $[M+H]^+$ of the Asu peptides synthesised according to [38]. Spectra were obtained by FAB mass spectrometry in glycerol.

Sequence	Peptide	$[M+H]^+$	Sequence	Peptide	$[M+H]^+$
Phe-Asp-Gly	Phe-Asu-$GlyNH_2$	319	**Gly-Asp-Phe**	Gly-Asu-$PheNH_2$	319
	Phe-Asu-GlyOH	320		Gly-Asu-PheOH	320

10.3 Incubations

A 50 mM phosphate buffer, pH 2.0, was prepared dissolving 6.2 mmol of sodium dihydrogen phosphate and 6.3 mmol of phosphoric acid in 250 ml of double distilled, deionized water. The ionic strength was adjusted to 0.2 M by addition of 2.56 g sodium chloride.

A 50 mM borate buffer, pH 10.0, was prepared dissolving 12.5 mmol of sodium tetraborate in approximately 180 ml of double distilled deionized water. The solution was titrated to pH 10.0 with 1 N sodium hydroxide solution and filled up to 250 ml with water. The ionic strength was adjusted to 0.2 M by addition of 0.096 g sodium chloride.

Solutions of pAMBA were prepared by dissolving 20 mg of pAMBA in 25 ml of buffer at pH 2 and in 25 ml of buffer at pH 10. These solutions were diluted with buffer to give two stock solutions with a final pAMBA concentration of 90 µg/ml. This concentration was chosen because the incubated samples were diluted 1:2, so that concentration of pAMBA during analysis was the same as for calibration (30 µg/ml).

8 mg of peptide were dissolved in 4 ml stock solution of pAMBA. This solution was divided in order to obtain two different incubation solutions for every sample. The peptides Phe-Asp-$GlyNH_2$ and Gly-Asp-$PheNH_2$ were incubated at 80 ± 1°C, while the succinimidyl peptide Phe-Asu-GlyOH was incubated at 30 ± 0.5°C. At selected time intervals 100 µl aliquots were withdrawn and added to 200 µl of ice-cold water in the case of the incubations at pH 2 and to 200 µl of ice-cold 100 mM phosphoric acid in the case of the incubations at pH 10. The samples were thoroughly mixed and stored at -20°C until analyzed. Each sample was injected in triplicate and the mean corrected peak-area ratios were evaluated. The mean value of the two incubations of the same sample was calculated and the peptide concentration was determined using the equations obtained from the respective calibration curves.

10.4 Capillary Electrophoresis with UV detection

Calibration of reference substances and analysis of incubated samples were performed on a P/ACE™ MDQ Capillary Electrophoresis System (Beckman Coulter, Unterschleißheim, Germany) equipped with a diode array detector. Data analysis was carried out with 32 Karat™ Software version 4.0. Untreated fused-silica capillaries (BGB Analytik Vertrieb, Schloßböckelheim, Germany) with 50 µm ID and 375 µm OD had an effective length of 40 cm and a total length of 50.2 cm. Prior to first use, capillaries were rinsed for 15 min with 100 mM sodium hydroxide, 10 min with water, 10 min with 100 mM H_3PO_4 and again 10 min with water. Between analyses the capillary was rinsed for 1 min with 100 mM sodium hydroxide, 1 min with water and 3 min with BGE. Sample solutions were injected at the anodic end by hydrodynamic injections at a pressure of 0.5 psi (1 psi = 6894.8 Pa) for 5 s. UV detection was carried out at the cathodic end of the capillary at 215 nm.

Buffer, voltage and temperature were optimized for the separation of all degradation products arising after incubation of the tripeptides. Five different CE-systems were developed. All buffers were prepared in double distilled deionized water, filtered (0.45 µm) and degassed in ultrasonic bath.

CE-System 1

This system was used for the analysis of most of the degradation products of the incubated peptides.

BGE:	50 mM phosphate, pH 3.0
Voltage:	25 KV (35.7 µA)
Temperature:	20°C

The buffer was prepared by dissolving 50 mmol sodium dihydrogen phosphate in 1000 ml of water and titrating the solution to pH 3.0 with 1 M sodium hydroxide. Fresh buffer was prepared every week and was stored at 4°C.

CE-System 2

This system was used for the separation of Gly-α-L-Asp-L-PheNH_2 and Gly-α-D-Asp-L-PheNH_2.

BGE:	50 mM phosphate, pH 3.0, 3 mg/ml S-β-CD
Voltage:	30 KV (50.1 µA)
Temperature:	20°C

The buffer was prepared by dissolving 50 mmol of sodium dihydrogen phosphate in 1000 ml of water and titrating the solution to pH 3.0 with 1 M sodium hydroxide. 30 mg S-β-CD were dissolved in 10 ml

of this buffer. After the addition of CDs, the pH of the buffer was controlled. The buffer was stored at 4°C.

CE-System 3

This system was developed for the separation and the analysis of L-Phe-β-L-Asp-GlyNH_2, L-Phe-α-L-Asp-GlyOH and L-Phe-α-D-Asp-GlyOH.

BGE:	50 mM phosphate, pH 3.0, 16 mg/ml CM-β-CD, containing 5% acetonitrile
Voltage:	25 KV (44.1 µA)
Temperature:	20°C

The buffer was prepared by dissolving 50 mmol of sodium dihydrogen phosphate in 1000 ml of water and titrating the solution to pH 3.0 with 1 M sodium hydroxide. 1.25 g CM-β-CD were dissolved in 50 ml of the buffer. This solution was titrated to pH 3.0 with 28 ml of 100 mM phosphoric acid (final concentration of CM-β-CD = 16 mg/ml). 2.63 ml of acetonitrile were added to this solution. In order to avoid evaporation of acetonitrile during analyses, the buffer was covered by a 1 mm thick film of light mineral oil according to [80].

CE-System 4

This system was used for the analysis of the diketopiperazine derivatives cyclo(Phe-Asp) and cyclo(Gly-Asp).

BGE:	50 mM formic acid, pH 3.0 (ammonia), containing 10% acetonitrile
Voltage:	30 KV (14.6 µA)
Temperature:	20°C

The buffer was prepared by dissolving 50 mM of formic acid in 1000 ml of water and titrating the solution to pH 3.0 with 25% aqueous ammonia. 10 ml of acetonitrile were added to 90 ml of this solution. In order to avoid evaporation of acetonitrile during analyses, the buffer was covered by a 1 mm thick film of light mineral oil according to [80].

CE-System 5

This system was developed for the separation of Phe-Asu-GlyOH, L-Phe-β-L-Asp-GlyOH and L-Phe-β-D-Asp-GlyOH after incubation of Phe-Asu-GlyOH at pH 10.

BGE:	50 mM phosphate, pH 2.9
Voltage:	25 KV (32.5 µA)

Temperature: 15°C

The buffer was prepared by dissolving 50 mmol of sodium dihydrogen phosphate in 1000 ml of water and titrating the solution to pH 2.9 with 1 M sodium hydroxide.

10.5 RP-HPLC with UV detection

RP-HPLC analyses with UV detection were performed on a Shimadzu system consisting of two LC-10AD VP pumps, a SPD-10A_{VP} detector, a SCL-10A_{VP} system controller and Class$_{VP}$ software version 5.0 (Shimadzu, Kyoto, Japan). The compounds were separated on a Grom-Sil 120 ODS-4 HE column (125 mm x 2 mm ID) (Grom Analytik, Rottenburg-Hailfingen, Germany). 10 µl of each sample were injected. Analyses were performed at a flow rate of 0.2 ml/min and detection was carried out at 215 nm.

Eluents and gradients were optimized for every sample. Five different HPLC-systems were developed. All buffers were prepared in double distilled, deionized water, filtered (0.45 µm) and degassed with helium.

HPLC-System 1

This system was used for the analysis of most degradation products and consisted of a gradient of two eluents:

Eluent A: 0.1% TFA in water
Eluent B: 0.1% TFA in water-acetonitrile (5:95 v/v)

The gradient was optimized for every sample:

HPLC-System 1a: for the separation of the degradation products arising from the incubation of Phe-Asp-GlyNH_2 at pH 2.
Gradient: 7-20% eluent B within 15 min

HPLC-System 1b: for the separation of the degradation products arising from the incubation of Phe-Asp-GlyNH_2 at pH 10.
Gradient: 2-13% eluent B within 30 min

HPLC-System 1c: for the separation of the degradation products arising from the incubation of Gly-Asp-PheNH_2 at pH 2.

Gradient: 1-39% eluent B within 20 min

HPLC-System 1d: for the separation of the degradation products arising from the incubation of Gly-Asp-PheNH_2 at pH 10.
Gradient: 10-20% eluent B within 15 min

HPLC-System 2
This system was used for the separation of L-Phe-α-L-Asp-GlyNH_2/L-Phe-β-L-Asp-GlyNH_2 and L-Phe-α-D-Asp-GlyOH/L-Phe-β-D-Asp-GlyOH

Eluent A: 15 mM aqueous sodium hydrogen phosphate, pH 5.0
Eluent B: water-acetonitrile (5:95 v/v)
Gradient: 2-13% eluent B within 30 min

10.6 CE-MS/MS

CE-MS/MS experiments were performed on a Hewlett Packard ^{3D}CE System (Agilent Technologies, Waldbronn, Germany) equipped with an Esquire 3000plus ion-trap mass spectrometer (Bruker Daltonik, Bremen, Germany) *via* the Agilent coaxial sheath-liquid sprayer interface (Agilent Technologies, Palo Alto, CA, USA). Post-processing software DataAnalysis version 3.0 and BioTools version 2.1 (Bruker Daltonik, Bremen, Germany) have been used. Untreated fused-silica capillaries (Polymicro Technologies, Phoenix, AZ, USA) with 50 µm ID and 375 µm OD had a length of 55 cm. Sample solutions were injected at the anodic end by hydrodynamic injections at a pressure of 50 mbar for 2-4 s.
Separation and detection conditions were as follows:

BGE: 200 mM formic acid, pH 2.9 (ammonia), containing 10% acetonitrile
Voltage: 30 KV
Temperature: 25°C
ESI-Voltage: 4500 V
Sheat liquid: 2 µl/min isopropanol/water (1:1)
Nebulizer gas: 3 psi
Scan speed: 13000 *m/z* per second
Mass range: 50-500 *m/z*

10.7 RP-HPLC-MS

RP-HPLC analyses with MS detection were performed on a HP 1100 series HPLC system (Agilent Technologies, Waldbronn, Germany) equipped with an API 165 single quadrupole MS system with turbo ion spray interface (Applied Biosystems, Langen, Germany). Data analysis was carried out with a HP ChemStation version Rev. A (Agilent Technolgies, Wldbronn, Germany). The compounds were separated on a LiChroCART 125-4 LiChrospher 100 RP-18 (5 µm) column (Merck, Darmstadt, Germany). 20 µl of sample were injected. Analyses were performed at a flow rate of 1 ml/min, at a temperature of 25°C.
Separation and detection conditions were as follows:

Eluent A:	0.1% TFA in water
Eluent B:	0.1% TFA in water-acetonitrile (5:95 v/v)
Gradient:	gradients of systems HPLC-1a,b,c,d
ESI-Voltage:	5200 V
Split:	1:4
Source temperature:	350°C
Focusing potential:	230 V
Declustering potential:	50 V
Entrance potential:	-10 V
Mass range:	100-400 *m/z*

10.8 Calibration and Validation

Calibration solutions were prepared in 50 mM phosphate buffer, pH 3.0, containing 30 µmol/ml pAMBA as internal standard. For every peptide seven solutions with decreasing concentrations (3.0, 1.5, 0.75, 0.3, 0.15, 0.06 and 0.015 µmol/ml) were prepared by diluting 15 µmol/ml stock solutions of the respective substances. Each sample was injected in triplicate and the mean of the corrected peak-area ratios (CPA of the analyte related to CPA of internal standard) were calculated. Calibration curves were obtained by plotting the analyte concentration on the x-axis *versus* the peak-area ratio on the y-axis. Validation was performed by analyzing two solutions of every peptide (0.75 and 0.06 µmol/ml) by three repetitive injections on three different days. The complete data for the calibration and validation are summarised in Appendix.

10.9 Materials, Chemicals and Instrumentation

10.9.1 General Instrumentation

Balances	Sartorius PT3100, BP210S, MC5 (Sartorius AG, Göttingen, Germany)
Drying oven	WTB Binder (Binder GmbH, Tuttlingen, Germany)
Filters	RC 55 Membrane Filters (Schleicher and Schuell, Dassel, Germany)
Filtration system	Glass Filter Holder 250 ml (Sartorius AG, Göttingen, Germany)
Hot plate stirrer	IKAMAG® RCT (Renner GmbH, Dannstadt, Germany)
Lyophylisator	Beta 1-8 (Martin Christ GmbH, Osterode, Germany)
pH meter	inoLab Level 1 (WTW GmbH, Weilheim, Germany)
Pipettes	Eppendorf Research 100, 200, 1000 (Eppendorf AG, Hamburg, Germany)
Rotary evaporator	VV 2000 with water bath WB 2000 (Heidolph Instruments GmbH, Kelheim, Germany)
SPPS syringes	5 ml Syringes (AbiMed Analysen-Technik GmbH, Langenfeld, Germany)
Ultrasonic bath	USR 9 (Merck Eurolab, Darmstadt, Germany)
Vacuum pump	CVC 2000 (Vacuubrand GmbH, Wertheim, Germany)
Vortex	Vortex Genie 2™ (Bender and Hobein AG, Zurich, Switzerland)
Water demineralizer	Seradest SD 6000 (Seral GmbH, Ransbach-Baumbach, Germany)

10.9.2 Chemicals

Acetonitrile	HPLC gradient grade, Merck KGaA, Darmstadt, Germany
Amino acids	Bachem AG, Heidelberg, Germany
CM-β-CD	Wacker-Chemie GmbH, Burghausen, Germany
DCM	Sigma-Aldrich Chemie GmbH, Taufkirchen, Germany
DIPEA	Sigma-Aldrich Chemie GmbH, Taufkirchen, Germany
Dipeptides	Bachem AG, Heidelberg, Germany
DMF	Sigma-Aldrich Chemie GmbH, Taufkirchen, Germany
Fmoc Amino Acids	Novabiochem, VWR International GmbH, Darmstadt, Germany
H_3PO_4 85%	J.T. Baker, Deventer, Holland
HBTU	Novabiochem, VWR International GmbH, Darmstadt, Germany
HCOOH	Merck KGaA, Darmstadt, Germany
Isopropanol	Merck KGaA, Darmstadt, Germany
$NaH_2PO_4 \cdot H_2O$	J.T. Baker, Deventer, Holland
NaOH Pellets	Merck KGaA, Darmstadt, Germany
NH_3 Solution 25%	Merck KGaA, Darmstadt, Germany
pAMBA	Sigma-Aldrich Chemie GmbH, Taufkirchen, Germany

S-β-CD	Sigma-Aldrich Chemie GmbH, Taufkirchen, Germany
TFA	Merck KGaA, Darmstadt, Germany

11. Zusammenfassung

Durch den Fortschritt in der Biotechnologie hat die Zahl der für den Markt zugelassenen biologisch aktiven Peptide, Proteine und Peptidomimetika in den letzten Jahren stark zugenommen. Während der Verarbeitung, Lagerung und des Transportes unterliegen diese Substanzen chemischen bzw. physikalisch-chemischen Abbauprozessen. Diese können sowohl zu Strukturveränderungen und somit zum Funktionsverlust der Pharmazeutika als auch zur Entstehung toxischer Abbauprodukte führen. Eine der instabilsten Aminosäuren in Peptiden und Proteinen ist die Asparaginsäure (Asp). Sie unterliegt im Besonderen der Isomerisierung und Enantiomerisierung über ein Aminosuccinimidyl (Asu) -Zwischenprodukt.

Ziel der vorliegenden Arbeit waren Studien zu Abbauprodukten von Aspartylpeptiden in sauren und basischen Milieu, besonders aber zu Isomerisierung und Enantiomerisierung der Asparaginsäurereste. Die Tripeptide Phe-Asp-GlyNH_2 und Gly-Asp-PheNH_2 wurden als Modellverbindungen verwendet. Sie wurden bei pH 2 und pH 10 über einer Zeitraum von maximal 10 Tagen bei 80°C inkubiert.

Die inkubierten Proben wurden zuerst mittels Kapillarelektrophorese (CE) mit UV-Detektion analysiert. Aufgrund der leicht unterschiedlichen pK_a-Werte ihrer freien Carboxylgruppen konnten Peptide mit α-Asp und β-Asp von den korrespondierenden Diastereomeren mit α-D-Asp und β-D-Asp getrennt werden. Die meisten Abbauprodukte konnten in einem 50 mM Phosphatpuffer, pH 3,0, analysiert werden. Trennungen, die in diesem System nicht möglich waren, wurden durch Zugabe von Cyclodextrinen zum Puffer erreicht.

Als Alternative zur Analyse der Abbauprodukte wurde zusätzlich eine RP-HPLC-Methode entwickelt. Die meisten Verbindungen konnten mit einem Gradienten von Acetonitril in wässriger Trifluoressigsäure (0,1% v/v) getrennt werden. Die Isomerenpaare L-Phe-α/β-L-Asp-GlyNH_2 und L-Phe-α/β-D-Asp-GlyOH wurden mit einem Gradienten von Acetonitril in Phosphatpuffer, pH 5,0, getrennt.

RP-HPLC und CE sind aufgrund ihrer unterschiedlichen Trennmechanismen komplementäre Techniken. Deshalb wurden Unterschiede in der Reihenfolge der Migration bzw. Elution erwartet. Beide Techniken erlaubten die Trennung der meisten Verbindungen. Während mit CE die zwei Paare von Diastereomeren Phe-α-L/D-Asp-GlyOH and Gly-α-L/D-Asp-PheNH_2 nicht getrennt werden konnten, war es mit HPLC problematisch, Peptide mit α-Asp und β-Asp Resten zu trennen. Generell waren Trennungen, die sich bei einer der Methoden als schwierig erwiesen, mit der jeweils anderen Methode problemlos erreichbar.

Die Abbauprodukte der Tripeptide wurden zuerst durch Koinjektion von Referenzsubstanzen identifiziert, die durch Festphasen-Peptidsynthese hergestellt wurden. Sowohl für CE als auch für HPLC wurde zusätzlich online-MS Detektion durchgeführt, um die Identifizierung über die koinjizierten Referenzsubstanzen zu bestätigen und vor allem, um unbekannte Abbauprodukte zu bestimmen. Alle Verbindungen konnten als $[M+H]^+$-Ionen detektiert werden. Die Analyse der MS-Spektren der Peptide erlaubte die Zuordnung der Abbauprodukte zur α-Asp- und β-Asp-Reihe. Unterschiede zwischen α-Asp- und β-Asp Peptiden wurden in dem Verhältnis zwischen den durch Spaltung der α/β-Asp-X und Y-α/β-Asp Bindung entstehenden b- und y-Ionen gefunden. Während α-Asp Peptide stärker zu b_2-Ionen und weniger zu y_2-Ionen fragmentierten, zeigten β-Asp Peptiden höhere y_2-Ionen Intensitäten. Zuverlässige Unterschiede in den Spektren von Peptiden mit D-Asp und L-Asp konnten nicht festgestellt werden. Für die Untersuchungen zur Stereochemie der Abbauprodukte musste deshalb der Vergleich mit synthetischen Peptiden bekannter Konfiguration durchgeführt werden.

Die Quantifizierung der Abbauprodukte erfolgte mittels CE. Die Methoden wurden mit Hilfe von Referenzsubstanzen validiert. Sehr gute Linearität, Wiederholpräzision (Präzision bestimmt mit Messungen am gleichen Tag) und laborinterne Vergleichspräzision (Präzision bestimmt mit Messungen in drei folgenden Tagen) wurden für alle Verbindungen nachgewiesen.

Inkubation im Sauren (pH2) führte hauptsächlich zur Hydrolyse der Peptidbindungen zu Dipeptiden und Aminosäuren, zu C-terminaler Deamidierung und zur Bildung von Succinimidyl-Peptiden. Die Spaltung der Peptidkette trat schneller auf als die Deamidierung. Zyklisierung des entstehenden Dipeptids führte zur Bildung eines Diketopiperazin-Derivates, das wiederum hydrolysierte. Unter diesen Bedingungen war der Succinimidyl-Ring stabil. Nach 10 Tagen Inkubation waren freie Aminosäuren die Hauptprodukte des Abbaus.

Bei pH 10 wurde sowohl für die nativen Amide als auch für die entstehenden deamidierten Tripeptide Isomerisierung und Enantiomerisierung von Asp beobachtet. Wie schon in der Literatur beschrieben [10, 55, 78], war die Menge an β-Aspartyl Peptiden in Inkubationen von Phe-Asp-GlyNH_2 größer als die an α-Aspartyl Peptiden. Inkubationen des Peptids Gly-Asp-PheNH_2 führten zu einer stärkeren Bildung von α-Aspartyl Peptiden. Die Ursache dafür ist vermutlich die sterische Hinderung durch den Phenylalanin-Rest. Die Entstehung von D-Asp Peptiden konnte in geringem Umfang nachgewiesen werden, was darauf hindeutet, dass die Enantiomerisierung langsamer als die Succinimidylringöffnung abläuft.

Der Abbau von Phe-Asp-GlyNH_2 und Gly-Asp-PheNH_2 folgte sowohl bei pH 2 als auch bei pH 10 einer apparenten Kinetik erster Ordnung. Für die Bildung und den weiteren Abbau der Reaktionsprodukte wurden kinetische Profile herstellt. Die erhaltenen Kurven wurden anhand der Bateman-Funktion gefittet. Für jedes Abbauprodukt konnte so die Halbwertszeit ermittelt werden.

Das Succinimidyl-Peptid Phe-Asu-GlyOH wurde bei pH 10 inkubiert, um die Kinetik der Ringöffnung und die damit verbundene Enantiomerisierung von L-Asp-Peptiden getrennt von den anderen Abbaureaktionen wie Deamidierung zu untersuchen. Die Bildung von L-Phe-α-L-Asp-GlyOH, L-Phe-α-D-Asp-GlyOH, L-Phe-β-L-Asp-GlyOH and L-Phe-β-D-Asp-GlyOH folgte einer apparenten Kinetik erster Ordnung. Im Gleichgewicht, das sich nach 2 Stunden einstellte, war das Verhältnis zwischen β-Aspartyl und α-Aspartyl Peptiden 3,4:1. Das Verhältnis von α-D-Asp/α-L-Asp wurde mit 0,23:1 und das von β-D-Asp/β-L-Asp mit 0,26:1 bestimmt.

12. References

[1] Walsh, G., Nat. Biotechnol. 21 (2003) 865-870.

[2] Walsh, G., Eur. J. Pharm. Biopharm. 55 (2003) 3-10.

[3] Manning, M.C., Patel, K., Borchardt, R.T., Pharm. Res. 6 (1989) 903-918.

[4] Aswad, D.W., Deamidation and Isoaspartate Formation in Peptides and Proteins, CRC Press, Boca Raton, 1995.

[5] Clarke, S., Stephenson, R.C., Lowenson, J.D. in Ahern, T.J., Manning, M.C. (Editors), Stability of Protein Pharmaceuticals, Part A: Chemical and Physical Pathways of Protein Degradation, Plenum Press, New York, 1992, 1-29.

[6] Oliyai, C., Borchardt, R.T., Pharm. Res. 10 (1993) 95-102.

[7] Oliyai, C., Borchardt, R.T., Pharm. Res. 11 (1994) 751-758.

[8] Capasso, S., Kirby, A.J., Savadori, S., Sica, F., Zagari, A., J. Chem. Soc. Perkin Trans. 2 (1995) 437-442.

[9] Radkiewicz, J.L., Zipse, H., Clarke, S., Houk, K.N., J. Am. Chem. Soc. 118 (1996) 9148-9155.

[10] Geiger, T., Clarke, S., J. Biol. Chem. 262 (1987) 785-794.

[11] Tam, J.P., Riemen, M.W., Merrifield, R.B., Peptide Res. 1 (1988) 6-18.

[12] Bodanszky, M., Principles of Peptide Synthesis, Springer, Berlin, 1984.

[13] Sandmeier, E., Hunziker, P., Kunz, B., Sack, R., Christen, P., Biochem. Biophys. Res. Comm. 261 (1999) 578-583.

[14] Nabuchi, Y., Fujiwara, E., Kuboniwa, H., Asoh, Y., Ushio, H., Pharm. Res. 14 (1997) 1685-1690.

[15] Roher, A.E., Lowenson, J.D., Clarke, S., Wolkow, C., Wang, R., Cotter, R.J., Reardon, I.M., Zürcher-Neely, H.A., Heinrikson, R.L., Ball, M.J., Greenberg, B.D., J. Biol. Chem. 268 (1993) 3072-3083.

[16] Orpiszewski, J., Schormann, N., Kluve-Beckerman, B., Liepnieks, J.J., Benson, M.D., FASEB J. 14 (2000) 1255-1263.

[17] Hekman, C.M., DeMond, W.S., Kelley, P.J., Mauch, S.F., Williams, J.D., J. Pharm. Biomed. Anal. 20 (1999) 763-772.

[18] Min Won, C., Molnar, T.E., Windisch, V.L., McKean, R.E., Int. J. Pharm. 190 (1999) 1-11.

[19] Ritz-Timme, S., Collins, M.J., Ageing Res. Rev. 1 (2002) 43-59.

[20] Goodfriend, G.A., Nature 357 (1992) 399-401.

[21] Mamula, M.J., Gee, R.J., Elliott, J.I., Sette, A., Southwood, S., Jones, P.-J., Blier, P.R., J. Biol. Chem. 274 (1999) 22321-22327.

[22] Reubsaet, J.L.E., Beijnen, J.H., Bult, A., van Maanen, R.J., Marchal, J.A.D., Underberg, W.J.M., J. Pharm. Biomed. Anal. 17 (1998) 955-978.

[23] Johnson, B.A., Aswad, D.W., Anal. Biochem. 192 (1991) 384-391.

[24] Carlson, A.D., Riggin, R.M., Anal. Biochem. 278 (2000) 150-155.

[25] Schurter, B.T., Aswad, D.W., Anal. Biochem. 282 (2000) 227-231.

[26] Zhang, W., Czupryn, M.J., Anal. Biochem. 307 (2002) 184-186.

[27] Cloos, P.A.C., Fledelius, C., Biochem. J. 345 (2000) 473-480.

[28] Bada, J.L., Methods Enzymol. 106 (1984) 98-115.

[29] Bada, J.L., J. Amer. Chem. Soc. 94 (1972) 1371-1373.

[30] Steinberg, S.M., Masters, P.M., Bada, J.L., Bioorganic Chemistry 12 (1984) 349-355.

[31] Manning, J.M., J. Amer. Chem. Soc. 92 (1970) 7449-7454.

[32] Sadakane, Y., Yamazaki, T., Nakagomi, K., Akizawa, T., Fujii, N., Tanimura, T., Kaneda, M., Hatanaka, Y., J. Pharm. Biomed. Anal. 30 (2003) 1825-1833.

[33] Radkiewicz, J.L., Zipse, H., Clarke, S., Houk, K.N., J. Am. Chem. Soc. 123 (2001) 3499-3506.

[34] Sabah, S., PhD Thesis, University of Münster (1998) 174-179.

[35] Chan, W.C., White P.D. (Editors), Fmoc Solid Phase Peptide Synthesis – A Practical Approach, Oxford University Press, 2000.

[36] Bodanszky, M., Tolle, J.C., Deshmane, S.S., Bodanszky, A., Int. J. Peptide Protein Res. 12 (1978) 57-68.

[37] Mergler, M., Dick, F., Sax, B., Weiler, P., Vorherr, T., J. Peptide Sci. 9 (2003) 36-46.

[38] Schön, I., Kisfaludy, L., Int. J. Peptide Protein Res. 14 (1979) 485-494.

[39] Stephenson, R.C., Clarke, S., J. Biol. Chem. 264 (1989) 6164-6170.

[40] Patel. K., Borchardt, R.T., Pharm. Res. 7 (1990) 787-793.

[41] Goolcharran, C., Borchardt, R.T., J. Pharm. Sci. 87 (1998) 283-288.

[42] Capasso, S., Vergara, A., Mazzarella, L., J. Am. Chem. Soc. 120 (1998) 1990-1995.

[43] Capasso, S., Mazzarella, L., Sica, F., Zagari, A., Salvadori, S., J. Chem. Soc. Chem. Commun. 12 (1992) 919-921.

[44] Capasso, S., Termochimica Acta 286 (1996) 41-50.

[45] Kašička, V., Electrophoresis 20 (1999) 3084-3105.

[46] Kašička, V., Electrophoresis 22 (2001) 4139-4162.

[47] Kašička, V., Electrophoresis 24 (2003) 4013-4046.

[48] Lai, M., Skanchy, D., Stobaugh, J., Topp, E., J. Pharm. Biomed. Anal. 18 (1998) 421-427.

[49] Sabah, S., Scriba, G.K.E., J. Pharm. Biomed. Anal. 16 (1998) 1089-1096.

[50] Sabah, S., Scriba, G.K.E., J. Chromatogr. A 822 (1998) 137-145.

[51] Vinther, A., Holm, A., Høeg-Jensen T., Jespersen, A.M., Klausen, N.K., Christensen, T., Sørensen, H.H., Eur. J. Biochem. 235 (1996) 304-309.

[52] Wan, H., Blomberg, L.G., J. Chromatogr. A 875 (2000) 43-88.

[53] Scriba, G.K.E., Electrophoresis 24 (2003) 4063-4077.

[54] Popa, T.V., Mant, C.T., Hodges, R.S., Electrophoresis 24 (2003) 4197-4208.

[55] Kaneda, M., Nakagomi, K., Sadakane, Y., Yamazaki, T., Tanimura, T., Akizawa, T., Fujii, N., Hatanaka, Y., J. Liq. Chromatogr. Rel. Technol. 25 (2002) 2445-2454.

[56] Roepstorff, P., Fohlman, J., Biomed. Mass Spectrom. 11 (1984) 601.

[57] Biemann, K., Methods Enzymol. 193 (1990) 886-887.

[58] Severs, J.C., Smith, R.D., in Cole, R.B. (Editor), Electrospray Ionization Mass Spectrometry: Fundamentals, Instrumentations and Applications, Wiley, New York, 1997, 343-382.

[59] Kelly, J.F., Ramaley, L., Thibault, P., Anal. Chem. 69 (1997) 51-60.

[60] Waterval, J.C.M., Hommels, G., Teeuwsen, J., Bult, A., Lingeman, H., Underberg, W.J.M., Electrophoresis 21 (2000) 2851-2858.

[61] von Brocke, A., Nicholson, G., Bayer, E., Electrophoresis 22 (2001) 1251-1266.

[62] Neusüß, C., Pelzing, M., Macht, M., Electrophoresis 23 (2002) 3149-3159.

[63] Figeys, D., van Oostveen, I., Ducret, A., Aebersold, R., Anal. Chem. 68 (1996) 1822-1828.

[64] Liu, T., Shao, X.-X., Zeng, R., Xia, Q.-C., J. Chromatogr. A 855 (1999) 695-707.

[65] Bateman, K.P., White, R.L., Thibault, P., J. Mass Spectrom. 33 (1998) 1109-1123.

[66] Zamfir, A., Peter-Katalinic, J., Electrophoresis 22 (2001) 2448-2457.

[67] Cao, P., Stults, J.T., Rapid Commun. Mass Spectrom. 14 (2000) 1600-1606.

[68] Hoitink, M.A., Hop, E., Beijnen, J.H., Bult, A., Kettenes-van den Bosch, J.J., Underberg, W.J.M., J. Chromatogr. A 776 (1997) 319-327.

[69] Lloyd, J.R., Cotter, M.L., Ohori, D., Doyle, D.L., Biomed. Env. Mass Spectrom. 15 (1988) 399-402.

[70] Hsu, Y.-R., Chang, W.-C., Mendiaz, E.A., Hara, S., Chow, D.T., Mann, M.B., Langley, K.E., Lu, H.S., Biochemistry 37 (1998) 2251-2262.

[71] Lehmann, W.D., Schlosser, A., Erben, G., Pipkorn, R., Bossemeyer, D., Kinzel, V., Protein Sci. 9 (2000) 2260-2268.

[72] Niessen, W.M.A., van der Greef, J., Liquid-Chromatography-Mass Spectrometry: Principles and Applications, Marcel Dekker, New York, 1992.

[73] Niessen, W.M.A., J. Chromatogr. A 1000 (2003) 413-436.

[74] Altria, K.D., Fabre, H., Chromatographia 40 (1995) 313-320.

[75] Wätzig, H., Degenhardt, M., Kunkel, A., Electrophoresis 19 (1998) 2695-2752.

[76] Schaeper, J.P., Sepaniak, M.J., Electrophoresis 21 (2000) 1421-1429.

[77] Mikulcik, P., Riede, J., Schmidbaur, H., Chem. Ber. 124 (1991) 2743-2746.

[78] Patel, K., Borchardt, R.T., Pharm. Res. 7 (1990) 703-711.

[79] Aylin, F., Konuklar, S., Aviyente, V., Org. Biomol. Chem. 1 (2003) 2290-2297.

[80] Baur, L., Sänger-van de Griend, C., Wätzig, H., J. Chromatogr. A 979 (2002) 97-103.

13. Appendix

13.1 Calibration of reference substances and validation of the method

13.1.1 Calibration and validation for CE-system 1 and CE-System 5

L-Phe-α-L-Asp-GlyNH$_2$						
Conc. (µmol/ml)	Intraday Precision			Interday Precision		
	CPA	SD	RSD (%)	CPA	SD	RSD (%)
0.015	0.042	0.001	1.81	-	-	-
0.06	0.128	0.002	1.89	0.133	0.004	3.35
0.15	0.293	0.006	2.14	-	-	-
0.3	0.567	0.006	1.03	-	-	-
0.75	1.365	0.014	0.99	1.365	0.002	0.18
1.5	2.709	0.042	1.54	-	-	-
3	5.419	0.098	1.81	-	-	-

L-Phe-α-D-Asp-GlyNH$_2$						
Conc. (µmol/ml)	Intraday Precision			Interday Precision		
	CPA	SD	RSD (%)	CPA	SD	RSD (%)
0.015	0.047	0.003	6.72	-	-	-
0.06	0.130	0.006	4.47	0.126	0.003	2.70
0.15	0.288	0.005	1.56	-	-	-
0.3	0.540	0.005	0.93	-	-	-
0.75	1.298	0.013	0.96	1.281	0.016	1.28
1.5	2.546	0.006	0.23	-	-	-
3	5.087	0.029	0.57	-	-	-

L-Phe-β-D-Asp-GlyNH$_2$						
Conc. (µmol/ml)	Intraday Precision			Interday Precision		
	CPA	SD	RSD (%)	CPA	SD	RSD (%)
0.015	0.041	0.003	7.17	-	-	-
0.06	0.122	0.011	9.1	0.126	0.005	3.65
0.15	0.273	0.012	4.56	-	-	-
0.3	0.494	0.026	5.37	-	-	-
0.75	1.179	0.024	2.00	1.167	0.011	0.96
1.5	2.265	0.019	0.83	-	-	-
3	4.371	0.062	1.43	-	-	-

L-Phe-β-L-Asp-GlyOH						
Conc. (µmol/ml)	Intraday Precision			Interday Precision		
	CPA	SD	RSD (%)	CPA	SD	RSD (%)
0.015	0.049	0.002	3.56	-	-	-
0.06	0.173	0.002	1.03	0.171	0.004	2.43
0.15	0.372	0.013	3.44	-	-	-
0.3	0.696	0.005	0.70	-	-	-
0.75	1.636	0.034	2.05	1.630	0.008	0.50
1.5	3.177	0.058	1.84	-	-	-
3	6.383	0.053	0.83	-	-	-

L-Phe-β-D-Asp-GlyOH						
Conc. (µmol/ml)	Intraday Precision			Interday Precision		
	CPA	SD	RSD (%)	CPA	SD	RSD (%)
0.015	0.052	0.002	3.33	-	-	-
0.06	0.180	0.005	2.59	0.1712	0.007	4.22
0.15	0.390	0.007	1.74	-	-	-
0.3	0.716	0.006	0.83	-	-	-
0.75	1.707	0.019	1.10	1.664	0.038	2.30
1.5	3.206	0.026	0.82	-	-	-
3	6.341	0.165	2.6	-	-	-

Gly-α-L-Asp-L-PheNH$_2$						
Conc. (µmol/ml)	Intraday Precision			Interday Precision		
	CPA	SD	RSD (%)	CPA	SD	RSD (%)
0.015	0.045	0.003	6.33	-	-	-
0.06	0.151	0.001	0.48	0.148	0.003	2.19
0.15	0.352	0.001	0.31	-	-	-
0.3	0.690	0.009	1.25	-	-	-
0.75	1.715	0.015	0.90	1.687	0.025	1.47
1.5	3.459	0.0279	0.80	-	-	-
3	6.793	0.021	0.30	-	-	-

Gly-α-D-Asp-L-PheNH$_2$						
Conc. (µmol/ml)	Intraday Precision			Interday Precision		
	CPA	SD	RSD (%)	CPA	SD	RSD (%)
0.015	0.040	0.001	3.23	-	-	-
0.06	0.150	0.005	3.27	0.150	0.001	0.72
0.15	0.365	0.002	0.64	-	-	-
0.3	0.704	0.005	0.70	-	-	-
0.75	1.744	0.002	0.11	1.741	0.009	0.54
1.5	3.464	0.031	0.90	-	-	-
3	6.922	0.054	0.78	-	-	-

Gly-β-L-Asp-L-PheNH$_2$						
Conc. (µmol/ml)	Intraday Precision			Interday Precision		
	CPA	SD	RSD (%)	CPA	SD	RSD (%)
0.015	0.050	0.0002	0.46	-	-	-
0.06	0.160	0.003	2.08	0.160	0.001	0.28
0.15	0.367	0.001	0.38	-	-	-
0.3	0.710	0.010	1.37	-	-	-
0.75	1.735	0.006	0.35	1.724	0.018	1.05
1.5	3.403	0.016	0.48	-	-	-
3	6.914	0.088	1.27	-	-	-

Gly-β-D-Asp-L-PheNH$_2$						
Conc. (µmol/ml)	Intraday Precision			Interday Precision		
	CPA	SD	RSD (%)	CPA	SD	RSD (%)
0.015	0.048	0.0003	0.80	-	-	-
0.06	0.159	0.005	3.15	0.160	0.001	0.87
0.15	0.374	0.006	1.49	-	-	-
0.3	0.724	0.003	0.45	-	-	-
0.75	1.771	0.013	0.72	1.768	0.007	0.37
1.5	3.484	0.058	1.66	-	-	-
3	6.860	0.094	1.37	-	-	-

Gly-α-L-Asp-L-PheOH						
Conc. (µmol/ml)	Intraday Precision			Interday Precision		
	CPA	SD	RSD (%)	CPA	SD	RSD (%)
0.015	0.040	0.001	3.06	-	-	-
0.06	0.134	0.002	1.32	0.132	0.001	1.09
0.15	0.304	0.002	0.57	-	-	-
0.3	0.591	0.017	2.88	-	-	-
0.75	1.444	0.019	1.3	1.435	0.015	1.05
1.5	2.801	0.025	0.91	-	-	-
3	5.657	0.068	1.20	-	-	-

Gly-α-D-Asp-L-PheOH						
Conc. (µmol/ml)	Intraday Precision			Interday Precision		
	CPA	SD	RSD (%)	CPA	SD	RSD (%)
0.015	0.045	0.001	2.53	-	-	-
0.06	0.163	0.004	2.69	0.164	0.001	0.82
0.15	0.379	0.008	2.25	-	-	-
0.3	0.734	0.008	1.14	-	-	-
0.75	1.779	0.028	1.55	1.782	0.005	0.29
1.5	3.445	0.077	2.23	-	-	-
3	6.747	0.112	1.66	-	-	-

Gly-β-L-Asp-L-PheOH						
Conc. (µmol/ml)	Intraday Precision			Interday Precision		
	CPA	SD	RSD (%)	CPA	SD	RSD (%)
0.015	0.049	0.001	3.07	-	-	-
0.06	0.182	0.002	1.14	0.180	0.002	1.15
0.15	0.414	0.005	1.31	-	-	-
0.3	0.795	0.024	3.03	-	-	-
0.75	1.921	0.027	1.39	1.908	0.017	0.92
1.5	3.723	0.031	0.84	-	-	-
3	7.501	0.083	1.11	-	-	-

Gly-β-D-Asp-L-PheOH						
Conc. (µmol/ml)	Intraday Precision			Interday Precision		
	CPA	SD	RSD (%)	CPA	SD	RSD (%)
0.015	0.042	0.003	7.67	-	-	-
0.06	0.176	0.014	7.8	0.176	0.008	4.60
0.15	0.428	0.008	1.8	-	-	-
0.3	0.819	0.020	2.43	-	-	-
0.75	2.000	0.045	2.25	1.900	0.091	4.79
1.5	3.961	0.105	2.66	-	-	-
3	7.779	0.050	0.65	-	-	-

Phe-Asu-GlyNH_2						
Conc. (µmol/ml)	Intraday Precision			Interday Precision		
	CPA	SD	RSD (%)	CPA	SD	RSD (%)
0.015	0.055	0.002	3.08	-	-	-
0.06	0.179	0.017	9.59	0.175	0.003	1.79
0.15	0.396	0.016	4.11	-	-	-
0.3	0.749	0.034	4.48	-	-	-
0.75	1.787	0.023	1.30	1.795	0.008	0.43
1.5	3.516	0.007	0.19	-	-	-
3	6.957	0.005	0.08	-	-	-

Phe-Asu-GlyOH						
Conc. (µmol/ml)	Intraday Precision			Interday Precision		
	CPA	SD	RSD (%)	CPA	SD	RSD (%)
0.015	0.068	0.005	6.99	-	-	-
0.06	0.207	0.010	4.75	0.204	0.002	1.15
0.15	0.453	0.010	2.17	-	-	-
0.3	0.859	0.022	2.56	-	-	-
0.75	2.031	0.004	0.18	2.002	0.026	1.31
1.5	3.944	0.087	2.20	-	-	-
3	7.708	0.106	1.37	-	-	-

Gly-Asu-PheNH$_2$						
Conc. (µmol/ml)	Intraday Precision			Interday Precision		
	CPA	SD	RSD (%)	CPA	SD	RSD (%)
0.015	0.038	0.003	6.72	-	-	-
0.06	0.140	0.003	2.43	0.139	0.002	1.30
0.15	0.335	0.002	0.76	-	-	-
0.3	0.680	0.014	2.09	-	-	-
0.75	1.699	0.049	2.88	1.680	0.017	1.04
1.5	3.369	0.053	1.57	-	-	-
3	6.805	0.173	2.55	-	-	-

Gly-Asu-PheOH						
Conc. (µmol/ml)	Intraday Precision			Interday Precision		
	CPA	SD	RSD (%)	CPA	SD	RSD (%)
0.015	0.0337	0.002	5.21	-	-	-
0.06	0.131	0.001	0.76	0.131	0.001	0.71
0.15	0.331	0.001	0.31	-	-	-
0.3	0.643	0.005	0.75	-	-	-
0.75	1.610	0.009	0.56	1.608	0.005	0.34
1.5	3.184	0.030	0.94	-	-	-
3	6.258	0.002	0.03	-	-	-

Phe-AspOH						
Conc. (µmol/ml)	Intraday Precision			Interday Precision		
	CPA	SD	RSD (%)	CPA	SD	RSD (%)
0.015	0.066	0.002	2.89	-	-	-
0.06	0.210	0.003	1.52	0.201	0.008	3.83
0.15	0.467	0.007	1.59	-	-	-
0.3	0.868	0.005	0.62	-	-	-
0.75	2.059	0.006	0.31	1.978	0.076	3.86
1.5	4.020	0.042	1.04	-	-	-
3	7.865	0.227	2.89	-	-	-

Gly-AspOH						
Conc. (µmol/ml)	Intraday Precision			Interday Precision		
	CPA	SD	RSD (%)	CPA	SD	RSD (%)
0.015	-	-	-	-	-	-
0.06	0.024	0.001	4.27	0.023	0.001	5.19
0.15	0.061	0.004	6.42	-	-	-
0.3	0.122	0.003	2.82	-	-	-
0.75	0.305	0.004	1.31	0.301	0.004	1.37
1.5	0.613	0.013	2.14	-	-	-
3	1.219	0.007	0.61	-	-	-

$PheNH_2$						
Conc. (µmol/ml)	Intraday Precision			Interday Precision		
	CPA	SD	RSD (%)	CPA	SD	RSD (%)
0.015	0.041	0.003	6.75	-	-	-
0.06	0.124	0.002	1.39	0.123	0.001	1.15
0.15	0.282	0.001	0.26	-	-	-
0.3	0.542	0.009	1.75	-	-	-
0.75	1.334	0.017	1.25	1.311	0.020	1.53
1.5	2.675	0.046	1.72	-	-	-
3	5.229	0.011	0.2	-	-	-

PheOH						
Conc. (µmol/ml)	Intraday Precision			Interday Precision		
	CPA	SD	RSD (%)	CPA	SD	RSD (%)
0.015	0.030	0.003	9.34	-	-	-
0.06	0.119	0.004	3.14	0.117	0.002	1.96
0.15	0.288	0.009	3.30	-	-	-
0.3	0.581	0.025	4.26	-	-	-
0.75	1.384	0.060	4.36	1.387	0.007	0.52
1.5	2.774	0.103	3.70	-	-	-
3	5.576	0.206	3.70	-	-	-

$GlyNH_2$						
Conc. (µmol/ml)	Intraday Precision			Interday Precision		
	CPA	SD	RSD (%)	CPA	SD	RSD (%)
0.015	-	-	-	-	-	-
0.06	-	-	-	-	-	-
0.15	-	-	-	-	-	-
0.3	0.013	0.001	9.88	-	-	-
0.75	0.031	0.001	4.5	0.032	0.001	3.02
1.5	0.064	0.003	4.11	-	-	-
3	0.125	0.004	3.12	-	-	-

13.1.2 Calibration and validation for CE-system 2

Cyclo(Phe-Asp)						
Conc. (µmol/ml)	Intraday Precision			Interday Precision		
	CPA	SD	RSD (%)	CPA	SD	RSD (%)
0.015	-	-	-	-	-	-
0.06	0.054	0.001	2.83	0.060	0.007	12.11
0.15	0.306	0.019	6.07	-	-	-
0.3	0.781	0.012	1.56	-	-	-
0.75	2.065	0.006	0.31	2.008	0.074	3.69
1.5	4.311	0.175	4.06	-	-	-
3	8.133	0.505	6.2	-	-	-

Cyclo(Gly-Asp)						
Conc. (µmol/ml)	Intraday Precision			Interday Precision		
	CPA	SD	RSD (%)	CPA	SD	RSD (%)
0.015	-	-	-	-	-	-
0.06	-	-	-	0.041	0.012	29.45
0.15	0.063	0.005	8.14	-	-	-
0.3	0.117	0.013	11.00	-	-	-
0.75	0.357	0.058	16.23	0.309	0.043	14.00
1.5	0.823	0.015	1.78	-	-	-
3	1.683	0.130	7.74	-	-	-

13.1.3 Calibration and validation for CE-system 3

L-Phe-β-L-Asp-GlyNH$_2$						
Conc. (µmol/ml)	Intraday Precision			Interday Precision		
	CPA	SD	RSD (%)	CPA	SD	RSD (%)
0.015	0.020	0.002	7.98	-	-	-
0.06	0.118	0.007	6.34	0.111	0.007	5.94
0.15	0.303	0.007	2.19	-	-	-
0.3	0.530	0.035	6.54	-	-	-
0.75	1.601	0.039	2.46	1.546	0.047	3.06
1.5	3.045	0.080	2.64	-	-	-
3	7.113	0.403	5.67	-	-	-

L-Phe-α-L-Asp-GlyOH						
Conc. (µmol/ml)	Intraday Precision			Interday Precision		
	CPA	SD	RSD (%)	CPA	SD	RSD (%)
0.015	0.019	0.002	8.34	-	-	-
0.06	0.097	0.001	0.86	0.091	0.005	5.73
0.15	0.240	0.006	2.71	-	-	-
0.3	0.479	0.007	1.54	-	-	-
0.75	1.239	0.030	2.45	1.159	0.078	6.76
1.5	2.279	0.033	1.46	-	-	-
3	3.932	0.171	4.35	-	-	-

L-Phe-α-D-Asp-GlyOH						
Conc. (µmol/ml)	Intraday Precision			Interday Precision		
	CPA	SD	RSD (%)	CPA	SD	RSD (%)
0.015	0.023	0.001	4.94	-	-	-
0.06	0.105	0.009	8.87	0.098	0.006	6.32
0.15	0.235	0.011	4.66	-	-	-
0.3	0.463	0.010	2.27	-	-	-
0.75	1.170	0.080	6.88	1.192	0.023	1.96
1.5	-	-	-	-	-	-
3	-	-	-	-	-	-

13.2 Incubation of Phe-Asp-GlyNH_2 at pH 2

L-Phe-α-L-Asp-GlyNH_2			
Incubation Time (h)	CPA	RSD (%)	Concentration (µmol/ml)
0	3.405	1.12	1.88
6	1.940	0.73	1.07
12	1.134	0.83	0.63
24	0.378	0.92	0.21
36	0.142	0.98	0.08
48	0.057	2.97	0.03
72	-	-	-
96	-	-	-
120	-	-	-
192	-	-	-
240	-	-	-

L-Phe-α-L-Asp-GlyOH			
Incubation Time (h)	CPA	RSD (%)	Concentration (µmol/ml)
0	-	-	-
6	0.212	0.66	0.13
12	0.207	2.18	0.13
24	0.113	4.68	0.07
36	0.052	4.00	0.03
48	0.021	15.34	0.013
72	-	-	-
96	-	-	-
120	-	-	-
192	-	-	-
240	-	-	-

Phe-Asu-GlyNH_2			
Incubation Time (h)	CPA	RSD (%)	Concentration (µmol/ml)
0	-	-	-
6	0.212	0.66	0.13
12	0.207	2.18	0.13
24	0.113	4.68	0.07
36	0.052	4.00	0.03
48	0.021	15.34	0.013
72	-	-	-
96	-	-	-
120	-	-	-
192	-	-	-
240	-	-	-

Phe-Asu-GlyOH			
Incubation Time (h)	CPA	RSD (%)	Concentration (µmol/ml)
0	-	-	-
6	0.048	9.45	0.02
12	0.102	7.75	0.04
24	0.171	2.97	0.07
36	0.215	2.23	0.08
48	0.247	1.45	0.09
72	0.301	0.86	0.12
96	0.341	1.16	0.13
120	0.365	1.75	0.14
192	0.393	2.56	0.15
240	0.388	2.54	0.15

Phe-AspOH			
Incubation Time (h)	CPA	RSD (%)	Concentration (µmol/ml)
0	-	-	-
6	0.965	1.07	0.36
12	1.419	0.85	0.54
24	1.667	0.84	0.63
36	1.536	0.18	0.58
48	1.329	0.6	0.50
72	0.986	0.94	0.37
96	0.758	0.71	0.29
120	0.607	0.89	0.23
192	0.405	1.66	0.15
240	0.338	1.02	0.13

PheOH			
Incubation Time (h)	CPA	RSD (%)	Concentration (µmol/ml)
0	-	-	-
6	0.015	33.41	0.01
12	0.060	18.77	0.03
24	0.193	3.57	0.10
36	0.319	1.68	0.17
48	0.429	2.04	0.23
72	0.626	4.85	0.34
96	0.787	2.13	0.42
120	0.903	2.62	0.49
192	1.191	3.09	0.64
240	1.351	2.74	0.73

$GlyNH_2$			
Incubation Time (h)	CPA	RSD (%)	Concentration (µmol/ml)
0	-	-	-
6	0.015	11.35	0.37
12	0.027	7.21	0.65
24	0.035	6.74	0.83
36	0.035	4.92	0.84
48	0.035	3.44	0.84
72	0.035	4.96	0.83
96	0.032	5.06	0.75
120	0.029	6.79	0.68
192	0.022	10.24	0.53
240	0.018	10.01	0.43

L-Phe-α-L-Asp-$GlyNH_2$			
Incubation Time (h)	CPA	RSD (%)	Concentration (µmol/ml)
0	-	-	-
6	0.095	12.7	0.03
12	0.236	8.97	0.09
24	0.686	4.70	0.25
36	0.943	4.54	0.34
48	1.101	2.55	0.40
72	1.290	1.82	0.47
96	1.285	1.43	0.47
120	1.253	2.26	0.46
192	0.909	7.62	0.33
240	0.816	7.22	0.30

13.3 Incubation of Phe-Asp-GlyNH_2 at pH 10

L-Phe-α-L-Asp-GlyNH_2			
Incubation Time (h)	CPA	RSD (%)	Concentration (µmol/ml)
0	3.469	0.55	1.92
6	2.519	1.42	1.39
12	1.892	0.66	1.05
24	1.042	1.03	0.58
36	0.597	1.12	0.33
48	0.357	0.95	0.20
72	0.145	1.54	0.08
96	0.070	1.77	0.04
120	0.033	5.19	0.02
192	-	-	-
240	-	-	-

L-Phe-α-D-Asp-GlyNH_2			
Incubation Time (h)	CPA	RSD (%)	Concentration (µmol/ml)
0	-	-	-
6	0.103	2.36	0.06
12	0.143	2.28	0.08
24	0.157	1.59	0.09
36	0.133	1.26	0.08
48	0.106	3.58	0.06
72	0.064	4.36	0.04
96	0.038	4.60	0.02
120	0.017	9.00	0.015
192	-	-	-
240	-	-	-

L-Phe-β-L-Asp-GlyNH_2			
Incubation Time (h)	CPA	RSD (%)	Concentration (µmol/ml)
0	-	-	-
6	0.394	3.75	0.19
12	0.602	2.66	0.29
24	0.750	3.48	0.36
36	0.663	8.62	0.32
48	0.515	8.22	0.25
72	0.258	7.71	0.12
96	0.121	5.46	0.06
120	0.059	14.44	0.03
192	-	-	-
240	-	-	-

L-Phe-β-D-Asp-GlyNH_2			
Incubation Time (h)	CPA	RSD (%)	Concentration (µmol/ml)
0	-	-	-
6	0.083	1.89	0.06
12	0.131	1.98	0.09
24	0.193	2.27	0.13
36	0.207	1.88	0.14
48	0.199	1.05	0.13
72	0.147	1.82	0.10
96	0.099	2.19	0.07
120	0.061	3.23	0.04
192	-	-	-
240	-	-	-

L-Phe-α-L-Asp-GlyOH			
Incubation Time (h)	CPA	RSD (%)	Concentration (µmol/ml)
0	-	-	-
6	0.517	3.43	0.33
12	0.799	4.41	0.52
24	1.245	3.93	0.80
36	1.364	6.34	0.88
48	1.328	6.84	0.86
72	1.155	6.33	0.75
96	0.995	4.48	0.64
120	0.892	8.02	0.58
192	0.563	11.52	0.36
240	0.333	18.93	0.21

L-Phe-α-D-Asp-GlyOH			
Incubation Time (h)	CPA	RSD (%)	Concentration (µmol/ml)
0	-	-	-
6	0.016	27.38	0.01
12	0.134	6.92	0.09
24	0.194	6.40	0.12
36	0.215	10.11	0.14
48	0.254	6.56	0.16
72	0.286	5.73	0.18
96	0.340	5.84	0.22
120	0.284	11.75	0.18
192	0.214	21.45	0.14
240	0.016	27.38	0.013

L-Phe-β-L-Asp-GlyOH			
Incubation Time (h)	CPA	RSD (%)	Concentration (µmol/ml)
0	-	-	-
6	0.094	2.41	0.04
12	0.238	1.56	0.11
24	0.593	1.31	0.28
36	0.908	1.55	0.43
48	1.161	1.01	0.54
72	1.468	1.42	0.69
96	1.638	0.75	0.77
120	1.668	1.07	0.78
192	1.556	1.74	0.73
240	0.933	5.60	0.44

L-Phe-β-D-Asp-GlyOH			
Incubation Time (h)	CPA	RSD (%)	Concentration (µmol/ml)
0	-	-	-
6	-	-	-
12	0.050	8.94	0.02
24	0.155	4.73	0.07
36	0.280	4.23	0.13
48	0.396	4.18	0.19
72	0.619	2.44	0.29
96	0.818	3.17	0.38
120	0.928	3.49	0.44
192	1.125	2.56	0.53
240	0.786	7.47	0.37

13.4 Incubation of Gly-Asp-PheNH$_2$ at pH 2

Gly-α-L-Asp-L-PheNH$_2$			
Incubation Time (h)	CPA	RSD (%)	Concentration (µmol/ml)
0	4.321	1.03	1.90
6	3.445	0.99	1.51
12	2.774	0.52	1.22
24	1.735	0.97	0.76
36	1.092	0.45	0.48
48	0.697	1.08	0.31
72	0.276	2.19	0.12
96	0.112	1.86	0.05
120	0.048	2.89	0.02
192	-	-	-
240	-	-	-

Gly-α-L-Asp-L-PheOH			
Incubation Time (h)	CPA	RSD (%)	Concentration (µmol/ml)
0	-	-	-
6	0.167	1.28	0.09
12	0.224	0.83	0.12
24	0.248	0.59	0.13
36	0.207	1.87	0.11
48	0.163	1.99	0.09
72	0.079	3.28	0.04
96	0.036	5.23	0.02
120	-	-	-
192	-	-	-
240	-	-	-

Gly-Asu-PheNH$_2$			
Incubation Time (h)	CPA	RSD (%)	Concentration (µmol/ml)
0	-	-	-
6	0.053	4.13	0.02
12	0.091	2.02	0.04
24	0.141	2.37	0.06
36	0.159	4.57	0.07
48	0.166	2.16	0.07
72	0.164	1.99	0.07
96	0.146	2.20	0.06
120	0.130	2.17	0.06
192	0.085	3.21	0.04
240	0.064	1.65	0.03

Gly-Asu-PheOH			
Incubation Time (h)	CPA	RSD (%)	Concentration (µmol/ml)
-	-	0	-
-	-	0	-
-	-	0	-
0.030	4.82	0.01	0.030
0.048	7.22	0.02	0.048
0.059	2.76	0.03	0.059
0.072	3.17	0.03	0.072
0.075	2.78	0.04	0.075
0.072	1.55	0.03	0.072
0.056	2.36	0.03	0.056
0.047	3.89	0.02	0.047

Gly-AspOH			
Incubation Time (h)	CPA	RSD (%)	Concentration (µmol/ml)
0	-	-	-
6	0.066	1.97	0.16
12	0.118	4.37	0.29
24	0.182	3.73	0.45
36	0.201	3.10	0.49
48	0.204	2.16	0.50
72	0.175	2.77	0.43
96	0.143	4.68	0.35
120	0.106	3.99	0.26
192	0.038	4.09	0.09
240	0.021	5.14	0.05

PheOH			
Incubation Time (h)	CPA	RSD (%)	Concentration (µmol/ml)
0	-	-	-
6	-	-	-
12	0.047	2.59	0.02
24	0.126	1.24	0.07
36	0.200	3.20	0.11
48	0.267	2.48	0.14
72	0.361	2.85	0.19
96	0.442	3.47	0.24
120	0.501	1.73	0.27
192	0.620	2.12	0.33
240	0.705	1.70	0.38

$PheNH_2$			
Incubation Time (h)	CPA	RSD (%)	Concentration (µmol/ml)
0	-	-	-
6	0.409	2.45	0.23
12	0.711	2.36	0.41
24	1.183	2.14	0.67
36	1.443	0.96	0.82
48	1.616	1.44	0.92
72	1.768	4.05	1.01
96	1.796	1.05	1.02
120	1.808	2.14	1.03
192	1.741	1.17	0.99
240	1.681	0.80	0.96

cyclo(Gly-Asp)			
Incubation Time (h)	CPA	RSD (%)	Concentration (µmol/ml)
0	-	-	-
6	-	-	-
12	-	-	-
24	0.044	48.55	0.08
36	0.062	22.17	0.11
48	0.075	33.69	0.14
72	0.068	27.02	0.12
96	0.054	35.62	0.10
120	0.054	23.25	0.10
192	-	-	-
240	-	-	-

13.5 Incubation of Gly-Asp-PheNH$_2$ at pH 10

Gly-α-L/D-Asp-L-PheNH$_2$			
Incubation Time (h)	CPA	RSD (%)	Concentration (µmol/ml)
0	4.241	0.67	1.86
6	3.714	2.49	1.63
12	3.251	1.32	1.43
24	2.428	1.44	1.07
36	1.850	1.76	0.81
48	1.412	0.85	0.62
72	0.815	0.95	0.36
96	0.473	1.19	0.21
120	0.282	0.98	0.12
192	0.063	2.32	0.03
240	0.022	7.81	0.013

Gly-α-L-Asp-L-PheNH$_2$			
Incubation Time (h)	% αLL	RSD (%)	Concentration (µmol/ml)
0	100.00	0.00	1.86
6	98.24	0.18	1.60
12	96.30	0.09	1.38
24	92.45	0.11	0.99
36	88.64	0.43	0.72
48	85.68	0.50	0.53
72	79.74	0.81	0.29
96	74.34	1.60	0.15
120	71.32	1.75	0.09
192	-	-	-
240	-	-	-

Gly-α-D-Asp-L-PheNH$_2$			
Incubation Time (h)	% αDL	RSD (%)	Concentration (µmol/ml)
0	0.00	-	-
6	1.76	10.32	0.03
12	3.70	2.31	0.05
24	7.55	1.33	0.08
36	11.36	3.33	0.09
48	14.32	2.99	0.09
72	20.26	3.21	0.07
96	25.66	4.63	0.05
120	28.68	4.35	0.04
192	-	-	-
240	-	-	-

Gly-β-L-Asp-L-PheNH$_2$			
Incubation Time (h)	CPA	RSD (%)	Concentration (µmol/ml)
0	-	-	-
6	0.039	5.43	0.02
12	0.057	12.09	0.02
24	0.091	3.24	0.04
36	0.098	4.74	0.04
48	0.098	3.20	0.04
72	0.083	4.14	0.04
96	0.069	7.76	0.03
120	0.056	7.31	0.02
192	-	-	-
240	-	-	-

Gly-β-D-Asp-L-PheNH$_2$			
Incubation Time (h)	CPA	RSD (%)	Concentration (µmol/ml)
0	-	-	-
6	-	-	-
12	-	-	-
24	0.042	7.23	0.02
36	0.058	1.63	0.02
48	0.066	3.22	0.03
72	0.070	3.83	0.03
96	0.065	4.04	0.03
120	0.058	4.06	0.02
192	-	-	-
240	-	-	-

Gly-α-L-Asp-L-PheOH			
Incubation Time (h)	CPA	RSD (%)	Concentration (µmol/ml)
0	-	-	-
6	0.482	2.29	0.26
12	0.857	2.99	0.45
24	1.384	3.01	0.73
36	1.706	3.90	0.90
48	1.919	2.40	1.02
72	2.131	1.93	1.13
96	2.225	3.20	1.18
120	2.259	2.48	1.20
192	2.144	1.39	1.14
240	2.031	1.84	1.08

Gly-α-D-Asp-L-PheOH			
Incubation Time (h)	CPA	RSD (%)	Concentration (µmol/ml)
0	-	-	-
6	0.024	9.83	0.01
12	0.108	4.86	0.05
24	0.286	1.37	0.13
36	0.470	0.80	0.21
48	0.628	1.05	0.28
72	0.875	2.14	0.39
96	1.015	1.65	0.45
120	1.090	1.65	0.48
192	1.113	1.46	0.49
240	1.072	2.14	0.47

Gly-β-L-Asp-L-PheOH			
Incubation Time (h)	CPA	RSD (%)	Concentration (µmol/ml)
0	-	-	-
6	-	-	-
12	-	-	-
24	0.028	7.97	0.01
36	0.053	12.19	0.02
48	0.077	12.70	0.03
72	0.129	11.96	0.05
96	0.176	10.84	0.07
120	0.224	13.89	0.09
192	0.315	10.25	0.13
240	0.339	11.53	0.14

Gly-β-D-Asp-L-PheOH			
Incubation Time (h)	CPA	RSD (%)	Concentration (µmol/ml)
0	-	-	-
6	-	-	-
12	-	-	-
24	-	-	-
36	0.018	20.70	0.01
48	0.042	26.02	0.02
72	0.076	7.42	0.03
96	0.112	8.00	0.04
120	0.141	7.31	0.05
192	0.212	2.95	0.08
240	0.245	3.61	0.09

13.6 Incubation of Phe-Asu-GlyOH at pH 10

Phe-Asu-GlyOH			
Incubation Time (min)	CPA	RSD (%)	Concentration (µmol/ml)
0	4.877	1.93	1.88
5	4.059	4.06	1.57
10	3.183	2.63	1.23
15	2.509	1.33	0.97
30	1.251	1.95	0.48
60	0.349	9.87	0.13
90	0.101	12.40	0.04
120	-	-	-

L-Phe-α-L-Asp-GlyOH			
Incubation Time (min)	CPA	RSD (%)	Concentration (µmol/ml)
0	-	-	-
5	0.072	11.86	0.05
10	0.115	3.51	0.07
15	0.158	3.08	0.10
30	0.211	3.14	0.14
60	0.300	9.60	0.19
90	0.295	6.00	0.19
120	0.306	9.06	0.20

L-Phe-α-D-Asp-GlyOH			
Incubation Time (min)	CPA	RSD (%)	Concentration (µmol/ml)
0	-	-	-
5	-	-	-
10	-	-	-
15	-	-	-
30	0.028	8.40	0.018
60	0.054	5.45	0.035
90	0.061	6.63	0.039
120	0.070	7.80	0.045

L-Phe-β-L-Asp-GlyOH			
Incubation Time (min)	CPA	RSD (%)	Concentration (µmol/ml)
0	-	-	-
5	0.415	6.33	0.195
10	0.629	4.11	0.295
15	0.800	3.40	0.375
30	1.103	3.81	0.518
60	1.328	1.87	0.623
90	1.388	2.47	0.651
120	1.395	2.48	0.655

L-Phe-β-D-Asp-GlyOH			
Incubation Time (min)	CPA	RSD (%)	Concentration (µmol/ml)
0	-	-	-
5	-	-	-
10	-	-	-
15	-	-	-
30	0.185	4.18	0.087
60	0.315	3.77	0.148
90	0.379	2.14	0.178
120	0.361	3.03	0.170

List of publications

Publications

1. De Boni, S., Neusüß, C., Pelzing, M., Scriba, G.K.E., Identification of Degradation Products of Aspartyl Tripeptides by Capillary Electrophoresis-Tandem Mass Spectrometry, Electrophoresis 24 (2003) 874-882.

2. De Boni, S., Oberthür, C., Hamburger, M., Scriba, G.K.E., Analysis of Aspartyl Peptide Degradation Products by High Performance Liquid Chromatography and High Performance Liquid Chromatography-Mass Spectrometry, J. Chromatogr. A 1022 (2004) 95-102.

3. De Boni, S., Scriba G.K.E., Kinetics of the Degradation of Aspartyl Peptides, in preparation for Pharm. Res.

Poster Presentations and Conference Contributions

1. De Boni, S., Scriba, G.K.E., Analysis of Aspartyl Peptide Degradation by Capillary Electrophoresis. *15th International Symposium on Microscale Separations and Analysis - HPCE* , April 13-18, 2002, Stockholm, Sweden.

2. De Boni, S., Neusüß, C., Pelzing, M., Scriba, G.K.E., Analysis of Aspartyl Peptide Degradation by CE and HPLC, *DPhG Annual Meeting*, October 9-12, 2002, Berlin, Germany.

3. De Boni, S., Psurek, A., Süß, F., Scriba, G.K.E., Separation of Peptide Stereoisomers by Capillary Electrophoresis – Application to Stability Studies. *Fachgruppentagung Arzneimittelkontrolle / Pharmazeutiche Analytik*, October 9, 2002, Berlin, Germany.

4. Neusüß, C., Pelzing, M., Unger, M., Holzgrabe, U., Dreyer, M., Bringmann, G., De Boni, S., Scriba, G.K.E., Structure Elucidation of Isomeric Forms of Small Molecules by CZE/MS^n. *16th International Symposium on Microscale Separations and Analysis - HPCE* , January 17-22, 2003, San Diego, California USA.

5. De Boni, S., Scriba, G.K.E., Analysis of Aspartyl Peptide Degradation Products by High Performance Liquid Chromatography-Mass Spectrometry. *DPhG Annual Meeting*, October 8-11, 2003, Würzburg, Germany.

6. De Boni, S., Neusüß, C., Pelzing, M., Scriba, G.K.E., Analysis of Degradation Products of Aspartyl Tripeptides: Comparison between HPLC-MS and CE-MS. *17th International Symposium on Microscale Separations and Capillary Electrophoresis - HPCE*, February 8-12, 2004, Salzburg, Austria.

7. Scriba, G.K.E., De Boni, S., Neusüß, C., Pelzing, M., Degradation of Aspartyl Tripeptides - Studies by Capillary Electrophoresis-Tandem Mass Spectrometry and High Performance Liquid Chromatography-Mass Spectrometry. *7th Sino-German-Symposium on Chromatography*, October 17-20, 2004, Chongqing, China.

Acknowledgments

I wish to express my gratitude to my supervisor, Prof. Dr. Gerhard Scriba, for his continuous support during the four years that I have spent in his group. His expertise and guidance have been essential for this work.

I am grateful to Prof. Dr. Dr. h.c. mult. Herbert Oelschläger and Prof. Dr. Jochen Lehmann for affording me a position at the Institute of Pharmacy of the University of Jena.

Furthermore I would like to thank all the people that in several ways helped me during my work:
Dr. Samir Sabbah for the synthesis of the amidated tripeptides,
Prof. Dr. Siegmund Reißmann, Dr. Bettina Müller and Dr. Georg Greiner, Institute of Biochemistry and Biophysics of the University of Jena, for the help and the advice on solid phase peptide synthesis,
Prof. Dr. Matthias Hamburger and Dr. Christine Oberthür, Department of Pharmaceutical Biology, Institute of Pharmacy of the University of Jena, for the assistance during HPLC-MS analysis.

I am particularly grateful to Dr. Christian Neusüß and Dr. Matthias Pelzing, Bruker Daltonik GmbH Leipzig, for the CE-MS/MS analyses and the interesting discussions on the CE-MS/MS results.

Finally, I wish to thank all my colleagues at the Department of Pharmaceutical Chemistry for the stimulating and friendly atmosphere, in particular Johannes Wange for the critical reading of the manuscript.

Lebenslauf

Name:	Silvia De Boni
Geburtsort:	Conegliano (Italien)
Geburtsdatum:	23. Juli 1975
Staatsangehörigkeit:	Italienisch

07.1994	Abitur am Liceo Scientifico Statale "G. Marconi", Conegliano (Italien)
1994-2000	Studium der Pharmazie (Chimica e Tecnologia Farmaceutiche) an der Fakultät für Pharmazie der Universität Padua (Italien)
09.1998-12.1998	Erasmus-Austauschstudium an der University of Wales, Bangor (UK) Laborpraktikum in Organischer Chemie: "Investigation into the Mode of Biological Action of Ptilomycalin A"
10.1999-10.2000	Diplomarbeit an der Universität Padua mit dem Thema: "Synthese, Charakterisierung und Aktivität eines aus 7-Aza-Tryptophan synthetisierten Analogon der 1-47 Domäne von Hirudin".
10.2000	Abschluss als Diplom-Pharmazeutin
seit 11.2000	wissenschaftliche Mitarbeiterin am Institut für Pharmazie der Friedrich Schiller Universität Jena Doktorarbeit über das Thema "Untersuchungen zur Enantiomerisierung von Asparaginsäure in Peptiden mittels der Kapillarelektrophorese" unter der Betreuung von Prof. Dr. G. Scriba

Selbstständigkeitserklärung

Die vorliegende Arbeit wurde am Institut für Pharmazie der Biologisch-Pharmazeutischen Fakultät im Zeitraum November 2000 bis Oktober 2004 unter Betreuung von Herrn Prof. Dr. Gerhard Scriba angefertigt.

Ich erkläre,

- dass ich die vorliegende Arbeit selbständig und nur unter Verwendung der angegebenen Hilfsmittel und Literatur angefertigt habe,
- dass die Arbeit weder teilidentisch noch identisch mit einer Arbeit ist, die der Friedrich-Schiller-Universität Jena oder einer anderen Hochschule zur Erlangung des akademischen Grades oder als Prüfungsleistung vorgelegt worden ist und
- dass mir die geltende Promotionsordnung der Biologisch-Pharmazeutischen Fakultät der Friedrich-Schiller-Universität bekannt ist.